Tomas Bata University
Faculty of Technology

Doctoral Thesis

# Design and Validation of the Methods for Comprehensive Characterization of the Hyperelastic Properties of Elastomers

# Návrh a validace metod pro komplexní charakterizaci hyperelastických vlastností elastomerů

Author:             **Eng. Rohitha Keerthiwansa**

Degree programme:   P3909 Production Engineering

Degree course:      3909V013 Tools and Processes

Supervisor:         Associate Prof. Ing. Jakub Javořík, Ph.D.

Reviewers:          Prof. Dr. Ing. Petr Horáček

                    Doc. Ing. Jan Krmela, Ph.D.

                    Doc. Ing. Dagmar Měřínská, Ph.D.

Zlín, 2020

This publication was issued in the year 2020

Key words: hyperelestic materials, data fitting, mechanical characterization, elastomers, rubber, strain energy density, hyperelestic material models

Klíčová slova: hyperelestické materiály, analýza experimentálních dat, elastomery, pryž, hustota deformační energie, mechanické vlastnosti, hyperelestické materiálové modely

# CONTENTS

# ABSTRACT

This thesis and the research work surrounding it, is oriented towards finding a solution to a problem in obtaining accurate material constants whenever only a single data set (i.e. uniaxial tension test data) is available in hyperelestic material characterization.

To begin with, the serious nature of the problem was highlighted through results of set of experiments. There, several material models were tried with two data fitting methods and the inaccuracy of data fitting with single data set could be proved beyond doubt from this exercise.

At the next stage, as a preliminary solution to the problem, a suggestion was given in the way of secondary data set generation from available data. The question at this point was about the method which could be adopted to generate the second data set. As an initial trial, exponential function was used with several exponents in order to generate data which could be consequently used as biaxial data. Amid some minor discrepancies, method delivered some promising results.

Second approach was sorted in order to get a better trajectory for the generated biaxial data. In this method, initial uniaxial data set was divided in to two segments and each segment was differently addressed. As a result, the trajectory of generated data nearly resembled the real biaxial data. Data fitting preceded the data generation, provided very encouraging results too. However, method had some serious shortcomings such as, unit incompatibility, and lack of use of uniaxial data in the later half. Due to these reasons, the method was not further examined for the use in the work.

Final experiments were done with six materials. Base material and other constituents were different in each of these cases and it resulted in varied data distributions in both uniaxial and biaxial data. An exponential function was once again used with a different exponent in finial tests. Proximity of generated data against real biaxial data was statistically tested. For the testing, 95% confidence interval was selected and most of the instances, generated data distribution was within the limit. Situations where, results differed, adjustment of confidence interval could be proposed with justification considering the hyperelestic material properties. Finally, Mooney-Rivlin model was used for data fitting as to further emphasize the results.

# ABSTRACT (CZECH)

Dizertační práce a výzkum provedený v průběhu doktorského studia se zaměřuje na nalezení řešení v oblasti získání přesných materiálových konstant, v případě, že je k dispozici pouze omezený soubor dat k charakterizaci hyperelastických materiálů.

Na začátku práce je zdůrazněna závažnost výše zmíněného problému skrze výsledky experimentů. Datové soubory z testování hyperelastických materiálů byly vyhodnoceny na několika materiálových modelech za použití dvou různých metod pro určení hyperelastických konstant. Nepřesnost určení konstant při využití dat pouze z měření jednoosého tahu byla jasně prokázána. V další fázi výzkumu, bylo navrženo předběžné řešení tohoto problému, a to ve formě generování druhého souboru dat (dvouosý tah) z dostupných dat pro jednoosý tah. Předmětem výzkumu tedy bylo stanovení vhodné metody pro generování druhého datového souboru. Pro prvotní testování byla pro toto generování zvolena exponenciální funkce.

Mimo drobné nesrovnalosti, byly výsledky této metody slibné. Dalším krokem řešení bylo v nalezení přesnější funkce pro generovaná biaxiálních dat. V rámci této metody se křivka pro dvouosý tah rozdělila na dva segmenty, přičemž každý segment byl řešen odděleně. Byla získána data, která blízce připomínala skutečný biaxiální datový soubor. Avšak tato metoda vykazovala vážné nedostatky, jako je například nekompatibilita jednotek generovaných dat a nedostatečný počet dat v druhém segmentu. Z těchto důvodů nebyla tato metoda dále použita. Finální experimenty byly provedeny se šesti různými elastomery. Ty se lišily základním materiálem kaučukové směsi a dalšími složkami, což se projevilo v různorodosti jednoosých i dvouosých dat. Shoda generovaných dat se skutečným dvouosým tahem, byla statisticky testována. Pro testování, byl zvolen interval spolehlivosti 95 %, a ve většině případů, byla shoda potvrzena. Pro situace, ve kterých se výsledky lišily, bylo navrženo upravení intervalu spolehlivosti, což bylo odůvodněno hyperelastickými vlastnostmi materiálů. V závěru práce je přínos výsledků ověřen při určení materiálových konstant pro Mooney-Rivlinův hyperelastický model.

# ACKNOWLEDGEMENT

Natural Rubber – It all starts from the Hevea Brasiliensis tree that grows in tropics.

# 1. INTRODUCTION

## 1.1 Hyperelastic Materials

Materials that exhibit large elastic strains at relatively moderate loads are called hyperelastic materials [1-4]. This material group consist of mostly, natural and artificial rubber, thermoplastic elastomers, and some biological materials such as human skin and tissues. Because of engineering properties such as, high flexibility, abrasion resistance, thermal and water resistance, these materials are used in the industry for wide range of applications [5]. These applications include, engine mountings, tires, vibration dampers, hydraulic hoses, structural bearings, medical tissues and membranes for medical devices and implants [1, 3]. Some of these applications are depicted in the figure 1.1.



**Fig. 1.1** Some industrial applications of elastomers {a. Tyres, b. Mountings, c. Dust covers, d. Mats, e. gloves, f. O-rings, g. gum boots} [*]

Constant development of new materials in this category with improved properties leads to ever increasing applications of elastomers. Considering these wide range of engineering applications in many fields, it is important to examine more about basic properties of these materials.

## 1.2 General Properties

Elastomers are unique set of engineering materials which exhibit elastic and viscous characteristics [6]. Chemically they are amorphous polymers [7]. Usually, these materials possess low elastic modulus and high bulk modulus [8] and considered incompressible or nearly incompressible [9]. Elastomers demonstrate high nonlinear stress-strain characteristic under moderate loads [1].

Because of such behaviour, the stress-strain relationship of such materials could only be defined through strain energy density functions (strain energy per unit volume) [1]. In addition to nonlinear behaviour at high loads, such materials possess high flexibility, extensibility, resiliency and durability [3].

With the advancement in new materials with improved inherent physical properties, application of elastomers in the industry is continuously increasing. This trend could be expected to continue over the next few decades, especially in the direction of thermoplastic elastomers. As interest for use of these materials grow, the research on elastomers both from fundamental theory and application point of views are equally gained attraction among scientific community [10]. This could be witnessed from the large number of research papers published over this particular research area during last few years.

When consider the research on elastomers, it is spread over several directions. Out of such large and diverse research domain, mechanical characterization plays a very vital role. The reason for that is the usefulness of the outcome in direct applications in product design and development.

## 1.3 Mechanical Characterization of Rubber like Materials

Examination based prediction of behaviour of material under mechanical loads could be defined as mechanical characterization. Whenever new products are designed, by selecting most suitable materials at initial design stage, time, effort and costs could be reduced drastically. In that aspect, mechanical characterization could be very vital tool. Not only that, such analysis could also be used for new material development, failure analysis and forecasts in the way of load limitations and capabilities.

When it comes to mechanical characterization of rubber like materials, the task is challenging. The reason for such difficulty is that, there are many governing theories involve in the behaviour of rubber, i.e., the large deformations, material nonlinearity, plastic and viscoelastic properties, stress softening. Hence, it is very difficult to analyse all of these phenomenon simultaneously [3].

In order to make the analytical task less complicated, normally most of these phenomenon is addressed separately at different stages of analysis [11-13]. In the present work, we are specifically concerned about the hyperelestic behaviour of these materials. At the same time, as stress-strain behaviour of these material is nonlinear, the mechanical characterization is usually done through set of pre-selected material models. A particular model is selected for a specific application after through consideration of the usage, related variables, and available data [6] and consequently the characterization is done.

## 1.4 Hyperelastic Material Models

Hyperelestic material models are basically mathematical relations that depict strain energy density in terms of either strain invariants or stretch ratios. When we consider hyperelestic models, there are many as forty different types available to date. Therefore, selection of a model for one particular application may not be simple. However, some of these models are applicable only to some specific materials and therefore generally less popular, while few others are frequently used in hyperelestic research domain.

At this stage, in order to get the background image of hyperelestic material characterization and its research history, in depth literature survey was done and observations could be briefly highlighted as follows.

## 1.5 A Brief Research History

The very first hyperelestic material model was introduced by Melvin Mooney as a general strain energy function in 1940 [14]. Reliable set of data required for the testing of models was then provided by Treloar in 1944 [15]. In 1948, Rivlin improved the first model, and it came in to existence as Mooney-Rivlin model [06]. This is the most frequently used model for the elastomer characterization. The simplest model of all, the Neo Hookean model [16], is a special case of the two parameters Mooney-Rivlin model. Further to these initial models, in 1967, Valanis and Landel [17], introduced a new method of representing the strain energy function. In this method, strain energy density was expressed as a function of stretch ratios instead of stain invariants. The model developed by Ogden [16], in 1972 is also frequently used for characterization. The Yeoh model [18], which came in to effect in 1990 is another common model. Arruda and Boyce also found a frequently used model as recent as 1993 [19]. There are many other models which are less known and could be used in specific applications [20-27].

A comparison of theory and experiment related to biaxial testing was done by Ogden [28]. James, Green, and Simpson [29], suggested an analytical forms of the strain energy density function for isotropic, incompressible materials as early as 1975. Tejasri and Basak [30] investigated the possibility of predicting the best model for a hyperelastic material like rubber using the Treloar's uniaxial test data. Comparative study was done by Destrade, Saccomandi, and Sgura [31] fitting of data belongs to three deformation ranges. A detailed comparison of hyperelastic models was also done by Marckmann and Verron [32] using twenty models including some of the less common models. By doing so, they could introduce a certain ranking for the fitting by the success of the results. Similar comparison was done by Kayacı and Serbest using several compounds [33]. Need for a second

data set, i.e., biaxial data for accurate result for data fitting is discussed by Johannknecht and Jerrams [34]. Importance of use of several data sets when characterising a model for mechanical response, is also emphasized by Morrow et. Al. [35]. The change of material constants with change of carbon black was studied by, Hassan, Abouel-Kasem and others [36]. Ogden and Saccomandi pointed out difficulties in getting unique optimal solution for data fitting [37]. Morrow et al. used Hotelling's $T^2$ test to evaluate the data fitting [35]. Further research on data fitting with hyperelestic models was done by H. P. Gavin [38]. His work based on The Levenberg-Marquardt algorithm. The paper discussed the methods of error minimizing in fitting and therefore, could be helpful in comparing different fitting results. Furthermore, literature survey on hyperelestic models done by G. Marckmann & E. Verron revealed the development methods of hyperelestic models across the board so far[39].

Considering all mentioned work of previous researchers we could initially formulate the topic discussed here in. Having mentioned briefly, the background study related to this work, it is appropriated to start with the research question at this point, and thereby extend the description towards explaining our intended answer to the problem.

## 1.6  Data Fitting

As general practice in characterization suggests, after selection of appropriate model for the characterisation, in order to complete the task, the relevant material constants are needed. They are obtained through nonlinear regression analysis, or simply by data fitting. The data collected through uniaxial, eqi-biaxial and pure shear laboratory experiments are used for the fitting.

## 2. THE OBJECTIVE

### 2.1 The Problem

As so far mentioned, hyperelastic material characterization leaped along several fronts over the last eighty or so years. Numerous models came in to existence and new methods of analysis were tried. In addition to that, advanced methods for testing of different strain modes were also established. Development of powerful computers and introduction of FEA tools also further simplified the hyperelastic material characterization.

However, amid all these new developments in the hyperelastic material research area, the problem of elimination of complicated laboratory tests such as eqi-biaxial testing for data collection, seems yet to be addressed. On the other hand, due to such complexities and cost concerns a single data set, i.e. uniaxial data, is frequently used. Amid repetitive use, method known to be erroneous. Therefore an investigation for an alternative solution to address this issue became a necessity and could be well justified.

### 2.2 The Aim

Having mentioned the necessity, we could clearly outlined the aim or the objective of the work as follows. That is to find a method of obtaining realistic and accurate material constants whenever only uniaxial data is available.

### 2.3 The Solution

Throughout this research work, possibilities of replacing data obtained through complicated and sometimes inaccurate biaxial experiments, by set of artificial data generated through uniaxial data is examined.

### 2.4 The Approach

First of all, uniaxial data set is obtained through typical standard test. Consequently, data set thus obtained is manipulated through a mathematical formula in such a way that, second set of data could be obtained. Thereafter, this second set of data, which could be considered as an alternative to the missing biaxial data could be used for the combined data fitting together with uniaxial data.

## 3. STATE OF THE ART

### 3.1 The Chemistry of Rubber

Rubber is, in simple terms, a material that can be stretched as much as twice or more of its original size and still could be formed in to its initial shape once released. The reason for such behaviour of these materials is their long chain like molecular structure. This structure gives the rubbery effect to the material. Chemically rubber is a hydrocarbon and its main constituent is polyisoprene. Typical appearance of these molecules is depicted in figure 3.1.
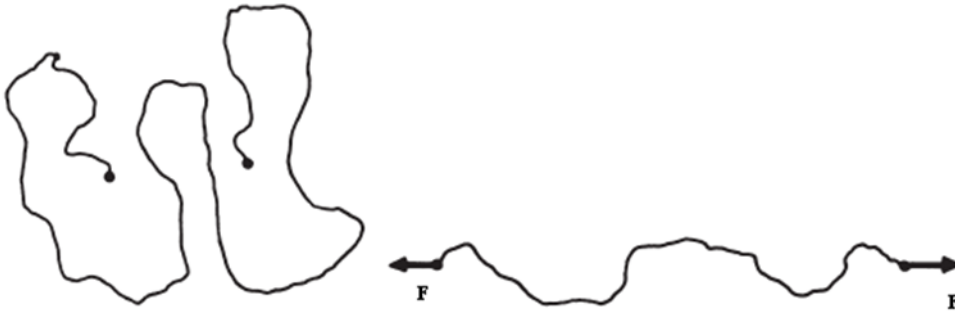


**Fig. 3.1** Chain like structure of rubber [40]

Just like in any other polymer, this long chained molecule structure of the rubber material is a direct result of repeated connection of basic unit cells. Constituent unit cells make these materials different from one another. However, long chain structural arrangement of these materials does not necessarily provide the rigid backbone required for them to function as engineering materials. Normally, these materials behave like viscous fluids. To improve the rubber material strength and to transform it to useful engineering material, during the early ages of the development, a process called vulcanization was introduced. The method first invented by American industrialist Charles Goodyear in 1844 and is still used for the very same reason.

### 3.2 The Vulcanizing Process

In this process, the long chain molecules of rubber materials are cross-linked through added foreign material at elevated temperature (140°–180° C) as shown in figure 3.2. For natural rubber, this material is often Sulphur. But, for other types of elastomers, there are different types of materials with similar characteristics. For example, Peroxides, and metal oxides are also used for such purpose [7].

14
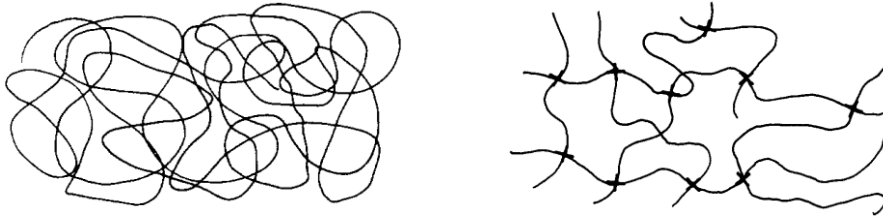
**Fig. 3.2** Rubber vulcanization process [40]

Amount of vulcanization or vulcanization density in general effect physical properties as given in the Fig. 3.3. According to the graph, the tensile strength increases with the improvement of cross linking density. The maximum tensile strength located somewhere in the vicinity of $13.5 \times 10{-5}$ mol/cm$^3$ of cross linking Density.
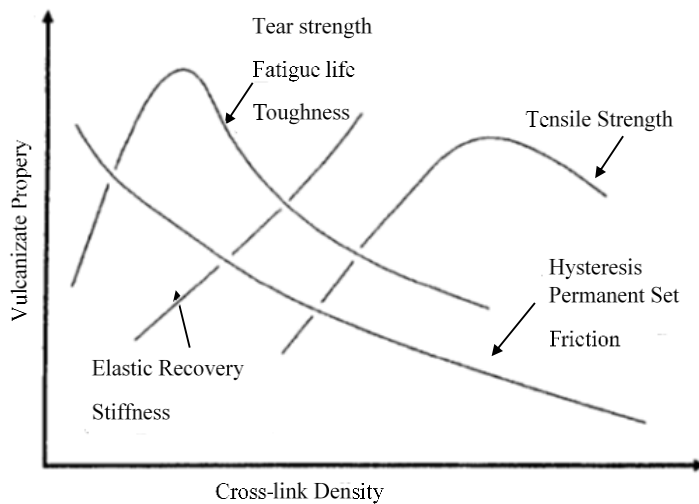


**Fig. 3.3** Vulcanization properties Vs cross-link density [41]

On the other hand, through the cross linking, the loose three dimensional molecular chain network could be improved to get a higher rigidity. In addition to cross linking, as a result of molecular intertwining, there are entanglements between long chains, in particular, with high molecular weight polymers. For rubber, these entanglements provide a permanent bonding to the material structure as depicted in figure 3.4.
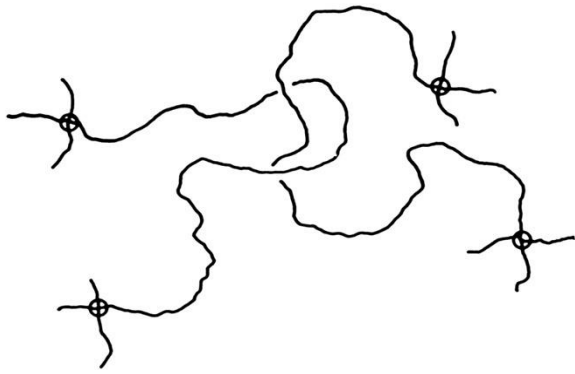
**Fig. 3.4** Entanglements between long chains [42]

However, number of cross links required for effective stability of the material is not very much clear even at situations where exact chemical composition is given. Therefore, it is suggested to express force-extension relationship in terms of strain energy density which subsequently expressed in terms of strain invariants or stretch ratios in order to clear ambiguity.

## 3.3 An Introduction to General Purpose Elastomers

Elastomers or rubberlike materials that are found in the industry can be broadly categorize in to two groups as general and special purpose elastomers. Bulk of rubber products manufactured today fall in to the group of general purpose elastomers. They comprised mostly, natural Rubber (NR), polyisoprene (IR), polybutadiene (BR), styrene-butadiene (SBR), nitrile-butadiene (NBR) and ethylene propylene rubber (EPR / EPDM). These elastomers are often used because of their good physical properties, processability and adoptability. In addition to that, they are economical too. Though there are many positives, some negative properties are also there. Less heat, oil and solvent resistant are dominant in negative side of these materials. Besides, some of them are susceptible to ozone and oxygen attacks too [43].

Natural Rubber (NR)

Natural rubber is produced from the milky white liquid extracted from the Hevea Brasiliensis tree (latex). The latex is first stabilized with preservatives (e.g., ammonia, formaldehyde, sodium sulphite). Then it is coagulation and hydroxylamine is added to produce technically-specified, constant-viscosity grades of natural rubber. The glass transition temperature ($T_g$) of natural rubber is around −70 °C and its structure composed of mostly cis-14-polyisoprene molecules (Fig. 3.5). In Addition to that, small amounts of fatty acids and protein

16

residues are also there. These ingredients enhance the sulphur vulcanization process [9].
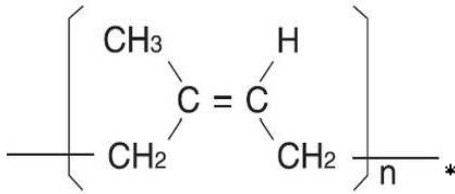


**Fig. 3.5** Unit cell of Natural Rubber

Styrene-Butadiene Rubber (SBR)

SBR is a copolymer of styrene and butadiene. Styrene content is about 23% wt. The glass transition temperature is around −55 °C. It is considered the most widely used synthetic elastomer. Material possesses a very good electrical resistance. The constituent unit cell is shown in the figure below (Fig. 3.6) [9].
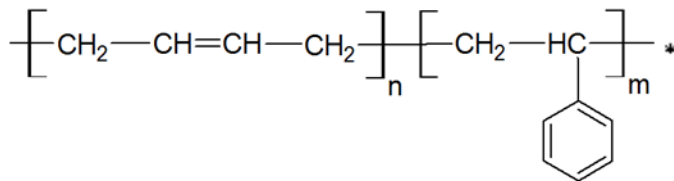


**Fig. 3.6** Unit cell of Styrene-Butadiene Rubber

Synthetic Polyisoprene (IR)

This synthetic material contains Poly-isoprene which is also the main ingredient of natural rubber. Therefore, properties of these two materials are similar and they include resilience, low hysteresis, low rolling resistance and high fatigue resistance. Both show poor resistance to oil, sunlight and ozone and have limited thermal capability. The structure of this rubber is given below (Fig. 3.7).
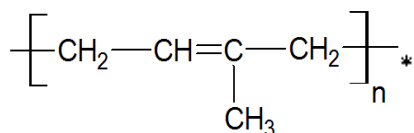


**Fig. 3.7** Unit cell of Synthetic Polyisoprene Rubber

Polybutadiene (BR)

The major use of polybutadiene is in tyre manufacture with over 70% of the elastomer produced going into treads and sidewalls. BR shows excellent abrasion resistance and low rolling resistance. It has high resilience. The glass transition temperature (Tg) Is less than –90C. The structure of material composed of unit cells given here (Fig. 3.8).
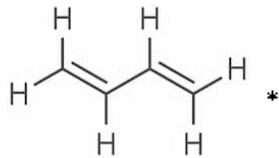


**Fig. 3.8** Unit cell of Polybutadiene Rubber

Acrylonitrile-Butadiene Rubber (NBR)

NBR, or as commonly known, nitrile rubber, is an emulsion copolymer of acrylonitrile and butadiene. Material has low density, show good heat stability and is a good oil resistant. Because of oil resistance and heat resistance, applications include fuel hoses, gaskets, rollers, and other similar products. The rolls for spreading ink in printing and hoses for oil products are other obvious uses. Typical glass transition temperature (Tg) is –60 °C. The NBR unit cell is given in figure 3.9.
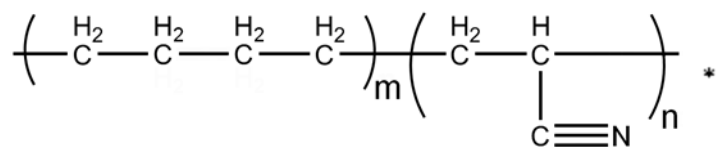


**Fig. 3.9** Unit cell of Acrylonitrile-Butadiene Rubber

Ethylene-Propylene Rubber (EPR, EPDM)

Ethylene propylene rubber is an elastomer prepared from ethylene and propylene monomers. It has a fair tensile strength and shows excellent resistance to weathering and ozone, and chemical attacks. Heat resistance lies between 150°C and 204°C. Because of good physical properties, material has a great acceptance in the sealing and electrical cable manufacturing industry. The unit cell of this material is given in figure 3.10.
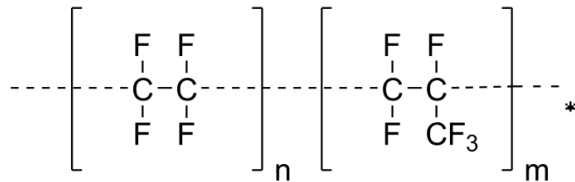
**Fig. 3.10** Unit cell of Ethylene-Propylene Rubber

Chlorobutyl (CIIR)

Chlorobutyl rubber is produced by the halogenation of butyl rubber. According to Mark et al. [44], these rubbers are highly impermeable to air and show very low water absorption, and exhibit good heat, oxygen and ozone resistance. Common uses of these are given as in liners of radial tires, covers and insulation of high-voltage electric cables, and automobile engine and radiator hoses. The unit cell of this material is given in figure 3.11.
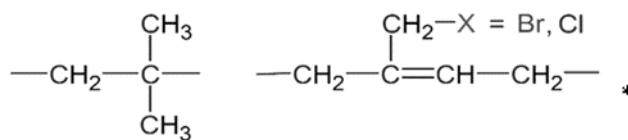


**Fig. 3.11** Structure unit of Chlorobutyl

Apart from main raw materials discussed above, in most of rubbers, there are additives that are used to get some specific properties for specialized applications.

## 3.4 Additives and Rubber Compounding

In the industry of rubber, there are many diverse applications as we already mentioned. These applications demand specific properties from rubber materials. Base materials alone cannot provide such exact properties. Therefore, they are mixed with various additives to achieve desirable effects. However, as indirect effect of additives, stress- strain properties of rubber compound also get changed. Apart from additives, fillers are used to reduce the cost of production of rubber materials. Then, there are some other mixing agents which are used to enhance the process. In order to give general idea about all these additives, fillers and ad mixtures frequently used, some common ones are discussed in detail here.

Carbon Black, Silica and Talc are the main additives in rubber making process. Besides, there are some other minor adding agents used at the rubber mixing stage such as oils, wax, and fatty acids for process improvement and pigments for aesthetics and colour.

Carbon Black

Carbon black is one of the main reinforcing ingredients find in the rubber mixture. It improves the tensile strength of the rubber. There are several types of carbon black and are classified according to the particle size and degree of surface oxidation.

Silica

Silica is also a reinforcement ingredient in rubber. It too increases the tensile strength and the tearing strength of the rubber material. However, addition of reinforcement fillers make rubber material move towards viscoelastic region [44].

Talc

Talc is used as a reinforcement filler in NBR, EPDM and Chloroprene (CR) rubber. It is a hydrated magnesium sheet silicate with the chemical formula $Mg_3Si_4O_{10}(OH)_2$. Talc in rubber reduces the viscosity of compound, thereby facilitate the processability of moulded parts. They also improve extruded product quality, increase production rates and enhance UV radiation resistance of exterior parts such as automotive profiles [44].

However, there are other factors such as mixing and dispersion, presence of contamination, curing, porosity which affect the stress strain behaviour of rubber compound [43].

## 3.5 The Mechanics of Hyperelasticity

Having discussed about chemistry and the major constituents of elastomers, the mechanics of these useful material group is worth mentioning here to understand the behaviour of them when subjected to various load conditions.

Mathematical relations that govern the behaviour of any material under loads is vital in forecasting stresses and strains experience by that material. In general, section of science that discuss this in detail is called mechanics and, the specific topic that deals with mechanical behaviour of materials where it is modelled as a continuous mass called continuum mechanics.

Continuum mechanics is originated from the man's interest in studying the movement and deformation of a body in space [16]. Basically, in relation to this topic, changes of a moving body over the time such as, translation, and rotation are examined and discussed. As basis here, two coordinate systems are used in tracking these physical changes. Coordinate system that is based on undeformed state or configuration called Eulerian or spatial while system based on deformed configuration is called Lagrange or material coordinates. Therefore, by adopting

similar nomenclature in defining a very small body $B_0$ in undeformed domain, the position could be marked with the coordinates $(\xi_1, \xi_2, \xi_3)$ (Fig. 3.12).
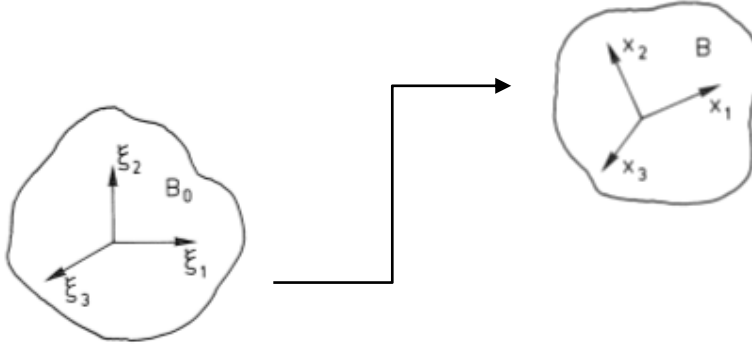


**Fig. 3.12** Change of configuration [45]

After state change in the space, supposing the body $B_0$ takes a shape of $B$ in deformed configuration with coordinates $(X_1, X_2, X_3)$, the function that maps this state change could be defined by, $X(\xi)$, as given in equation 3.1.

$$X(\xi): \xi \rightarrow X. \tag{3.1}$$

In the equation 3.1, the vector $X$ in deformed configuration and vector $\xi$ in undeformed configuration are named, Eulerian and Lagrange coordinates respectively. In the state change of small material body considered, translation and rotation which is also called rigid body motions should be eliminated from the equation in order to get the pure stress and deformation relationship. The rigid translation is eliminated through a matrix $F$ called deformation gradient. $F$ is defined as follows.

$$F_{i,j} = \frac{\partial x_i}{\partial \xi_j} \tag{3.2}$$

or,

$$F = x \nabla \xi \tag{3.3}$$

Here $\nabla \xi$ is the gradient operator worked out with differentiation with respect to material coordinates $(\xi_1, \xi_2, \xi_3)$. If equation (Eq. 3.3) is elaborated, it would appear as follows.

$$F = \begin{bmatrix} x_1 \\ x_2 \\ x_3 \end{bmatrix} \begin{bmatrix} \dfrac{\partial}{\partial \xi_1} & \dfrac{\partial}{\partial \xi_2} & \dfrac{\partial}{\partial \xi_3} \end{bmatrix} = \begin{bmatrix} \dfrac{\partial x_1}{\partial \xi_1} & \dfrac{\partial x_1}{\partial \xi_2} & \dfrac{\partial x_1}{\partial \xi_3} \\ \dfrac{\partial x_2}{\partial \xi_1} & \dfrac{\partial x_2}{\partial \xi_2} & \dfrac{\partial x_2}{\partial \xi_3} \\ \dfrac{\partial x_3}{\partial \xi_1} & \dfrac{\partial x_3}{\partial \xi_2} & \dfrac{\partial x_3}{\partial \xi_3} \end{bmatrix} \tag{3.4}$$

With this definition,

$$F = \nabla \xi x \qquad\qquad 3.5$$

New vector $x'$ is defined adding translation $c$ to the vector $x$.

$$x' = x + c \qquad\qquad 3.6$$

As $c$ is not a function of $\xi$, Differentiation with respect to it will result in,

$$F = x' \nabla \xi \qquad\qquad 3.7$$

Here, deformation gradient $F$ describe the deformation and the rotation while omitting the translation. In order to remove rotation, by decomposing $F$ in multiplicative sense:

$$F = RU \qquad\qquad 3.8$$

Assuming $R$ has the pure rotation and $U$, the pure deformation, the polar decomposition of equation 3.8 leads to separation of rigid rotation and pure deformations. When it comes to small deformations, this multiplicative decomposition is replaced by additive decomposition. As $U$ is difficult to ascertain, $U^2$ is calculated. As $R$ is an orthogonal matrix,

$$R^T = R^{-1}. \qquad\qquad 3.9$$

Therefore,

$$R^T R = I \qquad\qquad 3.10$$

Where, $I$ is the identity matrix. Pre-multiplication of equation 3.8 results in

$$C = U^2 = F^T F. \qquad\qquad 3.11$$

In the equation 3.11, $C$ measures the pure deformation. This is called the Right Cauchy-Green tensor. Since $C$ reduced to unit matrix for the undeformed state, at the beginning, tensor shows 1's which is little confusing. Therefore, as to get away with this ambiguity, Green-Lagrange strain tensor $\gamma$ is defined in describing large strains and used often.

$$\gamma = \tfrac{1}{2}\left(C - I\right). \qquad\qquad 3.12$$

Considering the principle stretch ratios $\lambda_1, \lambda_2, \lambda_3$ respective principle axis 1, 2, and 3, the deformation gradient can be expressed as follows.

$$F = \begin{bmatrix} \lambda_1 & 0 & 0 \\ 0 & \lambda_2 & 0 \\ 0 & 0 & \lambda_3 \end{bmatrix} \qquad\qquad 3.13$$

By adopting the equation 3.13, it can be derived the normal stretch for $1^{st}$

$$C_{11} = \lambda_1^2 \qquad\qquad 3.14$$

direction followed by other two directions similar to that. In undeformed configuration stretch ratio is 1. Considering the equation 3.12, the normal component for the $\gamma$ can be given as follows. First, $\gamma_{11}$ as given in equation 3.15, and then similarly, the other two, $\gamma_{22}$, $\gamma_{33}$.

$$\gamma_{11} = \tfrac{1}{2}\left(\lambda_1^2 - 1\right), \qquad\qquad 3.15$$

After a brief introduction to mechanics of hyperelasticity, in order to relate the topic to the current research work, essential theory component of the work is described here.

The theory related to this work can be divided in to four major sub topics. First section would present a short introduction to some of the often used hyperelastic models. Section that proceeds covers the mathematics related to manipulation of curves. In the third section, statistical theory related to present work would be discussed. Least square method and tools used to compare the suitability of fit are elaborated under this section. Finally, metrological principles and application of Digital Image Correlation (DIC) in stress-strain measurements are briefly introduced.

## 3.6 Mathematical Models

The independence of stresses on previous deformation history and the reversibility of imposed deformations in elastic materials allow us to prove that constitutive relations for both linear and nonlinear elastic solids can be derived from a strain energy potential function. This argument is very similar to the path independent work done on a particle in a potential field where the forces can be derived from a differentiable potential function [16]. By this analogy, if stresses take the place of forces, a differentiable potential function must exists and it is a function only of the deformations. In such cases stresses can be expressed as,

$$\sigma_{ij} = \frac{dW(e)}{de_{ij}} \qquad\qquad 3.16$$

Where $\sigma_{ij}$ is true (Cauchy) stresses, $w(e)$ is potential strain energy density function (strain energy per unit volume), $e$ is any deformation measure (e.g., finite Eulerian strain tensor, stretches). Any material for which such a potential strain energy function exists is called a green-elastic or hyperelastic material.

When one needs to select a hyperelestic model for mechanical characterization of a particular elastomer, there is a large group of $w(e)$ forms to select one from. However, it is established that the selection of model depends on factors such as material application, corresponding variables and available data [8]. Four major qualities of good material model are identified [9]. It is stated that, ability to produce the '*s*' shape, good functionality in all deformation modes, less material parameters and simple form of the formula as key qualities of such model. Having discussed about these governing rules, some of the popular models often found in the hyperelestic research domain are examined.

Model development history

According to James et al. [29], there are two main approaches, namely molecular method where molecular response due to deformation is considered, and the phenomenological approach where modified elastic theory is used together with experimental data to get the characteristic. In this sub topic, the initiation and evolvement of characteristic curves are briefly examined.

Neo-Hookean model

This is the simplest of all hyperelastic models. The model depends on first invariant $I_1$. General form of model is given in equation 3.17.

$$W = C_1(I_1 - 3)$$
3.17

In the equation, $W$ is the strain energy density, $I_1$ is the first strain invariant and $C_1$ is the material constant. Usually Neo-Hookean model is used for applications with low strains compared to other models. According to M. Kamper, A. Bekker and others [46] it works best at around 50% strain limits. This model can be used when there are less amount of data available for fitting [9].

Mooney-Rivlin model

This is the most frequently used model from all. Mooney-Rivlin is a phenomenological type model. This model is applicable for moderate strains up to 300% [8]. The description of the model can be given as below.

$$W = \sum_{i+j=1}^{N} C_{i,j}(I_1 - 3)^i(I_2 - 3)^j + D(J - 1)^2$$
3.18

In the strain energy density function, $I_1$, $I_2$ are first and second invariants while $D$, $C_{i,j}$ are material constants and $J$ is elastic volume ratio. Depending on $i$, $j$ and $N$, for the function can have multiple terms. However, Mooney-Rivlin function is so far used with up to maximum nine terms. Neglecting compressibility, consecutive three forms of the model can be written as follows (Eq. 3.19-3.21).

$$W = C_{10}(I_1 - 3) + C_{01}(I_2 - 3)$$
3.19

$$W = C_{10}(I_1 - 3) + C_{01}(I_2 - 3) + C_{11}(I_1 - 3)(I_2 - 3)$$
$$\qquad 3.20$$

$$W = C_{10}(I_1 - 3) + C_{01}(I_2 - 3) + C_{11}(I_1 - 3)(I_2 - 3) + C_{20}(I_1 - 3)^2 + C_{02}(I_2 - 3)^2$$
$$\qquad 3.21$$

Ogden model

This is a unique type of strain energy density function which expresses in terms of stretch ratios instead of strain invariants. The model is first introduced by Ogden in 1972 and is accurate over a large range of strains [47]. The general form of the model is given below (Eq. 3.22).

$$W = \sum_{i=1}^{N} \frac{2\mu}{\alpha_i^2} \left( \lambda_1^{\alpha i} + \lambda_2^{\alpha i} + \lambda_3^{\alpha i} - 3 \right) + \sum_{i=1}^{N} \frac{1}{D_i} (J - 1)^{2i}$$
$$\qquad 3.22$$

$\lambda_1$, $\lambda_2$, $\lambda_3$ are stretch ratios and $\mu$, $\alpha$, and $D$, are material constants.

Yeoh model

This model was first introduced in 1993. The model is based on first invariant only. According to Shahzad et al. [9], the Yeoh model is good for carbon black filled rubber characterization. Furthermore, according to them, the model is applicable over a large range of strains. The model can be described as follows (Eq. 3.23).

$$W = \sum_{i=1}^{N} C_{i0}(I_1 - 3)^i + \sum_{i=1}^{N} \frac{1}{D_i}(J - 1)^{2i}$$
$$\qquad 3.23$$

Arruda-Boyce model

The Arruda-Boyce model was introduced in 1993. The model is based on molecular chain network and depend only on first strain invariant (Eq. 3.24). Model function well with limited test data [9].

$$W = \mu \sum_{i=1}^{N} \frac{C_i}{\lambda_L^{2i-2}} \left( I_1^i - 3^i \right) + \frac{1}{D} \left( \frac{J^2 - 1}{2} - \ln J \right)$$
$$\qquad 3.24$$

In the equation, $C_i$ and $\lambda_L$ are material constants. The Initial shear module is given as $\mu$ and $J$ is the determinant of strain gradient tensor $F$. $D$ is a material constant.

Some other frequently used models

Apart from models discussed, there are few other models recurrently find in the hyperelestic material research area. Among them, the Gent and Thomas model, Humphrey-Yin model, Haines-Wilson model, Rivlin and Saunders model, the Hart-Smith and the Isihara are prominent.

## 3.7 Curve Theory

The main task of this work is to obtain a data set which matches a distribution similar to the typical biaxial data dispersion. Uniaxial data set is used to obtain this biaxial data dispersion. Therefore, in order to get a one dispersion from the other, it is vital to study mathematical options available for this task.

Generally, hyperelastic models are following some rules. Therefore, in order to generate artificial set of data that matches real data dispersion, it is important to understand these basic facts. Firstly, all hyperelastic curves start from origin. Secondly, the basic shape of curve resembles a stretched *s*. On the other hand, according to Kumar et al. [8], the curve changes its trajectory at every inflection point. Referring Moony-Rivlin model, they went on to say that, the number of such points depend on the number of terms in the model.

Power functions

Power function is a function that gives a specific shaped curve in the x-y domain. Referring equation 3.25, it can be noticed that there is a factor n, which decide the final shape the power curve.

$$y = x^n \qquad\qquad 3.25$$

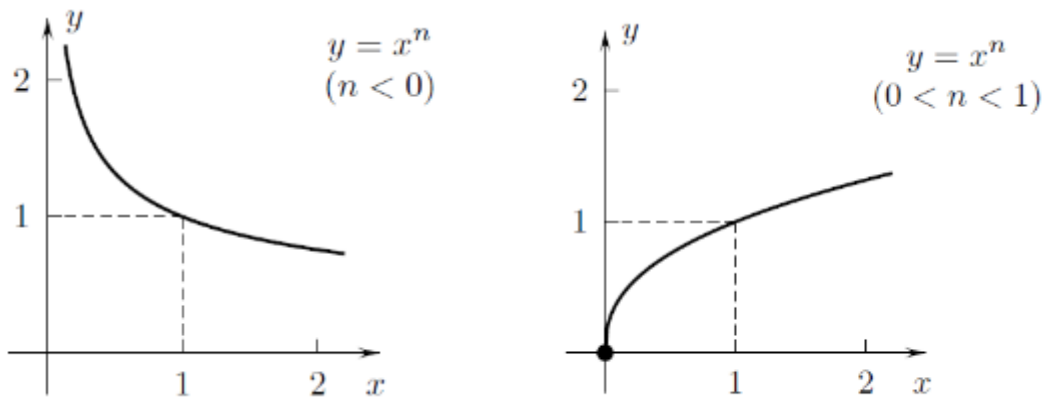Its influence on shape can be demonstrated from figure 3.13.



**Fig. 3.13 (a & b)** Power function configuration [48]

As it can be evident from two graphs, at the origin, first one lead to an asymptote while the second lead to zero.

Exponential functions

The exponential function in its general form is given in equation 3.26.

$$y = b^x \hspace{6cm} 3.26$$

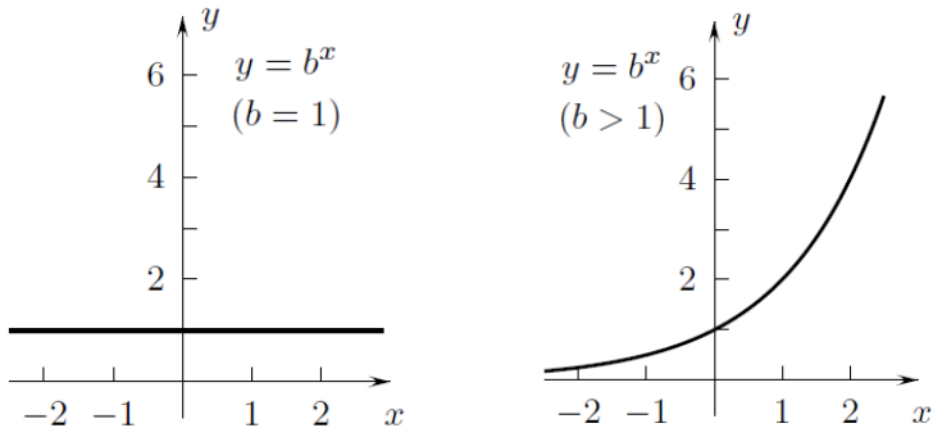By varying factor $b$, shape of the function can be changed (Fig. 3.14).



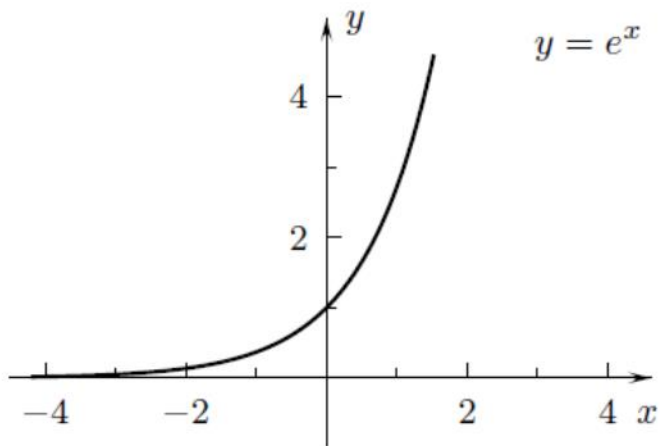**Fig. 3.14 (a & b)** Exponential function configurations [48]



**Fig. 3.15** Natural exponential function [48]

The natural exponential function

The natural exponential function (Eq. 3.27) is a special case of exponential function. The general shape appear to be similar to graph given in figure 3.15.

$$y = e^x \qquad\qquad\qquad 3.27$$

Here, $e$ is taking the value of 2.718.

Transition of curves

If a function f(x) needs to be moved up, down, left or right, it can be done with a use of positive number $k$ as given figure below (Fig. 3.16).
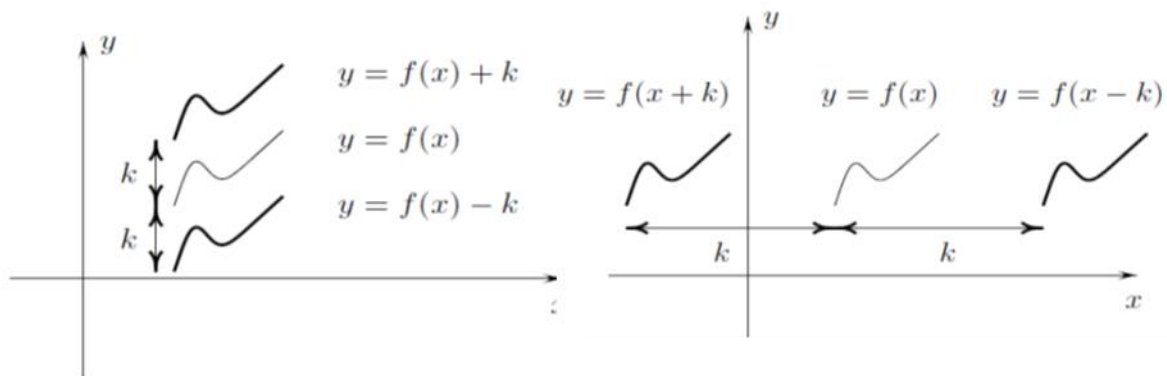


**Fig. 3.16 (a & b)** Transition of curves [48]

Enlargement and contraction

If a function $y = f(x)$ is multiplied by a constant $k$ with different values, the resultant graphs with respect to initial curve could be given as in figure 3.17. This operation could be used to magnify or contract a graph. In the left set of curves, distortion is more compared to the right set of graphs.
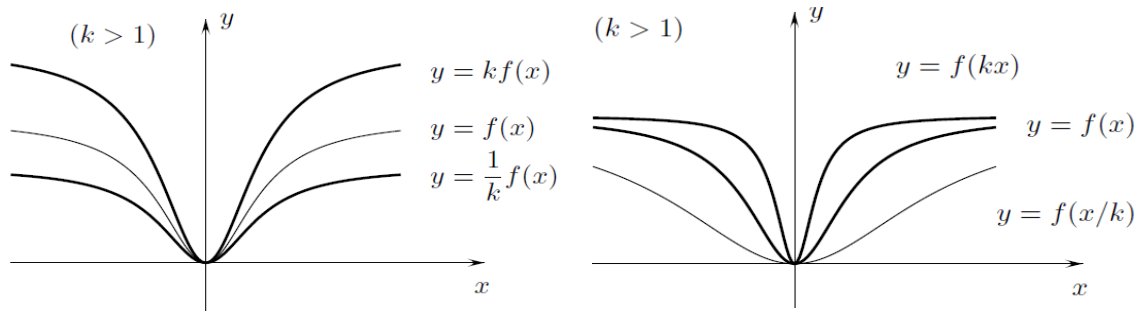
**Fig. 3.17 (a & b)** The enlargement and contraction of curve [48]

Reflection

In order to get a reflection of a graph, function or the variable should be multiplied by minus one (-1). Resulting shifts of graphs of f(x) are given in figure 3.18.
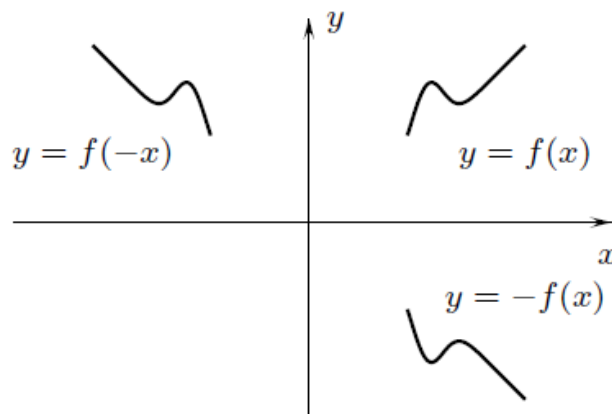


**Fig. 3.18** Reflection of a curve [48]

## 3.8  Statistical Tools

Statistical tools are normally used to evaluate raw data obtained through laboratory experiments to get a meaningful results for further analysis. In this particular case, data obtained through three basic tests are fitted in to a predetermined model using non-linear regression technique. Furthermore, such statistical tools are used in order to evaluate the fitting results. That is to examine

how good a certain model fits related to the set of data provided. Therefore, it is intend to elaborate the data fitting and analysis of best fit in this section.

Non-linear regression

As rubber like materials behave nonlinearly under large strains, in order to get the correct representation of it in the graphical domain, models should be described in polynomial form. The data extracted through laboratory tests could be fitted with these models to obtain the correct behaviour subsequently. Therefore, it is appropriate to describe the polynomial regression theory to elaborate the process [49]. As an example, for the demonstration purpose, a second order polynomial is considered as given in equation 3.28.

$$y = a_0 + a_1 x + a_2 x^2 + e$$

3.28

By considering data fitting to this equation with $n$ number of data points, the sum of squares of the residuals is given by equation 3.29.

$$S_r = \sum_{i=1}^{n} \left( y_i - a_0 - a_1 x_i - a_2 x_i^2 \right)^2$$

3.29

In order to generate the least squares fit, derivatives of above equation with respect to each unknown coefficient of the polynomial can be obtain as the first step. (Eq. 3.30-Eq. 3.32)

$$\frac{\partial S_r}{\partial a_0} = -2\sum \left( y_i - a_0 - a_1 x_i - a_2 x_i^2 \right)$$

3.30

$$\frac{\partial S_r}{\partial a_1} = -2\sum x_i \left( y_i - a_0 - a_1 x_i - a_2 x_i^2 \right)$$

3.31

$$\frac{\partial S_r}{\partial a_2} = -2\sum x_i^2 \left( y_i - a_0 - a_1 x_i - a_2 x_i^2 \right)$$

3.32

These equations can be set to zero and resultant group of equations are as follows. (Eq. 3.33- Eq. 3.35)

$$(n) a_0 + \left( \sum x_i \right) a_1 + \left( \sum x_i^2 \right) a_2 = \sum y_i$$

3.33

$$\left( \sum x_i \right) a_0 + \left( \sum x_i^2 \right) a_1 + \left( \sum x_i^3 \right) a_2 = \sum x_i y_i$$

3.34

$$\left( \sum x_i^2 \right) a_0 + \left( \sum x_i^3 \right) a_1 + \left( \sum x_i^4 \right) a_2 = \sum x_i^2 y_i$$

3.35

In these equations, $i$ takes values from 1 to $n$. When further examine above set of equations, one can see that they are all linear equations with finite number of

unknowns. In this particular case, it is three, namely, $a_1$, $a_2$, $a_3$. Hence, with known experimental data, these unknown can be calculated. If this second order form extend in order to accommodate $m^{th}$ order polynomial, the basic equation would look like as given in equation 3.36 below.

$$y = a_0 + a_1 x + a_2 x^2 + \ldots a_m x^m + e$$

3.36

Considering the previous case, it can be seen that unknown coefficients of general case also can be obtained by solving $(m+1)$ no of simultaneous linear equations. For the generalized case, the standard error is given by equation 3.37.

$$S_{y/x} = \sqrt{\frac{S_r}{n - (m+1)}}$$

3.37

## 3.9  Metrology and Theory of Digital Image Correlation (DIC)

Metrology is one major corner stone of any research.  It provides the data required for evaluation part to the research work. For hyperelestic material characterization, this involves in basically results of three tests. Namely these tests are, uniaxial, biaxial and pure shear.

These three tests are different from one another due to the method of application of force. However, in each of these tests, it is used to measure force and displacement. Consequently, stress and strain are calculated according to basic definitions. Final results are then presented as graphs of stress vs strain. However, correct calculation of stresses and strains depend on the accuracy of aforesaid test measurements. Altogether, mechanical characterization demands high accuracies related to basic measurements of force and length. Not only that, sometimes these measurements should be done in three dimensional space. For example, such is the case with bubble test related to the biaxial deformation. Unfortunately, some of conventional test methods so far used in mechanical characterization are neither standardized nor accurate. Therefore, when the measuring system demands such high norms, Digital Image Correlation technique or DIC technique as it is commonly known, is one good option. Hence, for the present research work, the DIC measuring technique is used in biaxial testing extensively. Therefore, it is important at this stage to get familiar with the basic theory behind the Digital Image Correlation measuring method. There are many ways of using this technique. However, the theory involved is the same.

An Introduction to DIC

Digital Image Correlation is a non-contact optical strain measuring technique. The measuring system comes complete with a digital camera, zoom objective
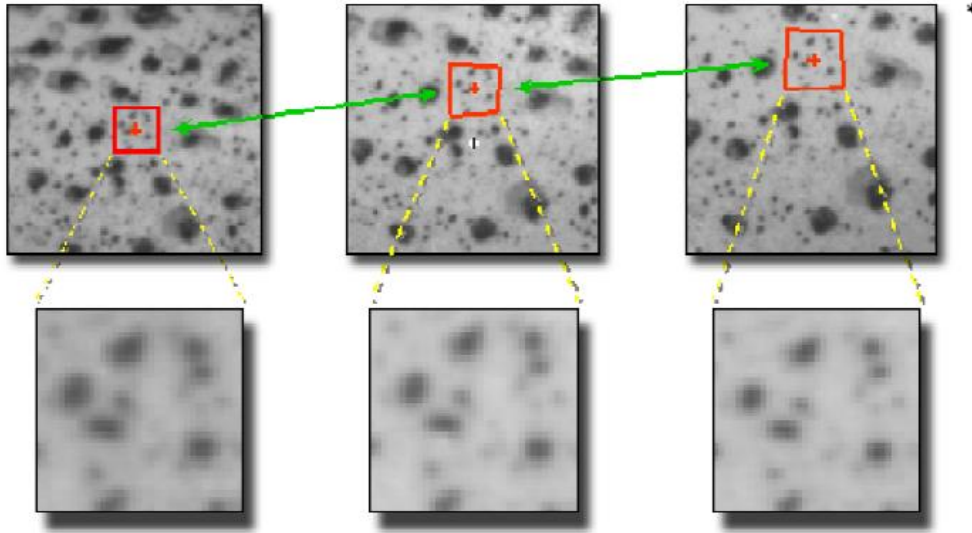


**Fig. 3.19** Migration of subset due to deformation

and PC software. It can accommodate more than one camera depending on the accuracy and the type of analysis. Literally, there are two major types of analysis related to the DIC namely, 2-D and stereo DIC.

In DIC, a shift in image pixel position is tracked through series of images when deformation is taking place due to the applied load on specimen during the test (Fig. 3.19).

For the evaluation of displacement, a correlation algorithm is applied through a software tool. Deformation of image is mapped through Cartesian coordinate system as depicted in figure 3.20. Highly optimized input parameters provide very accurate results [50].
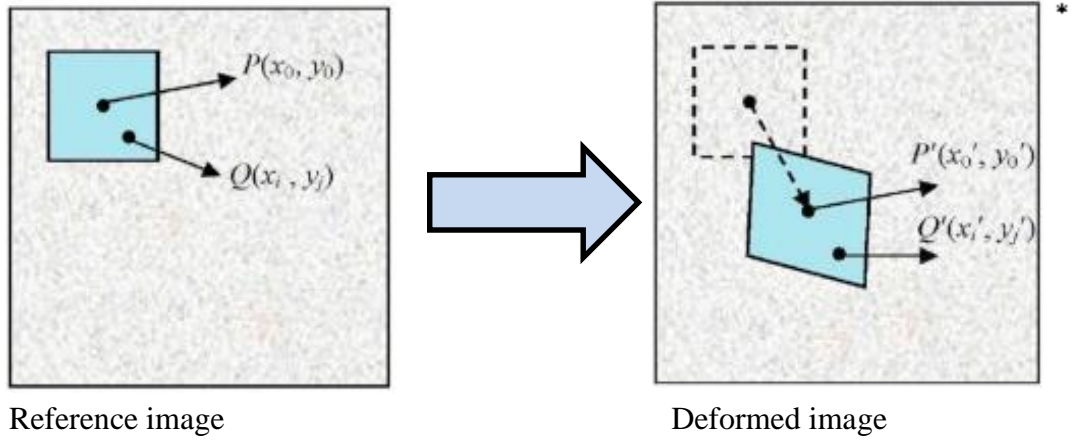
**Fig. 3.20** Mapping of deformation through coordinate system

## 4. MATERIALS AND METHODS

### 4.1 Laboratory Experiments

In order to gather uniaxial, biaxial and pure shear stress-strain data, there are three different experiments often done. They are named, uniaxial, eqi-biaxial and pure shear tests, according to their respective load applications. These experiments are done in several different configurations as we observed during the literature survey. However, in each of these cases basic idea behind the load application was followed in order to get the intended data set. By following these footsteps, we used the universal testing machine to collect uniaxial data while eqi-biaxial data were collected through a bubble test. Throughout these tests consistency was maintained as to collect unbiased data sets. Aforesaid experiments are described in detail below.

Uniaxial testing

Uniaxial test is the easiest form of test from three experiments mentioned. This is a standard test. The method is described in detail under ASTM D412 or ISO 37 : 2017. [11]
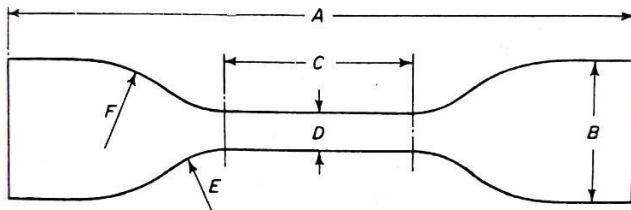


a.

b.

**Fig. 4.1** Uniaxial test: a. Standard sample b. Test apparatus

Initially, as a preparation for the test, several standard test pieces were cut from the uniformly thick sample material sheets according to the guide lines given in the said standard, which is used to explain the rubber general procedures for preparing and conditioning of test pieces for physical testing methods. From the specifications, type 1 dumbbell specimen was selected. Referring the figure 4.1 specimen dimensions could be given as below (Table 4.1).

**Table 4.1** Sample measurements

| Dimension (all measurements are in mm's.) | Type 1 |
|---|---|
| A – Overall length (min) | 115 |
| B – Width of ends | 25±1.0 |
| C – Length of narrow portion | 33±2 |
| D – Width of narrow portion | 6+0.4/-0 |
| E – Transition radius outside | 14±1 |
| F – Transition radius inside | 25±2 |
| Gauge length | 25±0.5 |

Test pieces were then mounted one at a time between two jaws of the standard tensile testing apparatus configured from the universal testing machine. According to ISO 37, standard grip separation rate is given as 500 mm/min.

After placement of specimen between jaws, uniaxial loading was applied continuously while tension and the elongation were recorded. Process was continued until the test sample gets failed. Results were obtained at equal time durations and were then recorded as engineering stress and engineering strain. Unit for the stress was taken as Mega Pascal (MPa) while strain was recorded as a percentage of initial length.

 Eqi-biaxial testing

Use of inflated rubber membrane for testing uniaxial tension has a long history. It was first introduced by Treolar in 1944.

Ever since, the method was frequently used by scientists in order to test rubber in biaxial tension [9, 11-12]. However, this method is not standardized and few variations could be observed [51-55]. Despite these variations, the basic elements of the test are the same for most of these cases. Essential principles of the bubble test performed is described in figure 4.2.

First, a uniform thin circular specimen was prepared from the test material. Then, the centre line and two parallel lines, each 5 mm apart to it were marked with white marker as given in figure 4.2 a. Thereafter, white paint was sprayed on the test piece as to get a speckle pattern near the marks. Then, it is held between two metal rings (jaws) of the apparatus. Subsequently, a flow of pressurised air is introduced into the chamber which is created by top wall of the specimen and the bottom part of ring assembly. With the increasing pressure, the volume inside the chamber is being enlarged while pushing the specimen membrane outward as given in figure 4.2.b. Due to this phenomenon, the rubber membrane takes a form of dome or bubble and theoretically, the topmost point of the bubble or the pole undergoes eqi-biaxial tension.
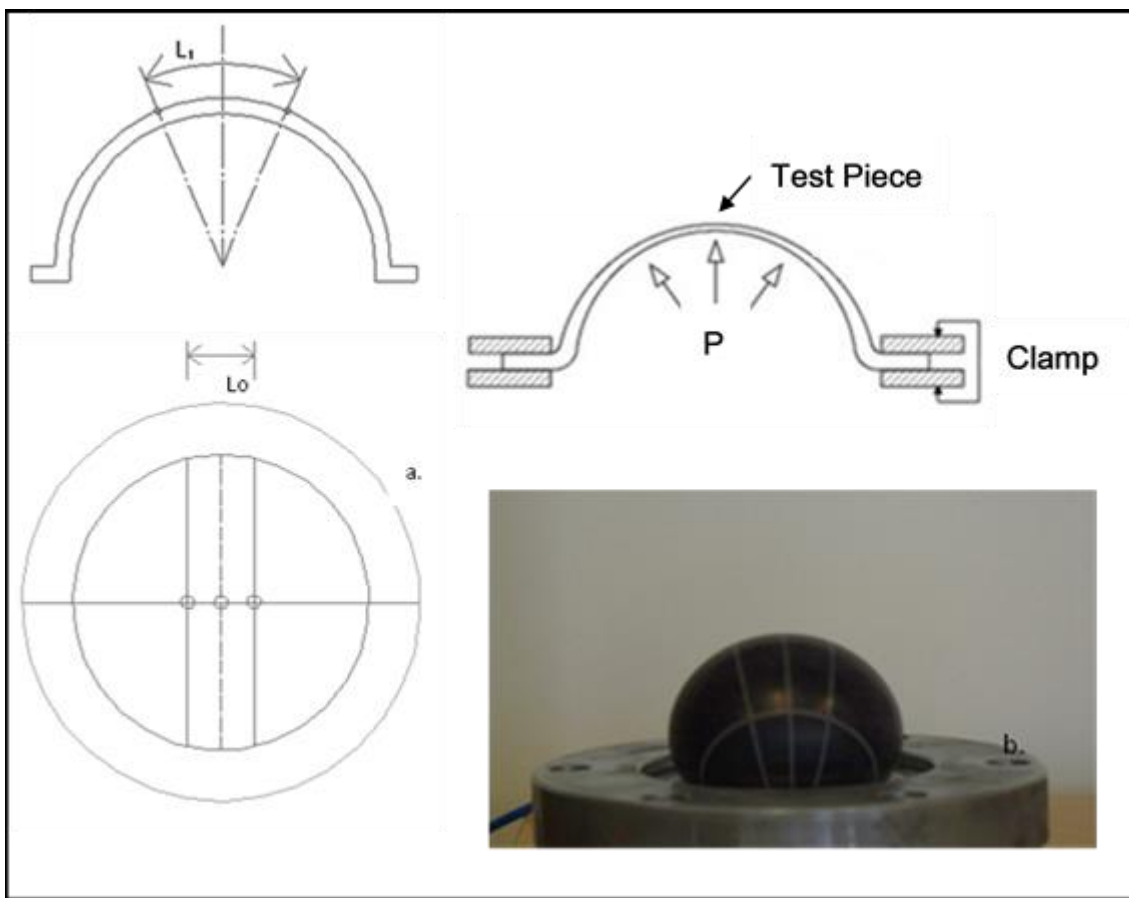


**Fig. 4.2** Biaxial test:  a. Standard sample   b. Test apparatus

During the experiment, two digital cameras were used to track down cross hairs corresponding to the marks and DIC technique was used to measure the bubble deformation. The calculation of the stress could be done as given below.

36

The stretch ratio lambda ($\lambda$) is calculated by comparing the length of curvature between marked positions ($l_1$) in each image with the undeformed specimen length ($lo$) corresponding to these points.

$$\lambda = l_1/lo \qquad\qquad\qquad 4.1$$

Considering material incompressibility hoop stress at the pole of the bubble ($\sigma_{\theta\theta}$) can be expressed as follows [56-58].

$$\sigma_{\theta\theta} = pr\lambda_{\theta\theta}^2/(2t_0) \qquad\qquad\qquad 4.2$$

In the equation 4.2, $p$ is the applied pressure, $t_o$ is the initial thickness of the specimen, $r$ is the radius of curvature and $\lambda_{\theta\theta}$ is the stretch ratio at the pole.

Pure shear testing

Theoretically the planar or pure shear experiment must be done with rectangle sample in which one dimension is constrained or restricted against deformation. In order to achieve this, the specimen dimensions are selected in such a way that deformation of one side could be neglected (bringing in to nearly zero value) compared to the deformation of the other side. Uniformly thick 240x24x2 mm rectangular rubber sample specimen was selected as a test piece here. Specimen thus prepared was then marked with a centre line across the larger dimension. Subsequently, along the centre line, two cross hair marks (20 mm apart) were inked, just for the tracking of the deformation.

After selection of specimen, the universal testing machine is used for pure shear tests too. Similar to uniaxial testing, while the load is gradually applied, tension and elongation were recorded at several positions and stress and the strain were thereby calculated.

## 4.2 Collection and Refinement of Raw Data

The data obtained through above mentioned tests, need to be refined as to produce a useable set of data for the fitting. Fifty to hundred data points are sufficient for a reasonable good fit [59]. There are often some erroneous minus points which should be eliminated. These adjustments could be done using a typical data editing program such as MS Excel or MATLAB [60-65]. Once, raw data is refined, it is then ready to be fitted in to the pre-determined model.

## 4.3 Fitting of Data

Once data is refined, next step of the process is to fit the data in to an appropriate model. As already discussed, there are many models to select from. The fitting could be done using a statistical software. Most finite element programs are also provided with some of the key models [66-68]. Single data set or multiple sets could be tried with several models and results could be compared. Comparison could be done by, a visual inspection of trajectory, suitability of fit

and values of material constants. By varying material constituents and proportions these trials could be repeated for all the selected models.

## 4.4 Materials Used in Experiments

The Styrene-Butadiene Rubber (SBR) commonly used in the tyre manufacturing industry was used as testing material during initial trials. For all experiments, specimens were taken from the same rubber sheet which is prepared under uniform process conditions.

Final experiments were done with six different materials, of which, properties are given in the table 4.2.

**Table 4.2** Material data for final tests

| Material Label | Shore A Hardness | Phr | Rubber Base |
|----------------|------------------|-----|-------------|
| M1 | 50 | 50 | NR,CIIR |
| M2 | 57 | 64 | NR,BR,SBR |
| M3 | 69 | 60 | NR |
| M4 | 86 | 65 | NR, BR |
| M5 | 78 | 84 | NR, SBR |
| M6 | 64 | 54 | NR,BR |

Phr - (parts of carbon black (and other additives) per hundred parts of rubber)

# 5. RESULTS

This chapter presents the results of experiments carried out during the full stretch of the work.  Apart from final set of experiments, five other experiments were done related to this work. These initial experiments were done using the data previously obtained. At the end, final experiments were done in order to test the proposed solution and reach ultimate objectives of the research.

At the very beginning, a scientific query of the problem was done. Initial solution for the problem was proposed through the experiment that followed it. In the third experiment, an additional improvement was done to the answer given in the second. While searching for a answer, certain intermediate queries came related to the Mooney material model and two of these experiments are allocated to such examinations. Therefore, results of these experiments are excluded from the final reporting.

## 5.1  Presentation of Problem (Experiment -1)

As a starting point to the research work, the risk of using only single data set, i.e. uniaxial data for fitting, in general to most hyperelastic material models, and in particular to Mooney-Rivlin model was established with scientific evidence. In this effort, a detailed comparison was done related to Mooney-Rivlin two, parameters, Mooney-Rivlin three parameters and Yeoh models.

Figure 5.1 to - figure 5.3 show resultant curves obtained for this analysis. From two graphs given in each figure, first graph (Fig. 5.1.a, 5.2.a, 5.3.a,) shows only uniaxial data fitted curves (O.U.) while second set (Fig. 5.1.b,5.2.b, 5.3.b,)  gives uniaxial, biaxial and pure shear combined data fitted (C.U.S) resultant curves. Two curves in each graph are identified as uniaxial, biaxial. Three data sets also plotted in the same graph as to visually inspect the results.
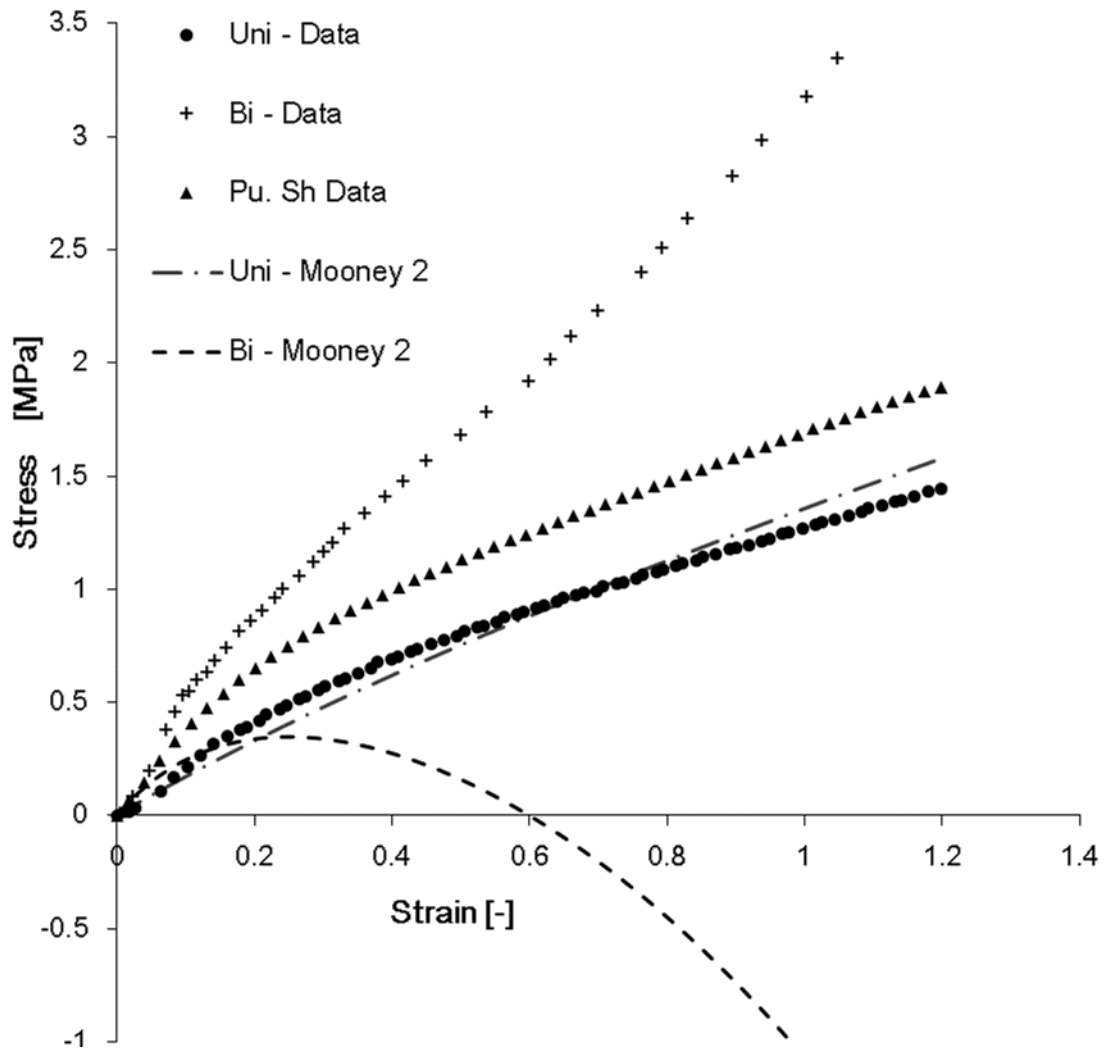
**Fig. 5.1. a** Mooney two parameter model comparison (Only uniaxial data fit).
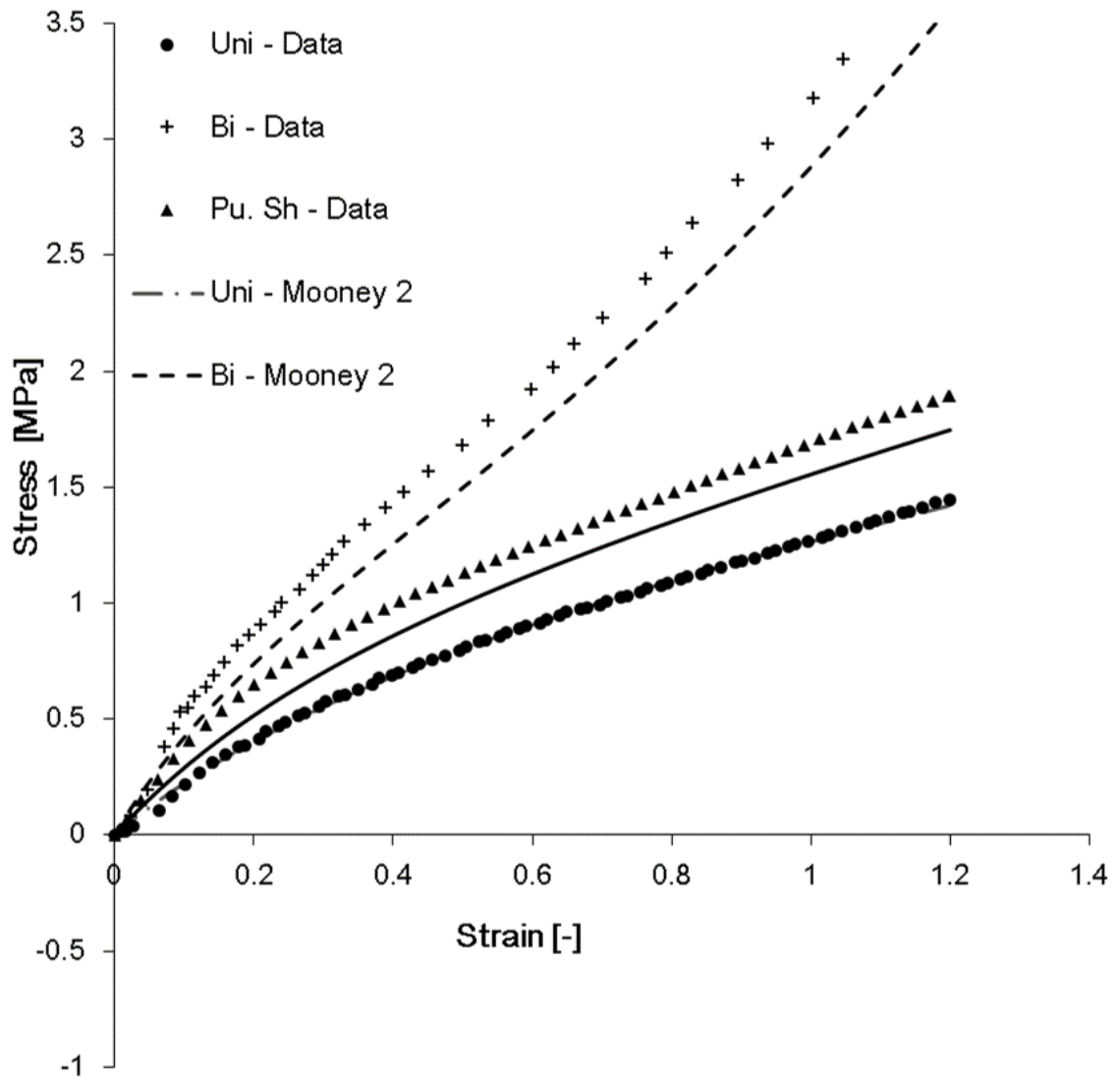
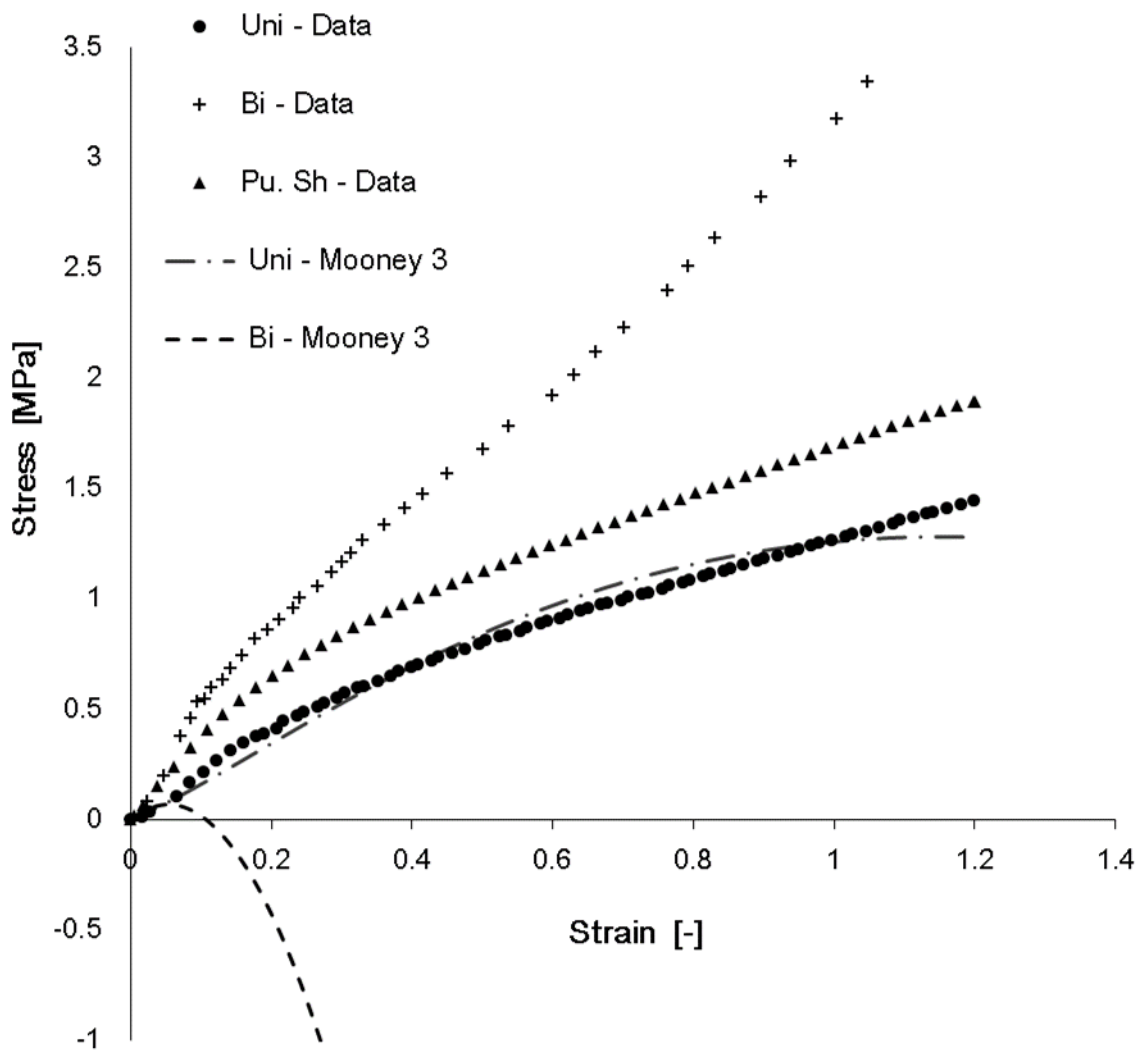**Fig. 5.1. b** Mooney two parameter model comparison (Combined data fit).

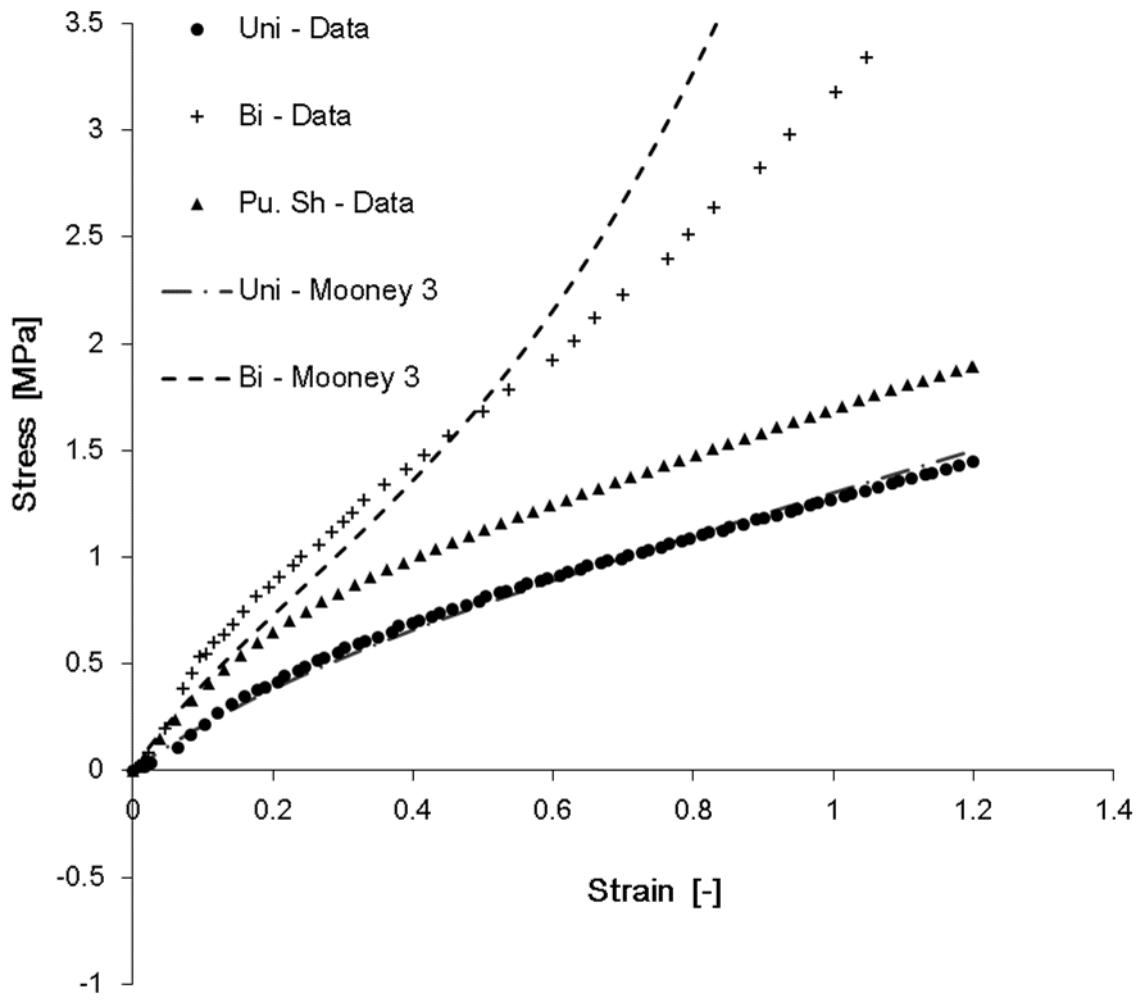**Fig. 5.2.a** Mooney three parameter model comparison (Only uniaxial data fit).

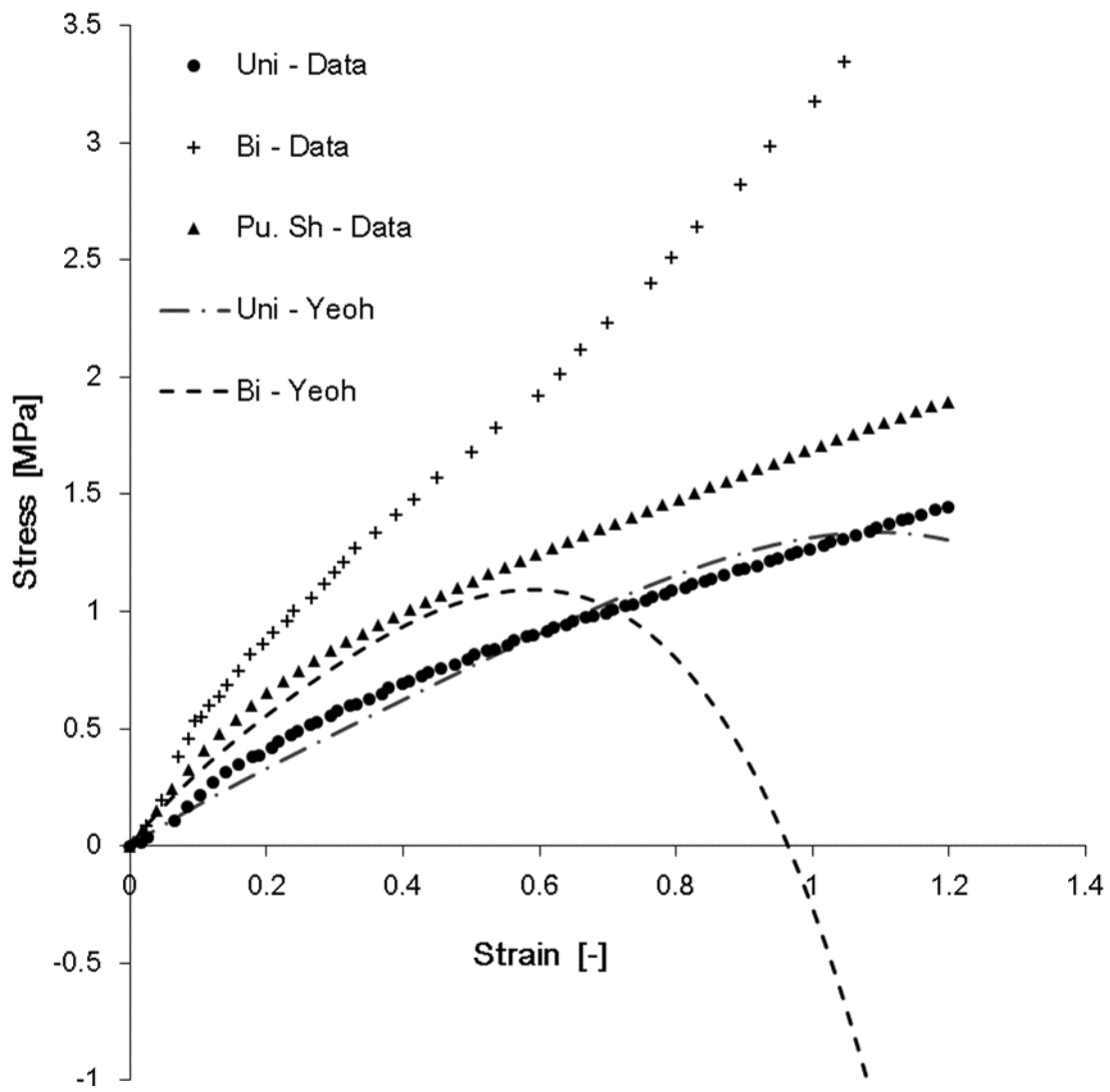**Fig. 5.2.b** Mooney three parameter model comparison (Combined data fit).

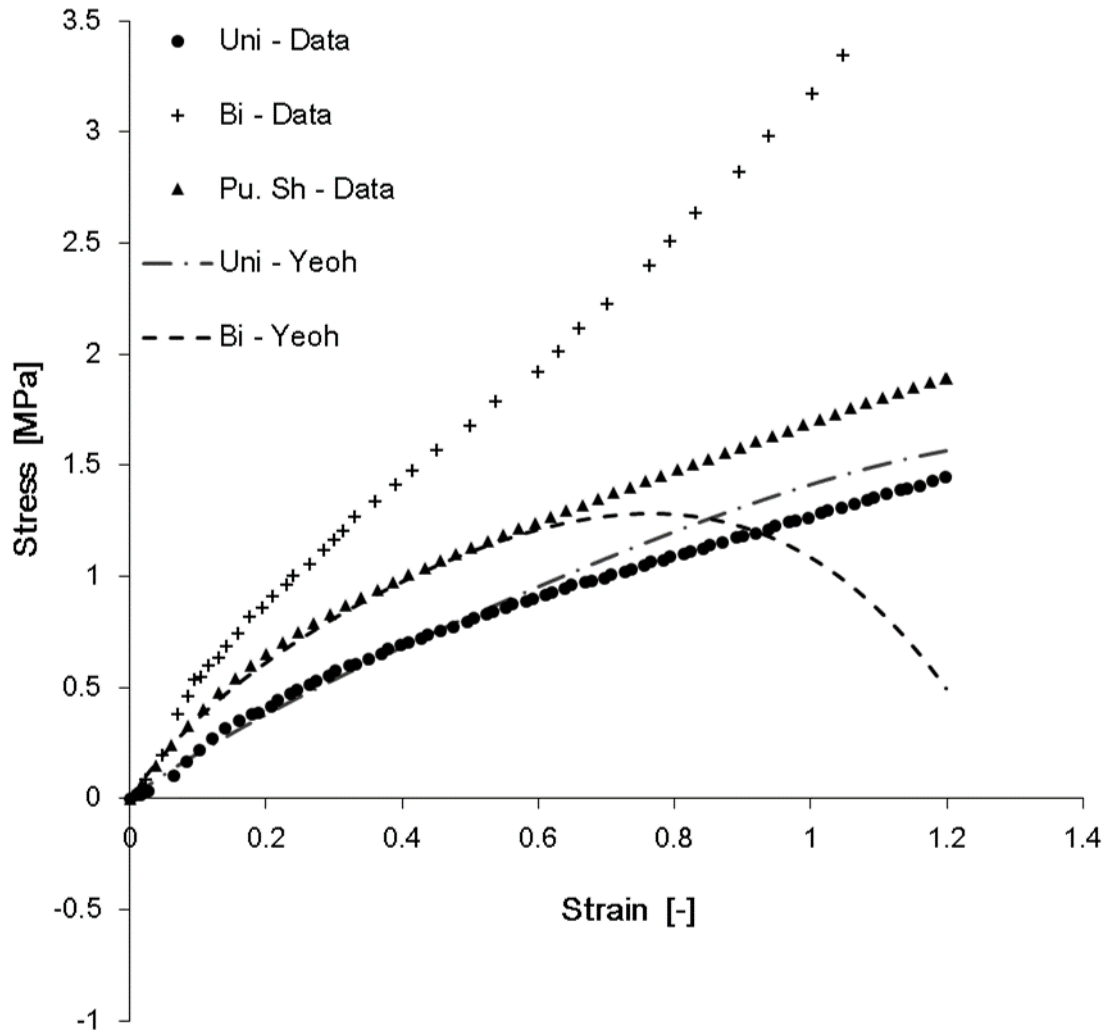**Fig. 5.3.a** Yeoh model comparison (Only uniaxial data fit).

**Fig. 5.3.b** Yeoh model comparison (Combined data fit)

## 5.2 Initial Attempt in Solving the Problem (Experiment -2)

It was proven from first experiment that one data set used alone in data fitting, is not sufficient to obtain accurate results for material constants and thereby, for the mechanical characterization of rubber like materials. Hence, the question that follows is, how to get an additional data set whenever uniaxial data is available.

The status quo of the problem is as such, an effort was exerted in order to address the problem and several attempts were made to get a feasible solution to it. At this stage, a second experiment was done related to the topic and results of the experiment are presented here.

In this experiment, a set of stress-strain data was collected using uniaxial tension upon SBR rubber samples and it was then manipulated using a simple mathematical formula to get a hypothetical second data set. The data set thus generated consequently used in place of missing biaxial data for combined data fitting. The results obtained for the experiment were evaluated first, with the real biaxial data and, then with data fitted curves for three models mentioned.

The equation used to obtained hypothetical data is a simple exponential curve function. It is given in equation 5.1. The general dispersion of actual biaxial data takes a shape of inverted S. This was considered when selecting exponential curve for generation of data.

$$y_b = e^{a y_u}$$

5.1

In the formula given in equation 5.1, $y_b$ is the generated biaxial stress while $y_u$ is the corresponding uniaxial stress. A factor '$a$' is included and it is tested initially with three values 0.6, 0.7 and 0.8. Strain is considered as same for both cases. Once the most suitable data set is selected from these three different data sets, combined data fitting was done together with uniaxial data. Results were obtained in the way of three curves, uniaxial, biaxial and pure shear.

For the initial comparison, three generated biaxial data sets related to 0.6, 0.7 and 0.8, were plotted alongside real biaxial data set (Fig. 5.4). After a close visual inspection, data set that resembles most to the original data set was selected.
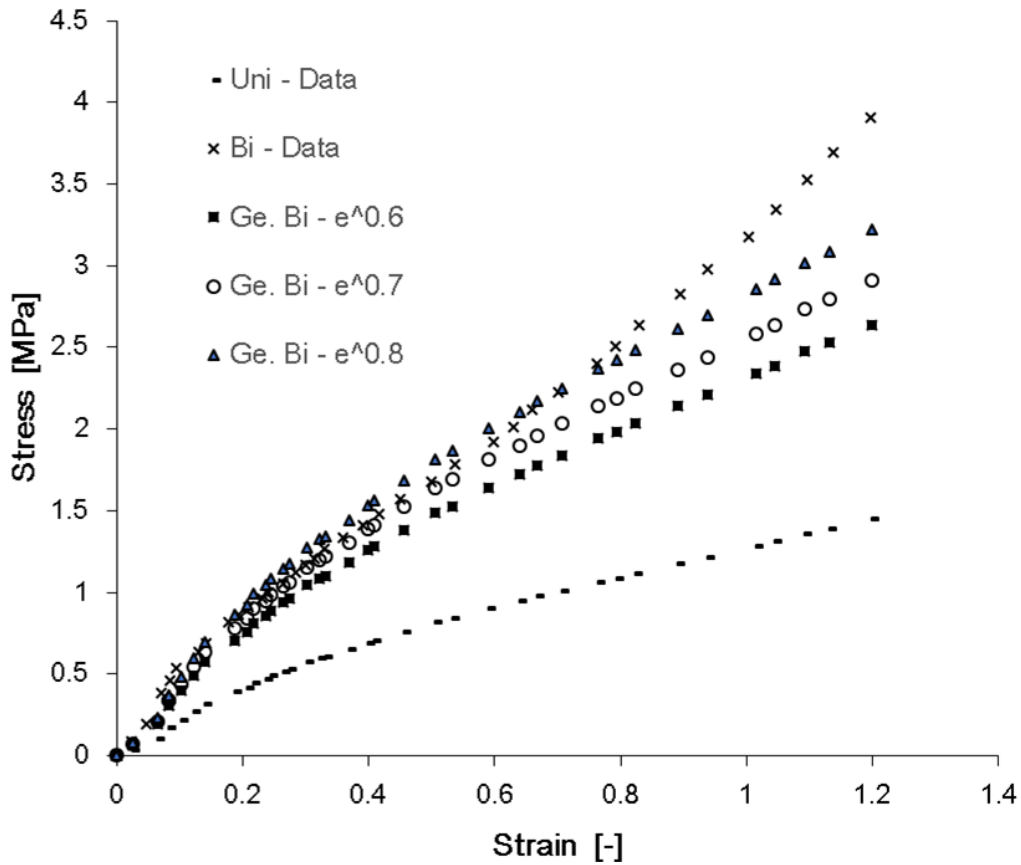
**Fig. 5.4** Comparison of generated biaxial data

The results of the data fitting part of the experiment is given in figure 5.5. The model used here was the Mooney two parameter model. In order to ascertain the improvement due to newly adopted method, a comparison was done between combine data fitting which utilized the data of uniaxial and newly generated biaxial and single data set fitting, i.e. uniaxial data, of results previously given in figure 5.1 (a). In order to ascertain the improvement, apart from simple visual inspection, a detailed statistical analysis also was done. In this analysis, two different data fitting cases, only uniaxial fitting and combined fitting were compared related to residue error. The main purpose was to examine the closeness of curves to each other in each of these cases. Calculated residue values are given in table 5.1.
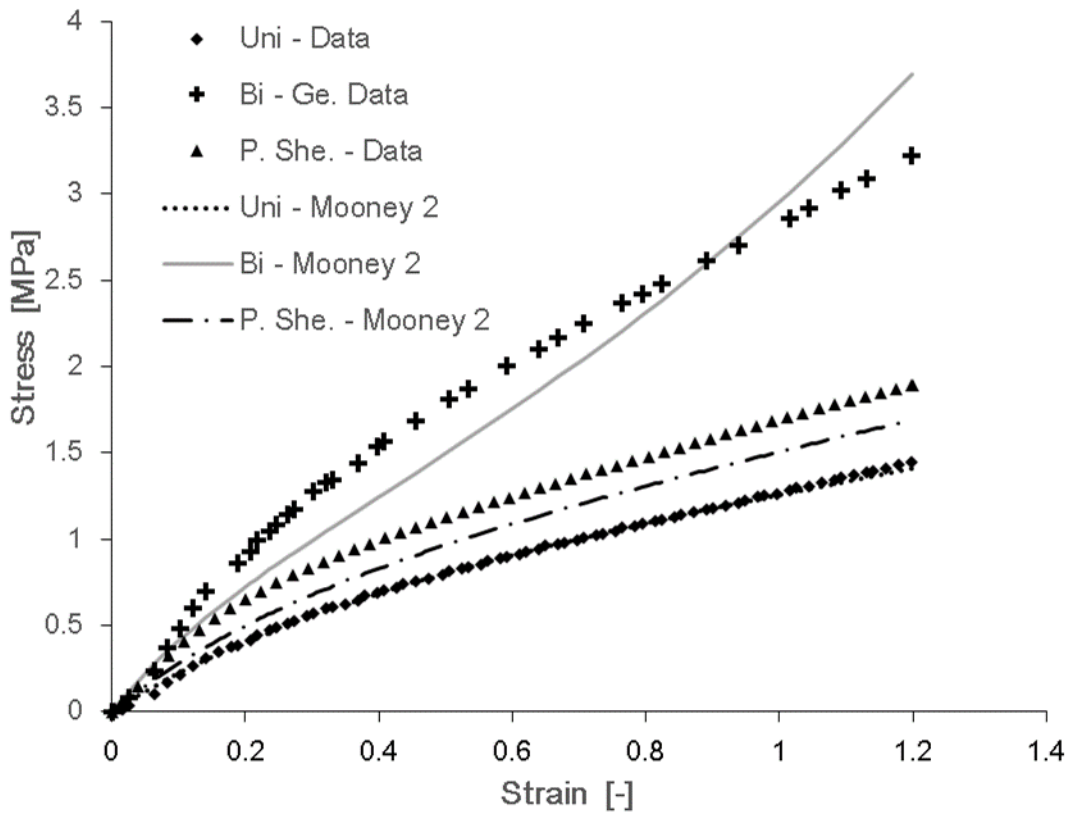
**Fig. 5.5** Data fitting with combined data (Ex. uni. +Gen. Bi.)

**Table 5.1.** Residue Error values for two cases.

| Curve type | R.S.S. for only uniaxial data fitting (Fig. 5.1 (a) | R.S.S. for combined data fitting (Exp. uniaxial and gen. biaxial data) (Fig. 5.5) |
|---|---|---|
| Uniaxial | 1.7155 | 3.1275 |
| Biaxial | 32.025 | 1.1595 |
| Pure shear | 8.2099 | 1.6638 |
| Sum | 41.9504 | 5.9508 |

## 5.3  An Improvement to the Initial Solution ((Experiment -3)

Since there had been some discrepancies in the generated data set compared to real biaxial data in the previous experiment, further refinement of formula was needed. In order to improve results, some changes were done. The method which was adopted for the refinement of data is briefly given here.

As trajectory of the uniaxial data curve changes from the inflection point, current data distribution was divided in to two parts from that point. In the case at hand, it seems that inflection point lies at 0.6 in the strain scale. Therefore, having separated the uniaxial data set in to two segments, they were treated separately with two different formulas. With the use of two new equations, the biaxial stress data was generated. Two formulas used for the purpose is given in equations 5.2 and 5.3.

For X<0.6,  $$Y_b = e^{0.7} \times y_u$$  5.2

For X> or = 0.6,  $$Y_b = y_{u=0.6} + e^{2 \times (x_u - 0.6)}$$  5.3

The data set obtained through the method then plotted in a graph alongside real biaxial and uniaxial data in order to examine the compatibility (Fig. 5.6). Furthermore, data fitting was done separately with four different models as to investigate the success of the method.

The Models considered here were Mooney 2, Mooney 3, Yeoh, and Ogden. Figures 5.7 to 5.10 give results of this comparison. Both data sets, experimental biaxial data and generated biaxial data are separately fitted and respective curves were plotted in each model graph, so that a comparison could be done easily. Uniaxial, Biaxial and pure shear curves are named in these graphs as U, B and P respectively.
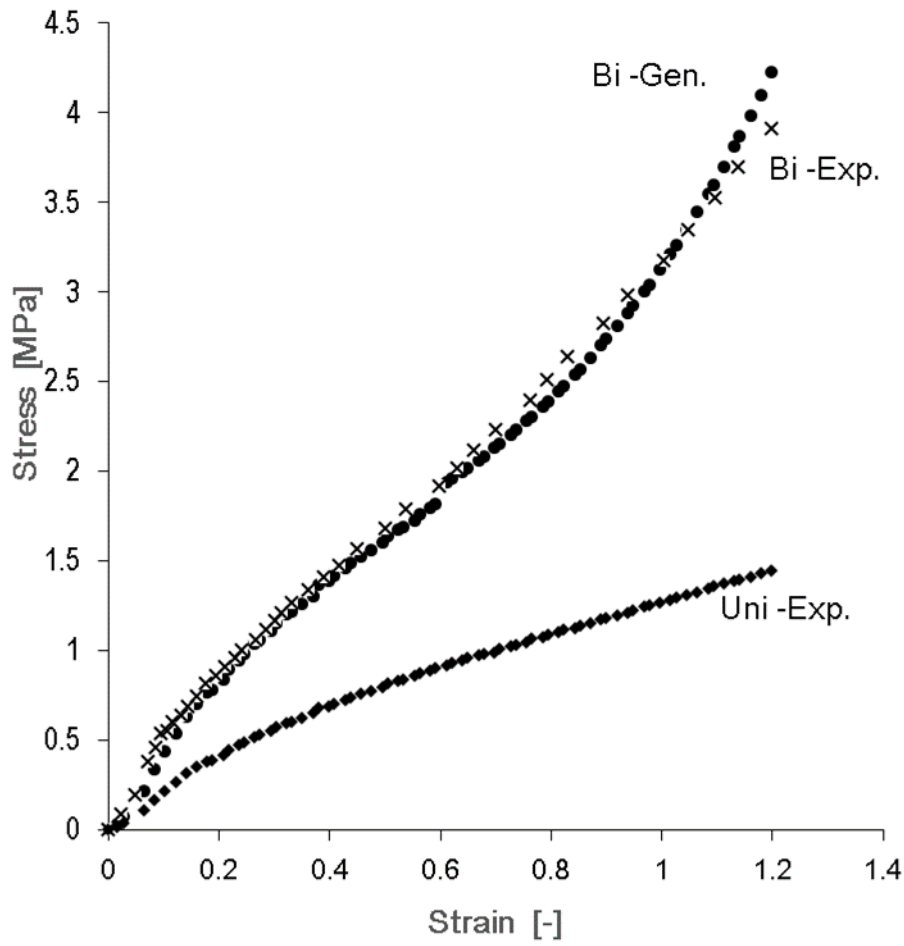
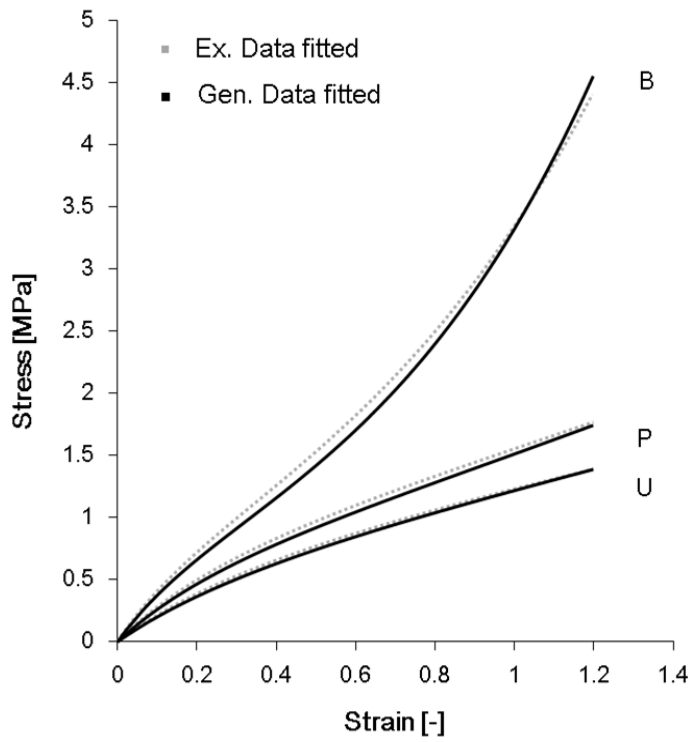**Fig. 5.6** Gen. Bi. Data and Exp. Bi. Data with Uni. data
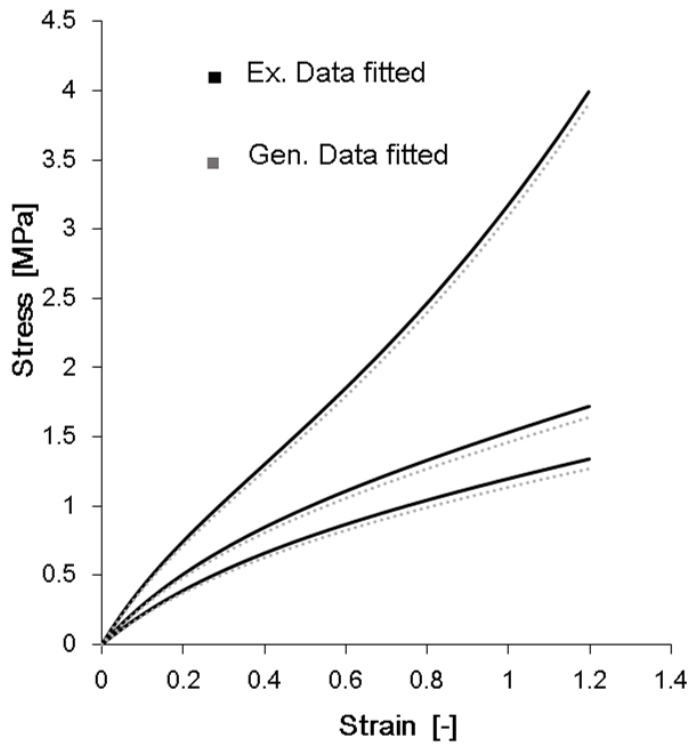


**Fig. 5.7** Mooney-2 model comparison

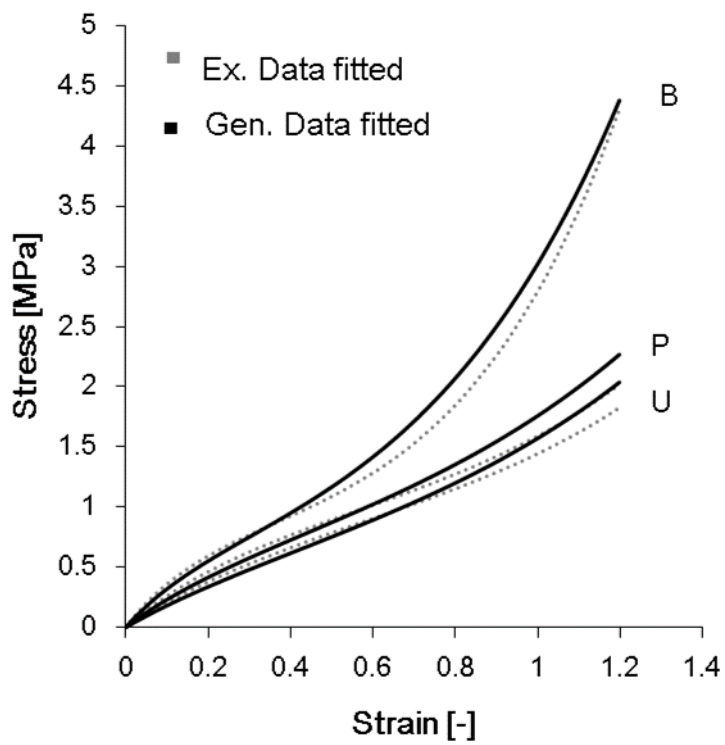**Fig. 5.8** Mooney 3 comparison
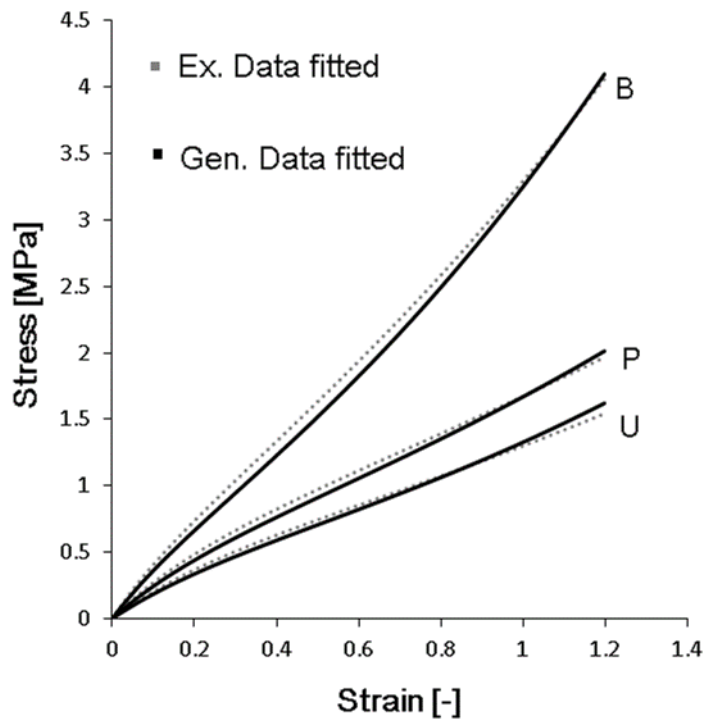


**Fig. 5.9** Yeoh comparison

51

**Fig. 5.10** Ogden comparison

## 5.4  The Detailed Solution to the Problem (Final Experiments)

As to prove our approach in finding additional biaxial data set and thereby to establish the validity of the method, a set of experiments were done. The experiments which were planed here consisted of 30 uniaxial experiments and 10 biaxial experiments for each material. As already mentioned, there were six different types of material to be tested (Table 4.2). Therefore, given number of experiments were planned and carried out for each of them. In this section, the results of these experiments are discussed in detail.

Results of these experiments could be divided in to three segments. First section discusses the resultant data distribution related to both biaxial and uniaxial experiments. The next section would be dealing with the statistical analysis. Final and the last section discusses the fitted model curves related to real data and the generated data. Additional topic would be allocated to discuss the possibility of optimizing the solution.

### 5.4.1 Data Distribution Comparison

In order to get a relationship between uniaxial data and biaxial data, first of all, each material needed to be represented by single unique uniaxial and biaxial data set. As there were more than one set of data from each material, this was achieved by obtaining the average of multiple data sets. All thirty data sets were adjusted to have same number of data points and thereafter averaged data values were calculated by taking simple average with 30 number of points.
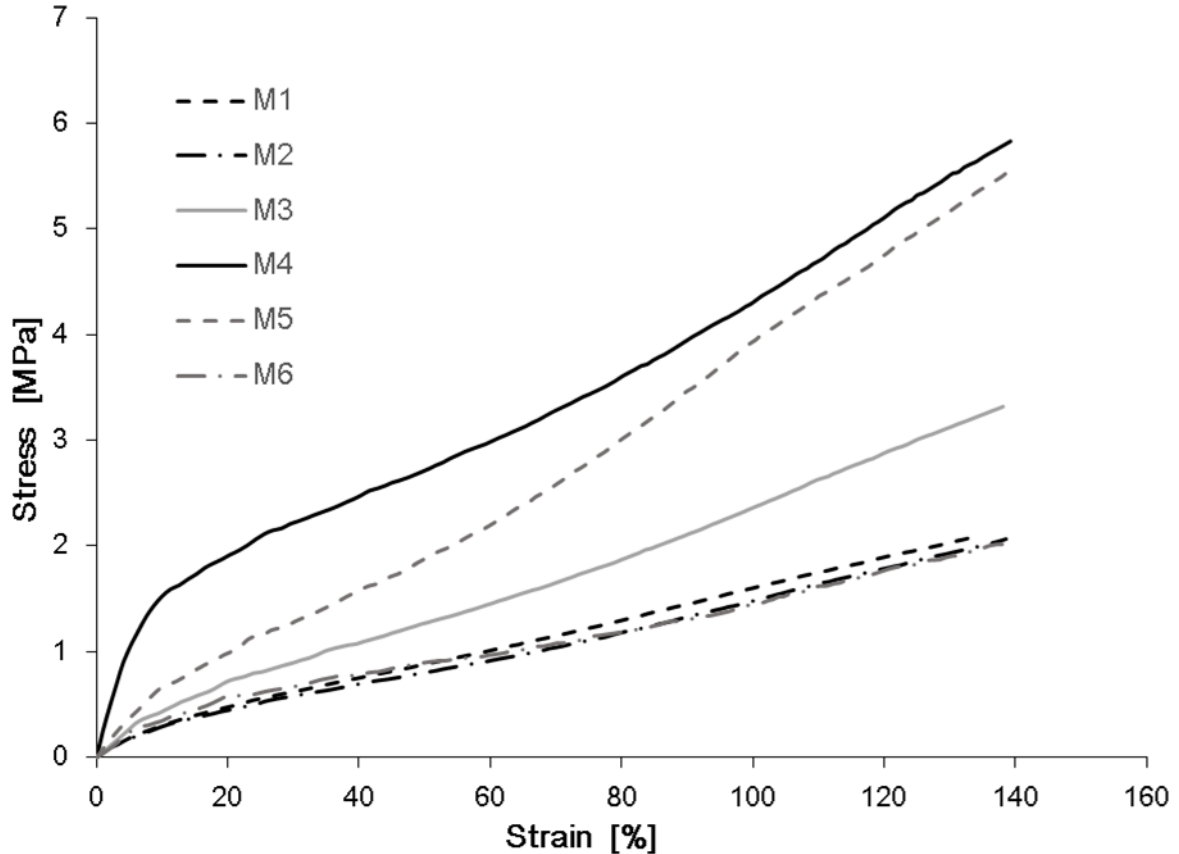


**Fig. 5.11** Distribution of uniaxial data

Averaged uniaxial data distributions of all materials are given in Fig.5.11. According to the figure, in general, all data sets depict typical uniaxial distributions. However, if we consider each distribution separately and observe closely, there are some minor differences. Two materials namely M4 and M5 stand out from others. They show unique distribution pattern. Furthermore, materials M1, M2 and M6 lies very close to each other. Position of material M3 is somewhat away from the rest. If we take the material M4, it is some out of general shape of biaxial data distribution. The trajectory in this case is unique and visibly has two portions to it. First segment appear to be rapidly increasing from zero up to around 10% strain. During the second half, data dispersion seems flattening.

By and large, all data sets seems having the sag in the middle potion. In some data sets, the middle portion sag is prominent while in others it is less dominant.
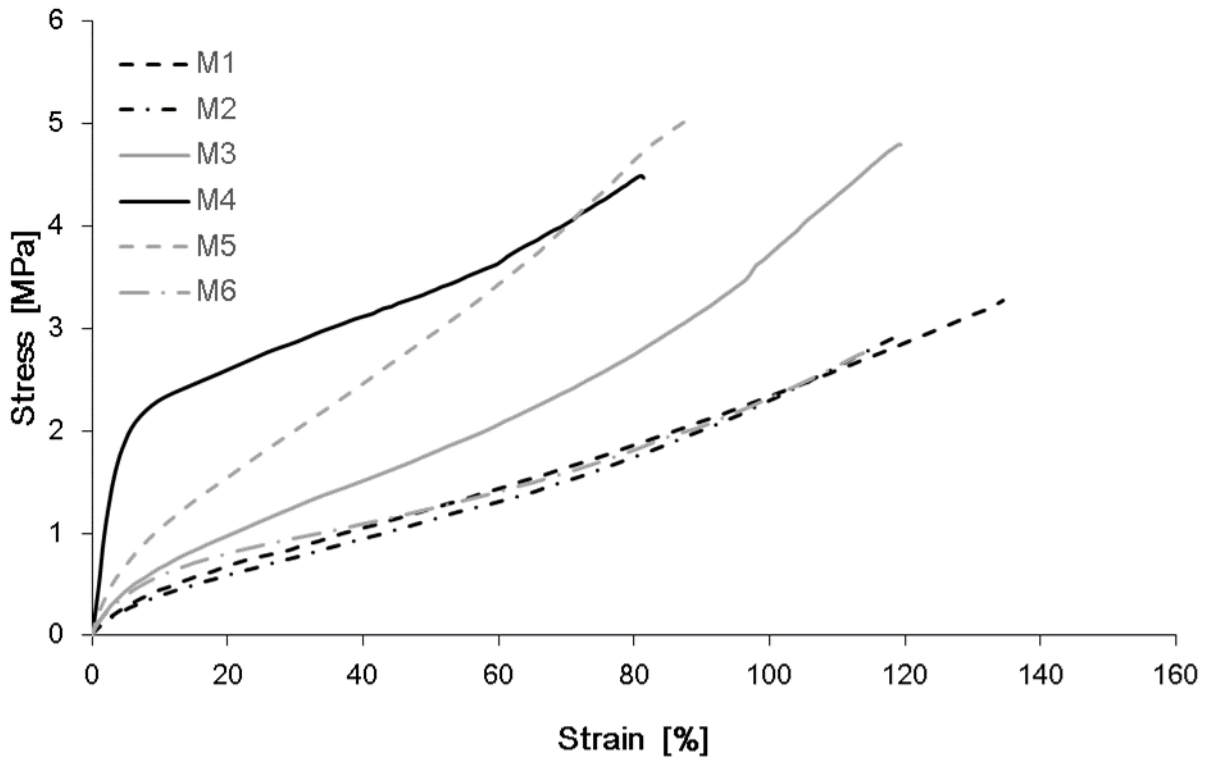


**Fig. 5.12** Distribution of biaxial data

Distribution related to biaxial data for same six materials are given in figure 5.12. Initial visual inspection of this figure reveals a picture similar to the uniaxial data distributions previously discussed. However, in this case, differences between each individual set seems much dominant than previous instance.

In this case, all data distributions are shifted more towards stress axis as with the biaxial data distributions. Like in previous case, same three data sets are visibly separated from the rest. Though it might not be significant, two data sets, M4 and M5 are crossing each other at somewhere in the vicinity of 70% strain. Data set M4, change its trajectory in this case at around 6% strain which is little earlier than in previous case. Out of two segments of this distribution, first segment seems steeper than in previous instance.

### 5.4.2 The Relationship between Uniaxial and Biaxial Data Distributions

In order to construct a relationship between uniaxial data and biaxial data, each data set must be representative average curve of the respective material. Therefore, in the previous section, these average curves were obtained for each material for both uniaxial and biaxial deformation modes. Considering the data distributions of these materials, and the relationship we already discussed, a mathematical formula which is given in equation 5.4 is arranged in order to link two data sets.

$$\sigma_b = \sigma_u \times e^x \qquad\qquad 5.4$$

In the equation, $\sigma_b$ is the biaxial stress at an arbitrary point in the stain axis while $\sigma_u$ is the corresponding uniaxial stress at the same point. Exponent $x$ of the exponential function is a positive real number.

Using this relationship, several biaxial data sets were calculated after assigning different values to the unknown number $x$. From these initial trials, it could be selected a suitable value for $x$ somewhere near 0.4, considering the generated biaxial data and the actual biaxial data. After that, further improvements were done and $x$ was fixed at 0.35.

With selection of particular value for $x$, using above equation, corresponding biaxial values could be generated for each uniaxial stress. Using this method, all biaxial stresses were calculated and plotted together with related uniaxial and experimental biaxial data, as given below from figures 5.13-5.18. Newly created substitute data for biaxial stress- strain distributions are, for identification purposes called hereafter as generated data whenever given in the text.
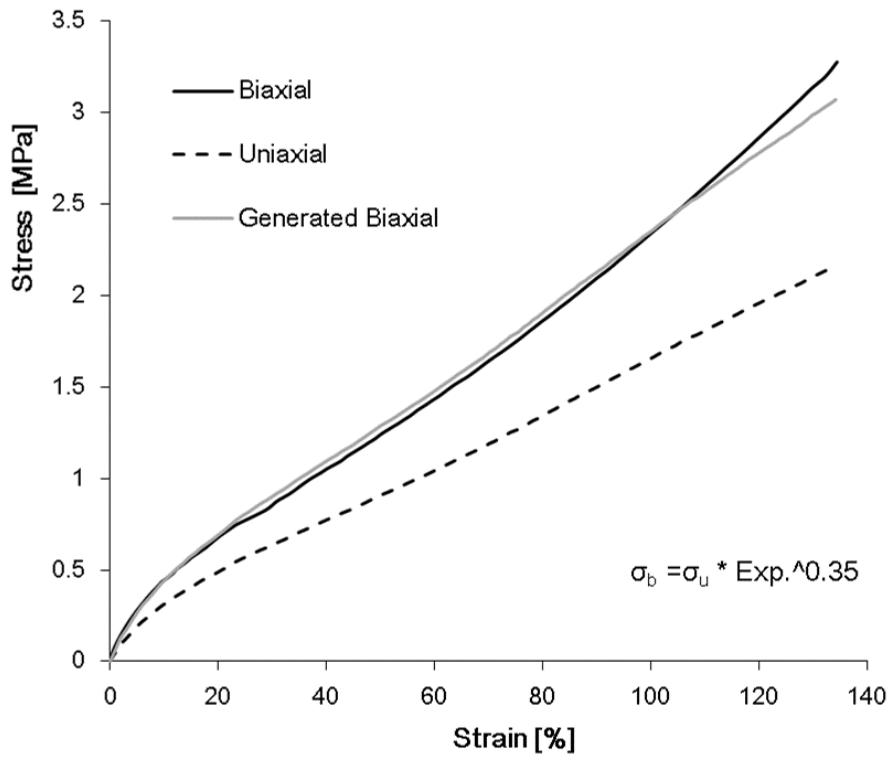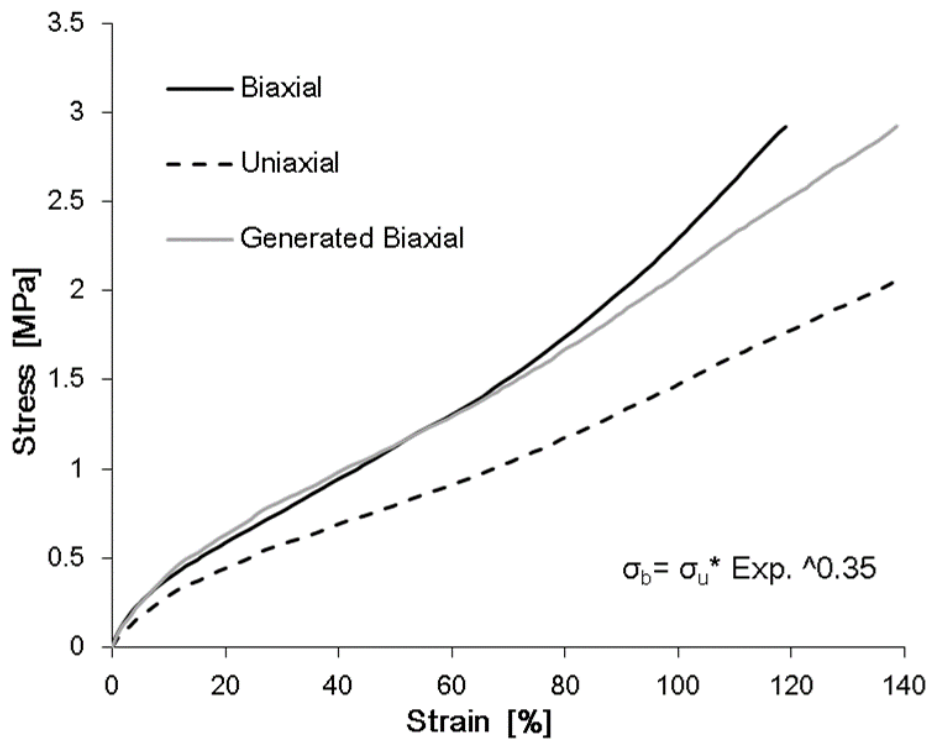
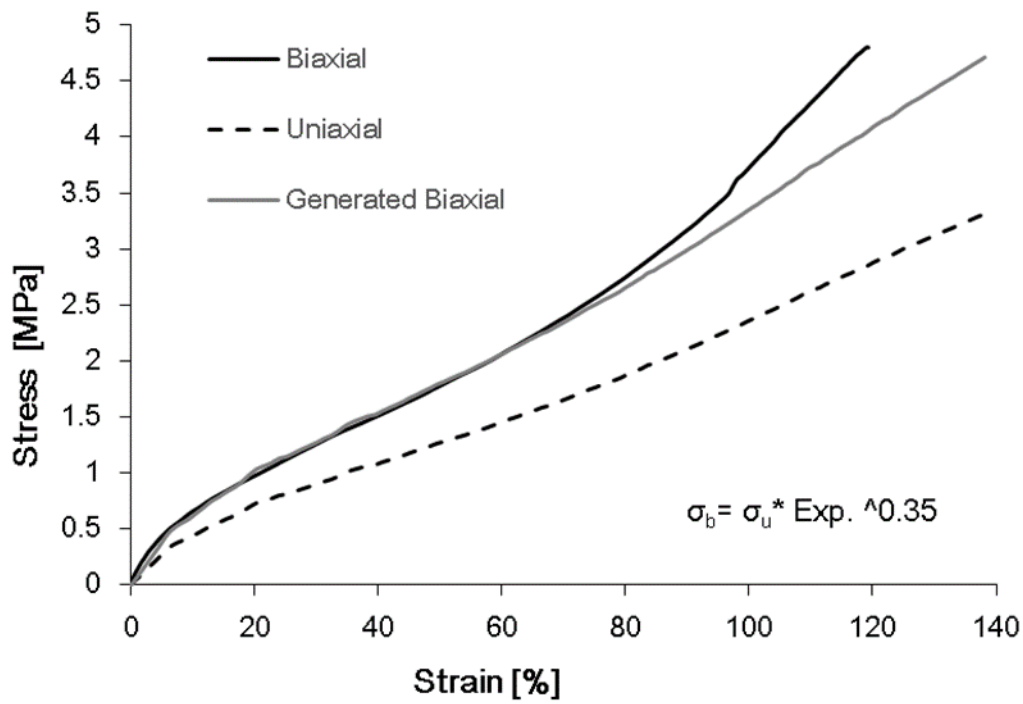**Fig. 5.13** Generated data for M1



**Fig. 5.14** Generated data for M2
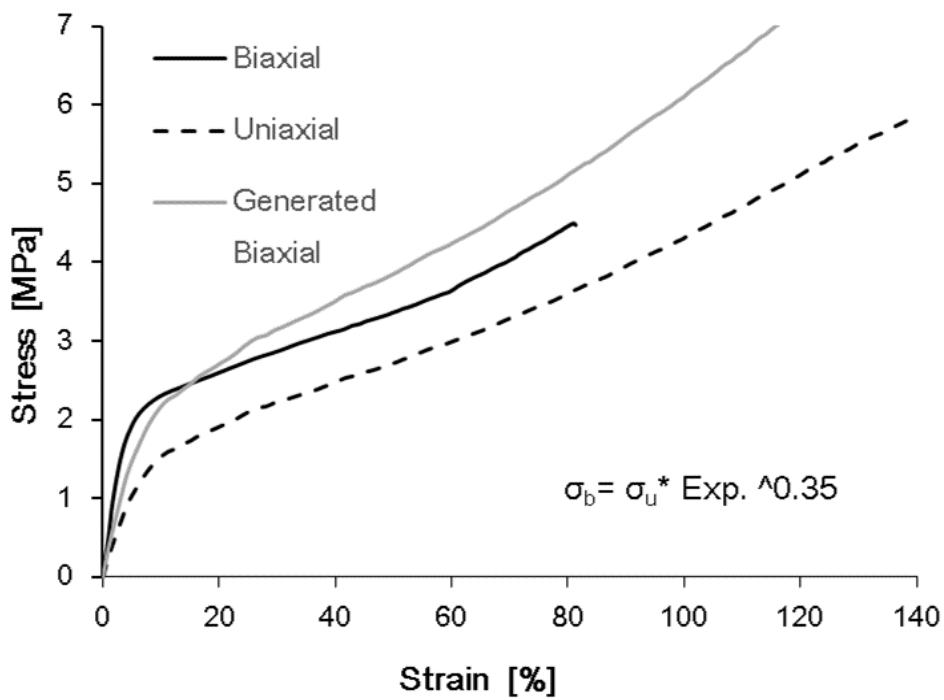
**Fig. 5.15** Generated data for M3
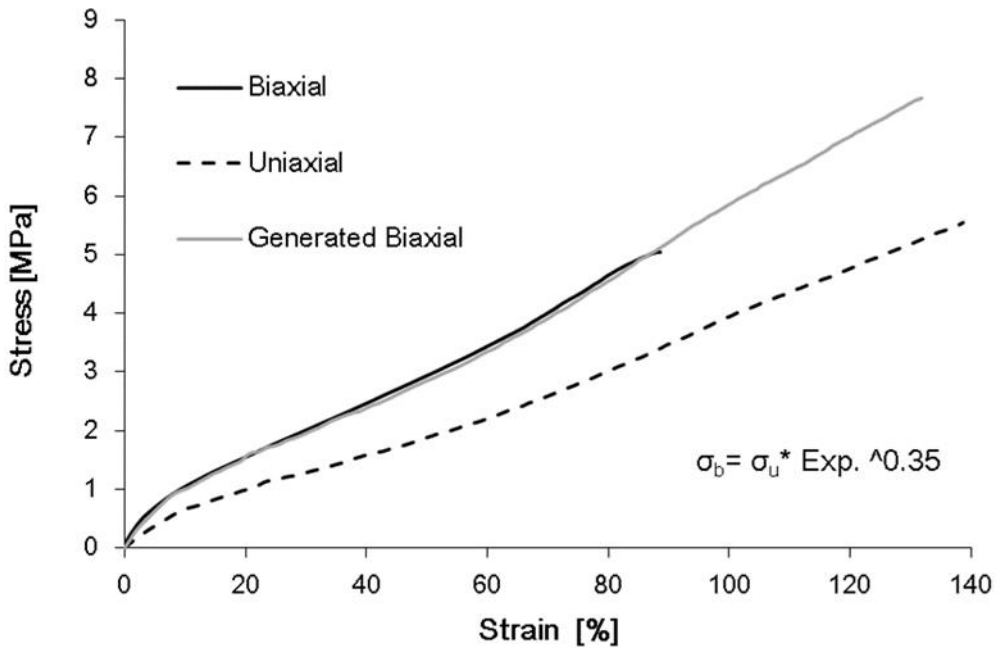


**Fig. 5.16** Generated data for M4

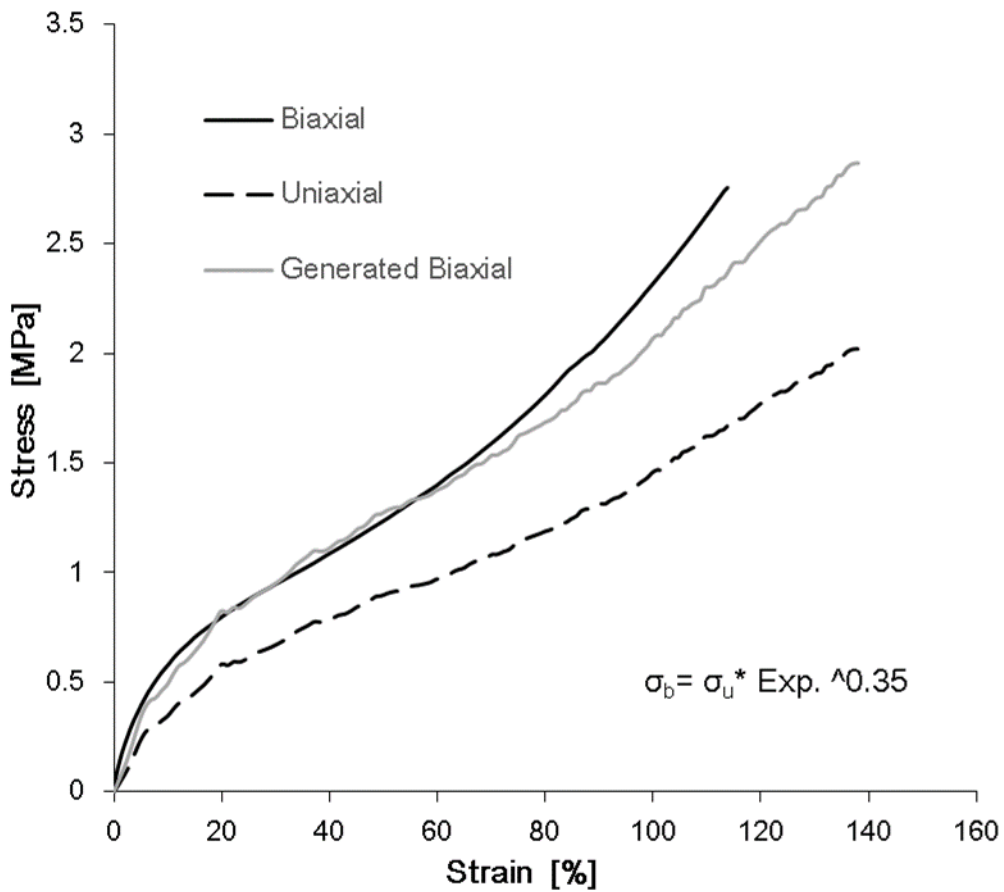**Fig. 5.17** Generated data for M5



**Fig. 5. 18** Generated data for M6

As visible from these graphs, generated data sets are located in general, close proximity to the respective experimental data sets. Only exception is the M4 data set where generated data set is taking a trajectory similar to uniaxial and hence not showing close resemblance to the biaxial experimental data distribution. However, in this particular case, the said difference could be observed when compare uniaxial and biaxial experimental data sets as well. On the other hand, when we examine all generated curves closely, a certain deviation could be observed at the later part of strains for each material. These deviations are happened to be in various proportions according to each of these materials.

Out of all generated biaxial data sets related to these six materials, the data generated using uniaxial data of material 5 seems the best and the closest to the original data.

### 5.4.3  The Statistical Reasoning

After generating biaxial data distributions for each and every material tested, next task was to test statistically how close these generated data to the real data. In order to do verify this, we followed a typical significant test devised as to suite this particular case.

Significant testing is normally done in order to estimate the level of confidence with witch one can forecast the population from a sample. This is a typical statistical testing method and here, it is adopted to include this particular situation as follows.

According to the method discussed here, first of all averaged biaxial data set is divided in to five equal segments. This is done according to the stress obtained by dividing maximum average stress in to five (Fig. 5.19). Idea behind this effort is to get five different points in the data distribution to compare real and generated biaxial data.
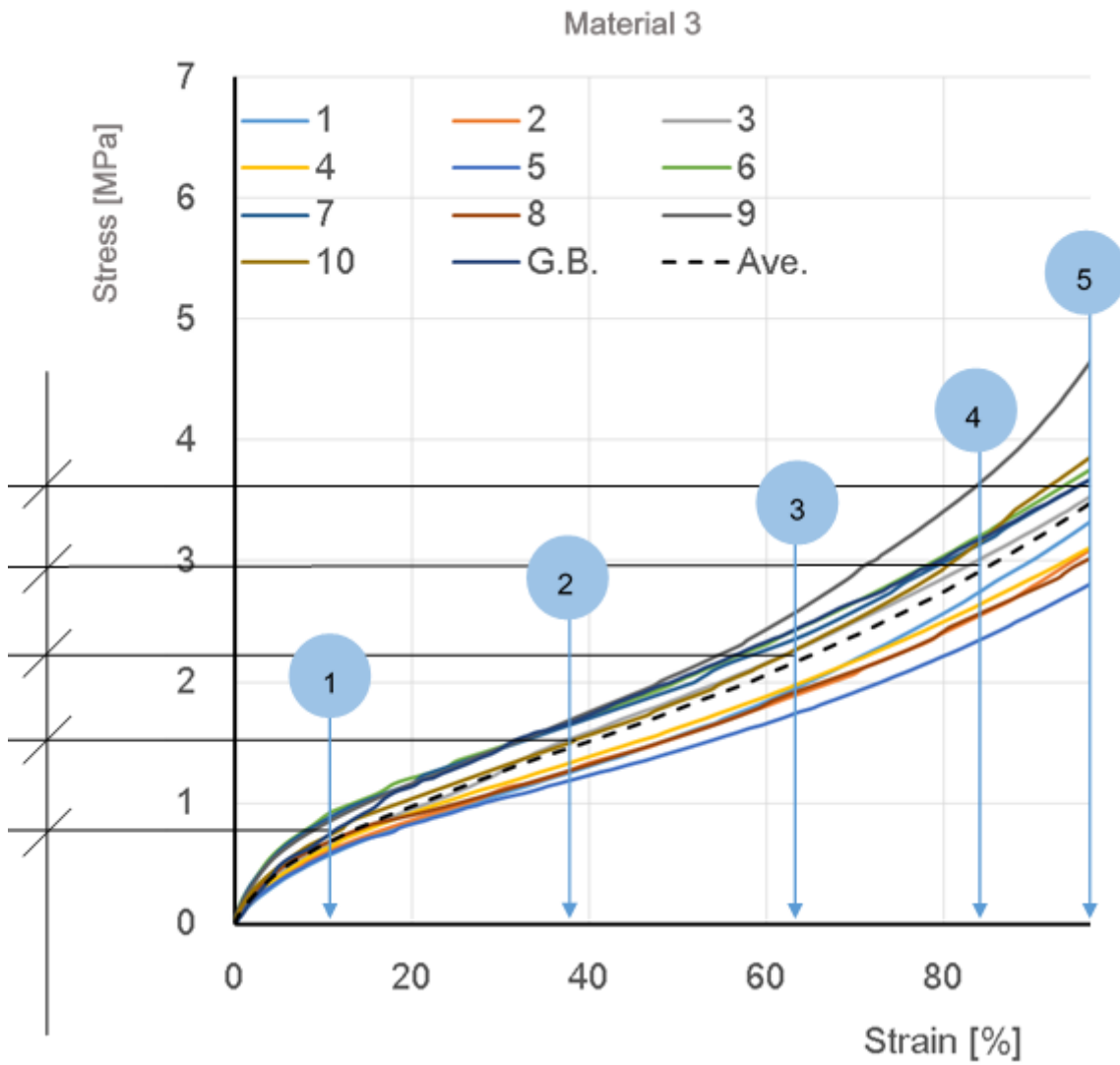
**Fig. 5.19** five tapping points

Thereafter, corresponding strain values were selected. By plotting generated biaxial data distribution according to the material in the same graph, equivalent generated biaxial stress values for these strain tapping points could be calculated. At the same time, all experimental biaxial data were plotted in the same graph and equivalent stress values corresponding to each tapping point strain is also collected.

For the demonstration purpose, the stress values obtained for material M1 is given in the table 5.2, below for the ten sample graphs and for that of generated graph. The first column of the table gives each tapping point strains collected through average curve maximum stress dividing in to five.

**Table 5. 2** Stress values for five tapping points for M1

| Tap. Pt. strain [%] | Curve number & corresponding stress [Mpa] | | | | | | | | | | Gen. curve Stress [MPa] |
|---|---|---|---|---|---|---|---|---|---|---|---|
| | 1 | 2 | 3 | 4 | 5 | 6 | 7 | 8 | 9 | 10 | |
| 11.53 | 0.68 | 0.54 | 0.52 | 0.52 | 0.48 | 0.51 | 0.42 | 0.56 | 0.46 | 0.57 | 0.49 |
| 38.85 | 1.21 | 1.18 | 0.99 | 1.05 | 1.00 | 1.02 | 0.76 | 1.08 | 0.93 | 1.17 | 1.07 |
| 63.51 | 1.71 | 1.71 | 1.42 | 1.50 | 1.46 | 1.48 | 1.14 | 1.54 | 1.36 | 1.68 | 1.55 |
| 87.83 | 2.22 | 2.31 | 1.91 | 2.01 | 1.98 | 2.01 | 1.84 | 2.04 | 1.86 | 2.30 | 2.08 |
| 108.43 | 2.70 | 2.87 | 2.37 | 2.50 | 2.47 | 2.51 | 2.37 | 2.52 | 2.35 | 2.95 | 2.53 |

Ten stress data values were examined against respective generated stress value using statistical significant test. For the statistical significant test or t-test, null and alternative hypothesis arguments were constructed as follows.

Null Hypothesis

Ho : $\mu = \bar{x}$                      5.5

Alternative Hypothesis

H1 : $\mu \neq \bar{x}$                    5.6

Where, $\mu$ is the Generated stress while $\bar{x}$ is the mean of ten values of ten curves at the same taping point. Results of this significant test are tabulated here. (Table 5.3)

**Table. 5.3** *p* values derived using student's t-distribution

| Material | Stain point & value [%] | | *p* value |
|---|---|---|---|
| M1 | 1. | 11.53 | 0.095 |
| | 2. | 38.85 | 0.454 |
| | 3. | 63.50 | 0.378 |
| | 4. | 87.83 | 0.551 |
| | 5. | 108.43 | 0.676 |
| M2 | 1. | 9.32 | 0.389 |
| | 2. | 27.82 | 0.113 |
| | 3. | 49.88 | 0.197 |
| | 4. | 69.16 | 0.861 |
| | 5. | 85.15 | 0.178 |
| M3 | 1. | 7.21 | 0.179 |
| | 2. | 25.67 | 0.522 |
| | 3. | 47.94 | 0.391 |
| | 4. | 67.32 | 0.951 |
| | 5. | 83.29 | 0.425 |
| M4 | 1. | 0.94 | 0.016 |
| | 2. | 3.08 | 0.001 |
| | 3. | 8.76 | 0.001 |
| | 4. | 37.94 | 0.000 |
| | 5. | 65.42 | 0.000 |
| M5 | 1. | 4.04 | 0.000 |
| | 2. | 16.90 | 0.041 |
| | 3. | 34.07 | 0.462 |
| | 4. | 49.88 | 0.086 |
| | 5. | 64.35 | 0.257 |
| M6 | 1. | 4.04 | 0.001 |
| | 2. | 15.79 | 0.059 |
| | 3. | 39.77 | 0.676 |
| | 4. | 62.66 | 0.929 |
| | 5. | 79.90 | 0.227 |

By referring the third column of the table, we can see that critical *p* values for most of the significant tests are above 0.05. This means that the forecast can't be rejected or in other words, with 95 percent confidence we can say that null hypothesis cannot be rejected in such cases.

However, there are few exceptions where, the *p* value is less than 0.05. In particular, for the material M4, with relation to all points of concern, shows such

low values. As we have already mentioned, this particular material seems deviating from others and behaving differently from the group. Therefore, such a result could be expected for the statistical test as well.

In other cases where P value is less than 0.05, it would be appropriate to lower the confidence interval and check the results once again. This suggestion could be justified as typical behavior of rubber materials allow such wide margins in the testing.

### 5.4.4  The Generated Biaxial Data Set Optimization

As part of the generalized biaxial generating formula is an exponential function, the exponent can take many values. The value of exponent affect the relative position of the generated data set. Therefore, we examine the possibility of getting a unique value for the exponent which would provide the optimal position for the data set related each material.  At the end, further examination was done as to find one optimal value representing whole material group.

The method used here is explained as follows. Considering the five tapping points used for extraction of data for statistical calculation, by referring figure 5.20, in order to minimize the error between biaxial experimental data and generated data ($\Delta y$), following formula could be drawn (Eq. 5.7-5.9).
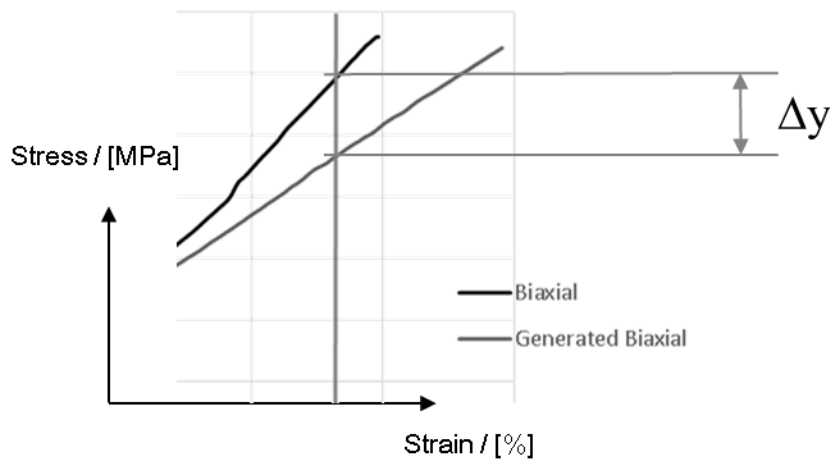


**Fig. 5.20** Error between real and generated biaxial data

$$f(x) = \sum_{1}^{5}\left[\left(y_{bi} - y_{gbi}\right)^2\right] \qquad 5.7$$

$$f(x) = \sum_{1}^{5}\left[\left(y_{bi} - y_{ui} \times e^x\right)^2\right] \qquad 5.8$$

$$f(x) = \sum_1^5 y_{bi}^2 - 2 \times \sum_1^5 y_{bi} \times y_{ui} \times e^x + \sum_1^5 y_{ui}^2 \times e^{2x} \qquad 5.9$$

Using this formula, by allocating values to exponent x, from 0.005 to 0.7, $f(x)$ vs x was drawn. Graph drawn for material M1 to M6 are given below from Fig. 5.21 to 5.26 looks as follows. From these graphs, it is possible to find the value of exponent x where, error of real biaxial data set and generated data is minimal.
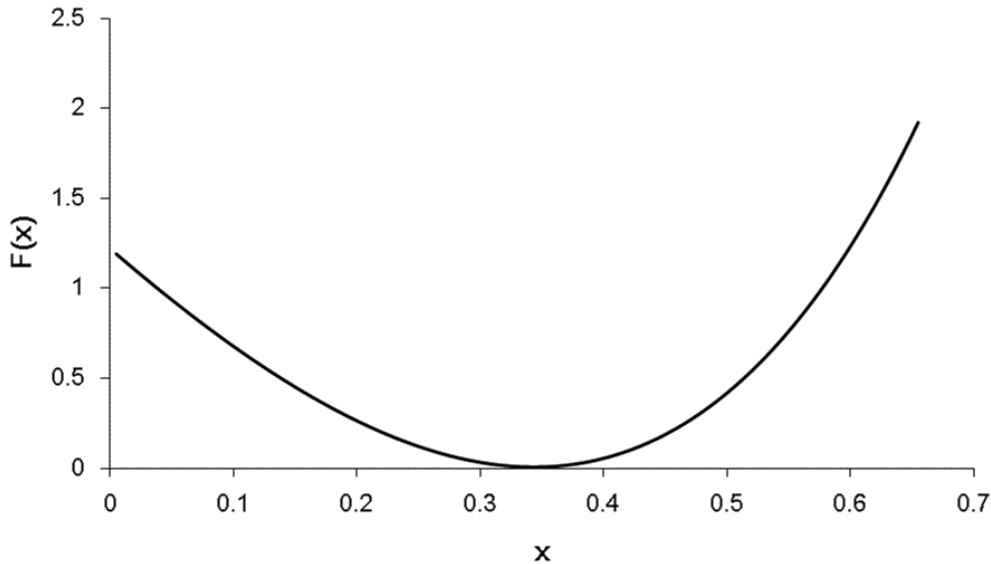

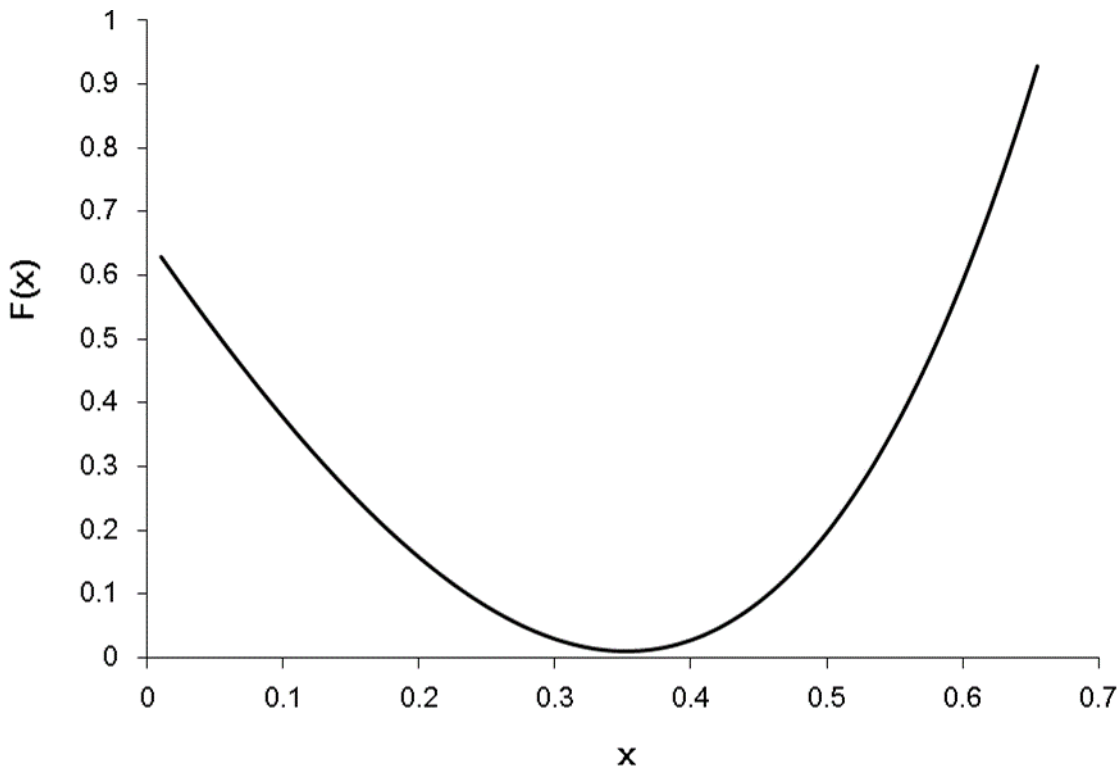
**Fig. 5.21** Error calculation for M1
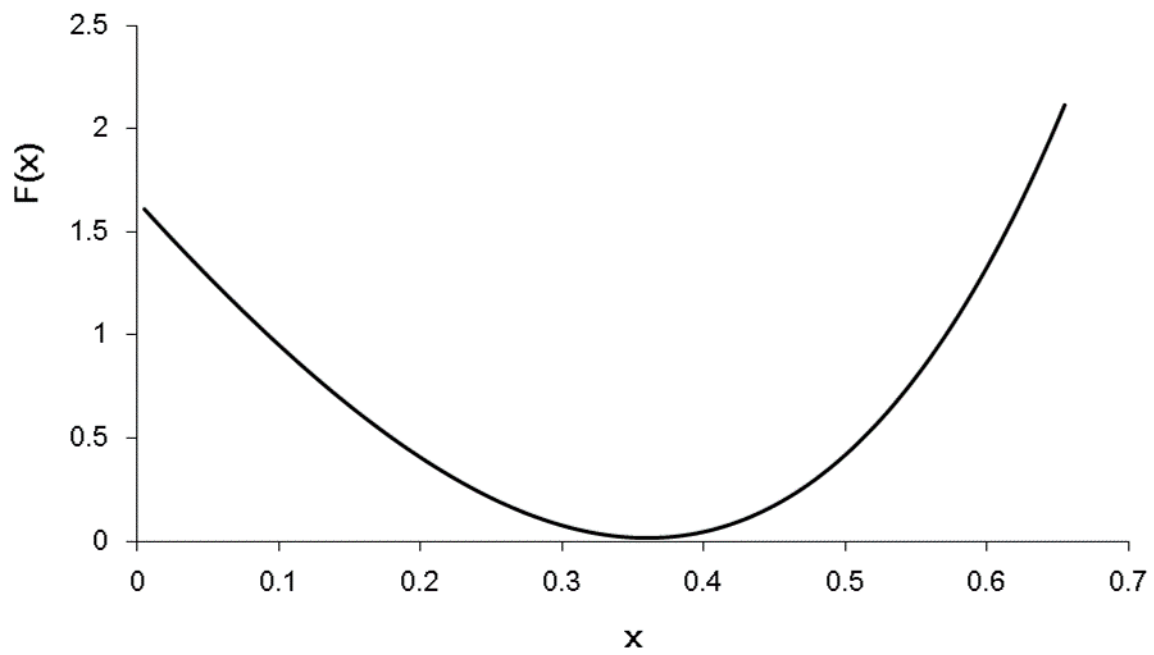


**Fig. 5.22** Error calculation for M2

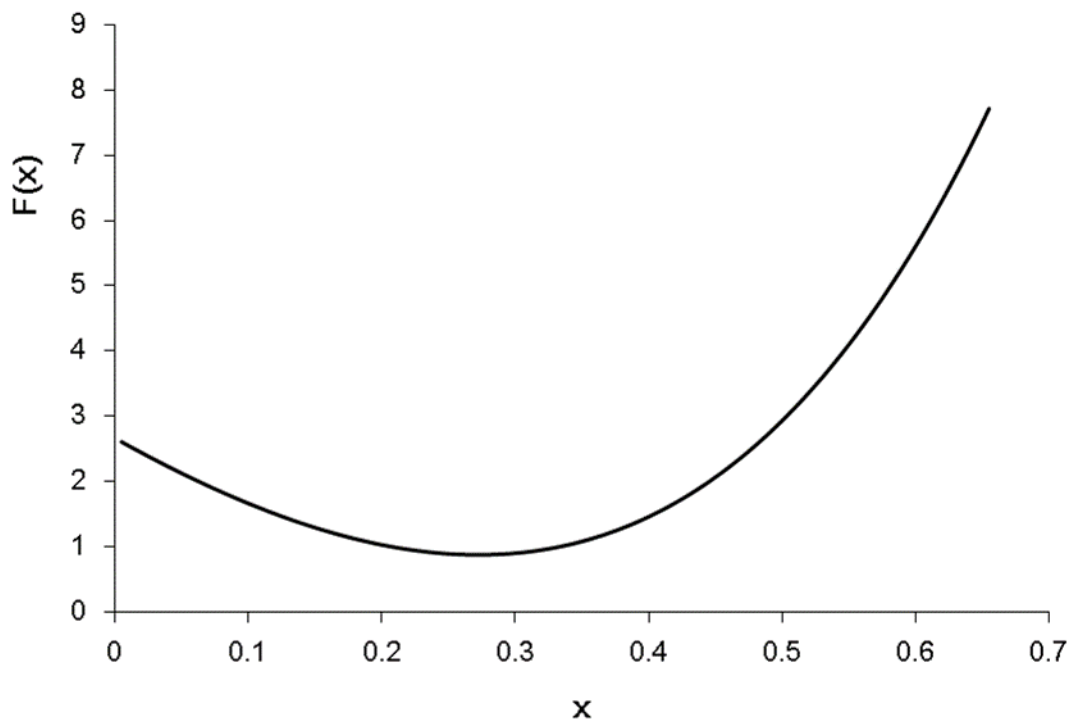**Fig. 5.23** Error calculation for M3
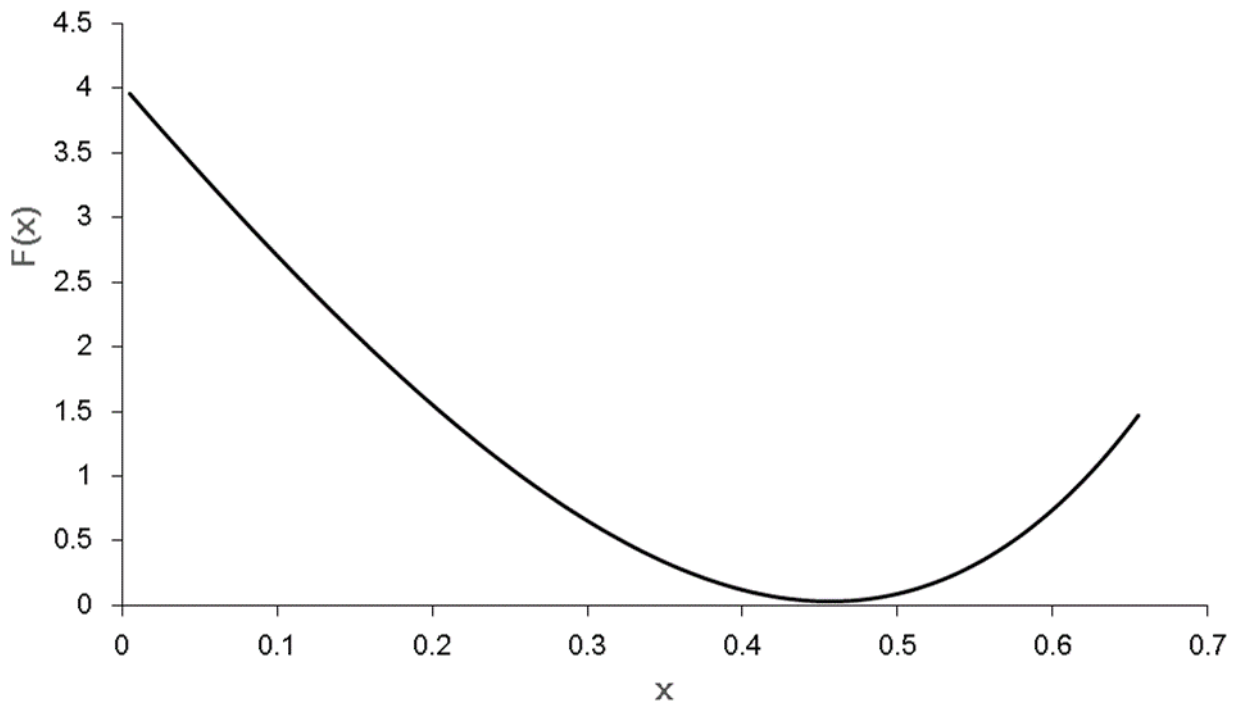


**Fig. 5.24** Error calculation for M4
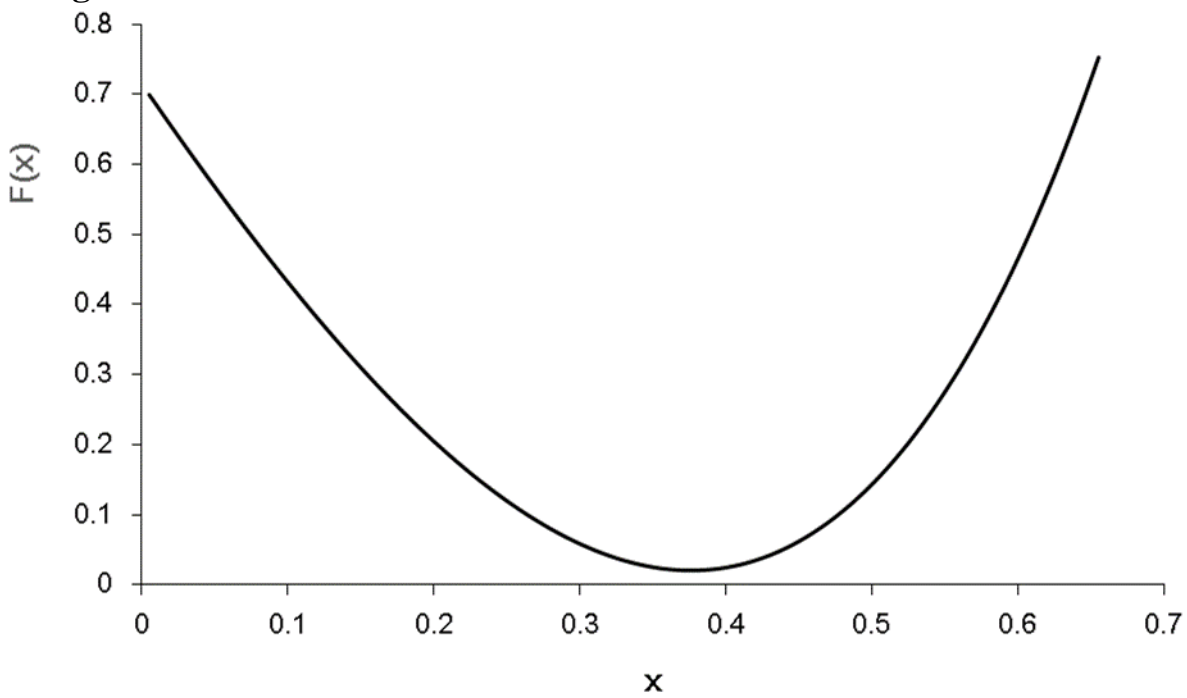
**Fig. 5.25** Error calculation for M5



**Fig. 5.26** Error calculation for M6

From these graphs, it can be evaluated the optimal value of $x$ for materials M1 to M6 as follows.

**Table 5.4** Optimal values for Exponent.

| Material | Optimal Value |
|----------|---------------|
| M1       | 0.35          |
| M2       | 0.35          |
| M3       | 0.36          |
| M4       | 0.27          |
| M5       | 0.46          |
| M6       | 0.38          |

Furthermore, considering all the data together, it is possible to get a one exponent for all materials. Idea is to get a one formula for the material group. For this task, calculations were done and related plot was presented in Fig. 5.27.
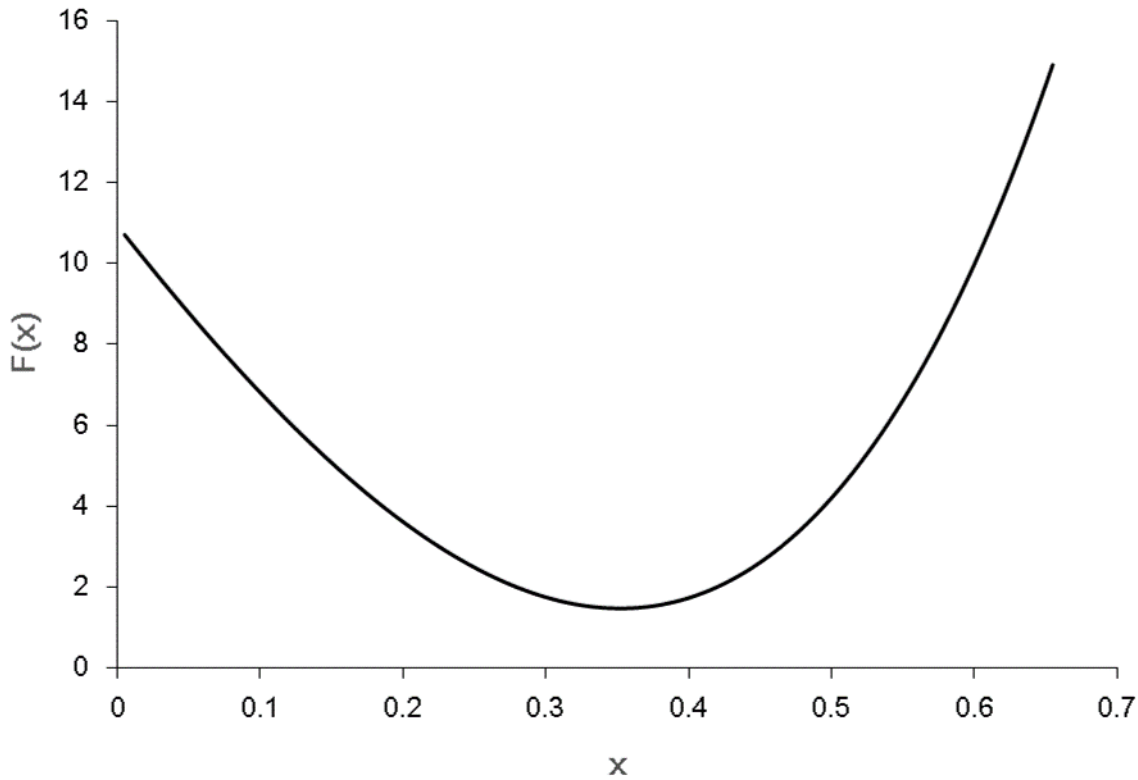


**Fig. 5.27** Error calculation for all materials together

Considering the overall graph, optimal value for this material group could be fixed at 0.3525.

The model testing for the newly generated biaxial data

Having examined and obtained positive results for the statistical testing, next and the last step was to see how these artificial data would work with some of the common models when used for combined data fitting with uniaxial data. In this section of the work, several models were examined for the compatibility and to

obtain the correct model to represent the material group. However, some of the material models tested were not compatible with this material group and showed inconsistence results. Mooney two parameter model was the most compatible. Results of this model fitting for six materials separately are given from figures 5.28 to 5.33.
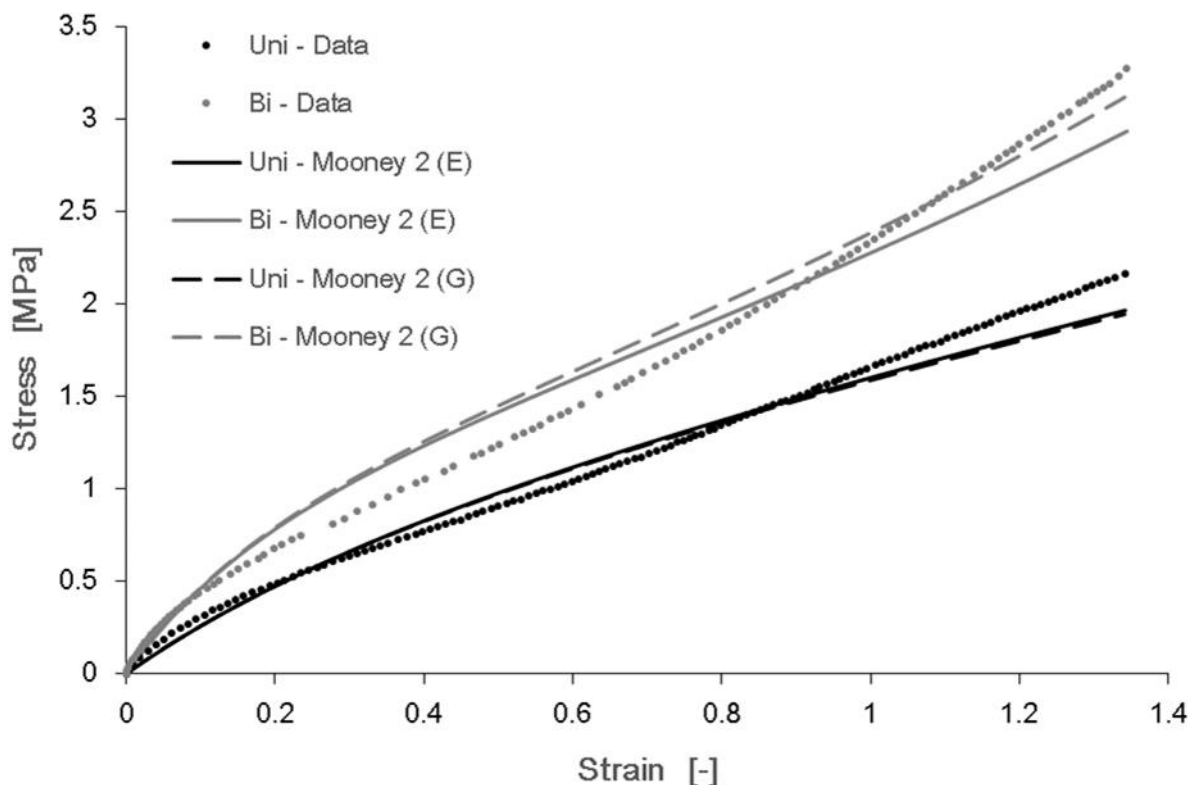


**Fig. 5.28** Mooney-2 Model: Generated and real data comparison – M1

Combined data fitting of both real biaxial data with uniaxial data and generated biaxial data with uniaxial data were done separately. Uniaxial model seems coinciding in these two instances.

Data fitting results given in for material 2 in figure 5.29, also shows similar results like in previous case. However, unlike previous instance, in these cases, data and the model curves seems somewhat compatible with each other.

Material 3 data fitting results given in figure 5.30 also gives a set of curves somewhat similar to M2 curves, though with higher stresses.

As it was the case with M4, the model curves seems deviating from the data distributions (Fig. 5.31). On the other hand, two combined data fitted modal curves are deviating from each other from early strain value

**Fig. 5.29** Mooney-2 Model: Generated and real data comparison – M2



**Fig. 5.30** Mooney-2 Model: Generated and real data comparison – M3
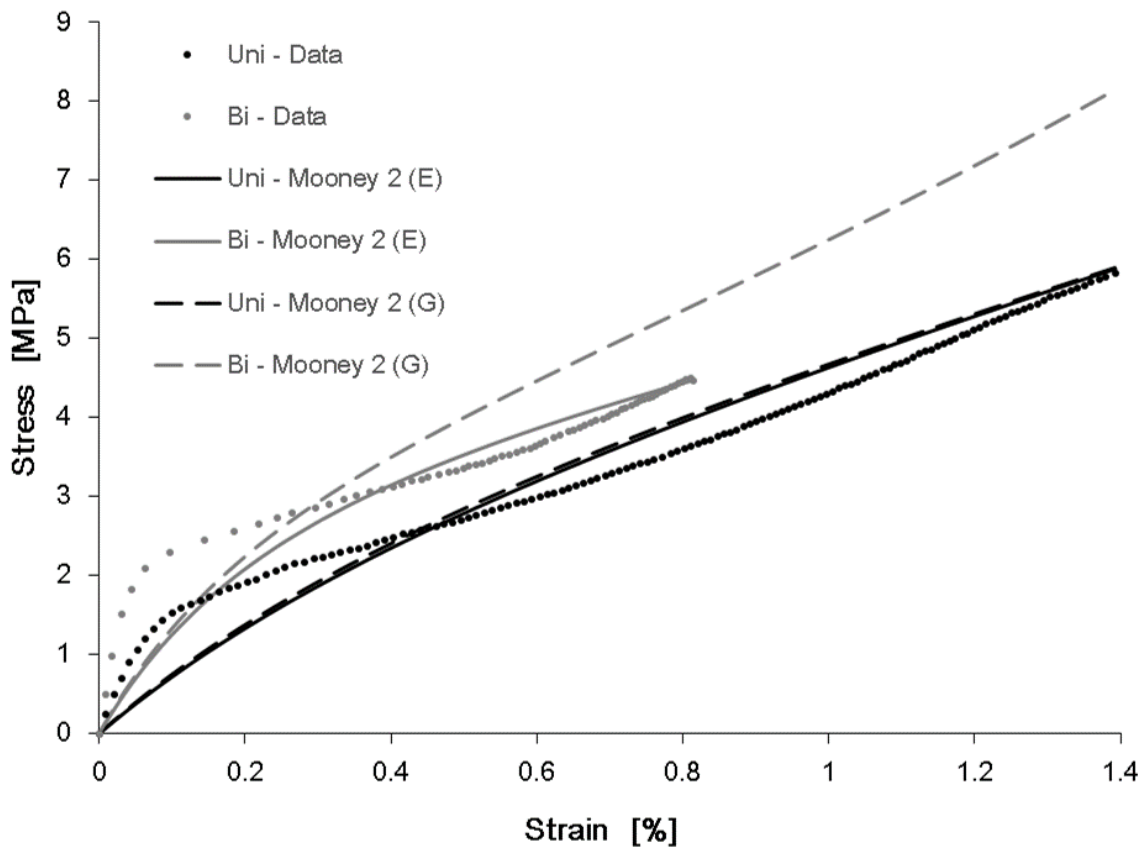
**Fig. 5.31** Mooney-2 Model: Generated and real data comparison – M4



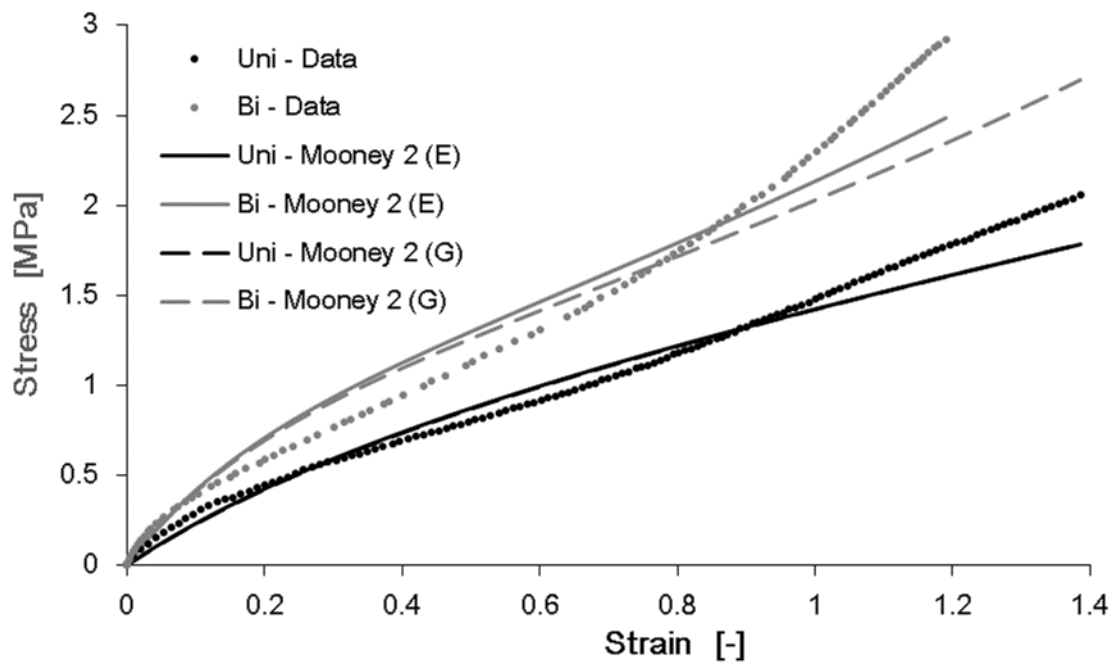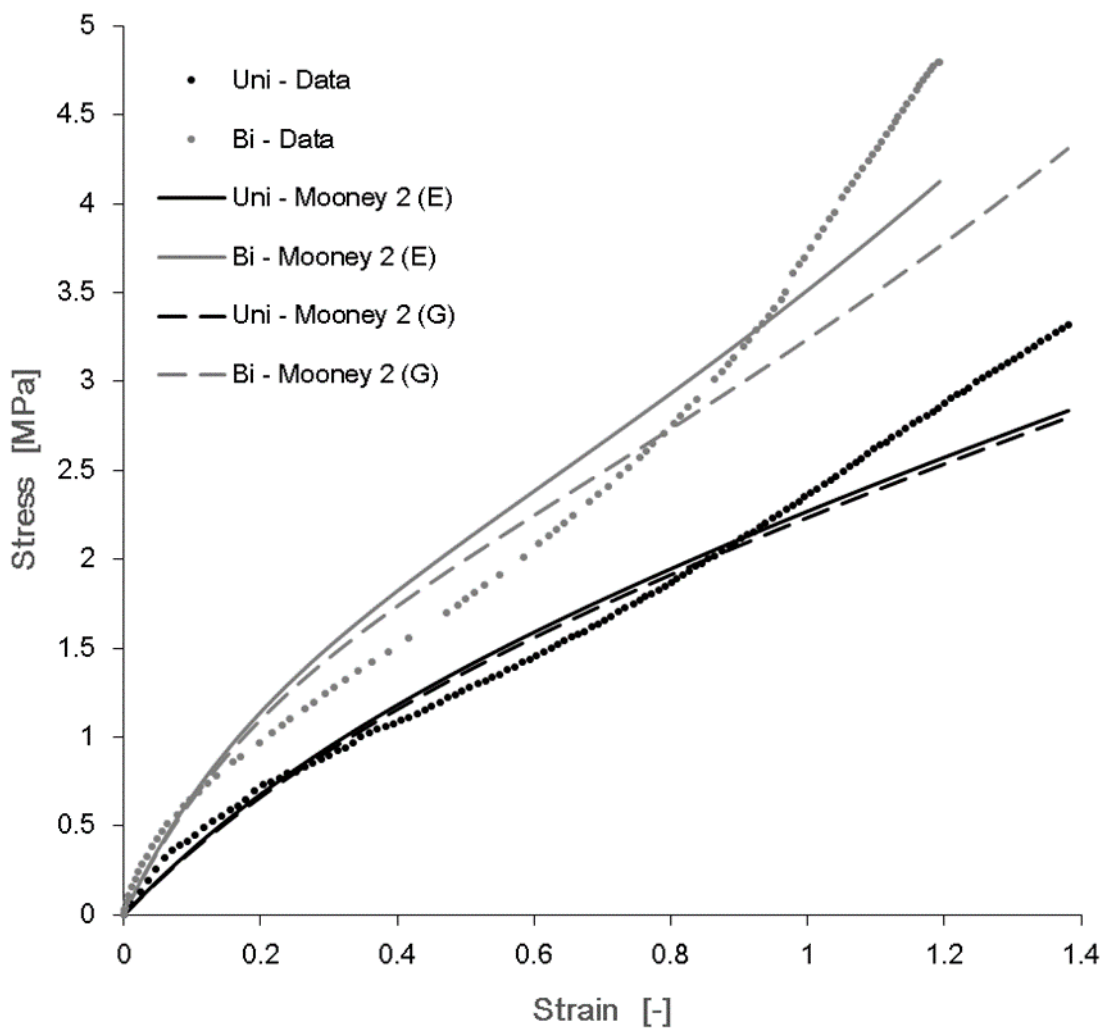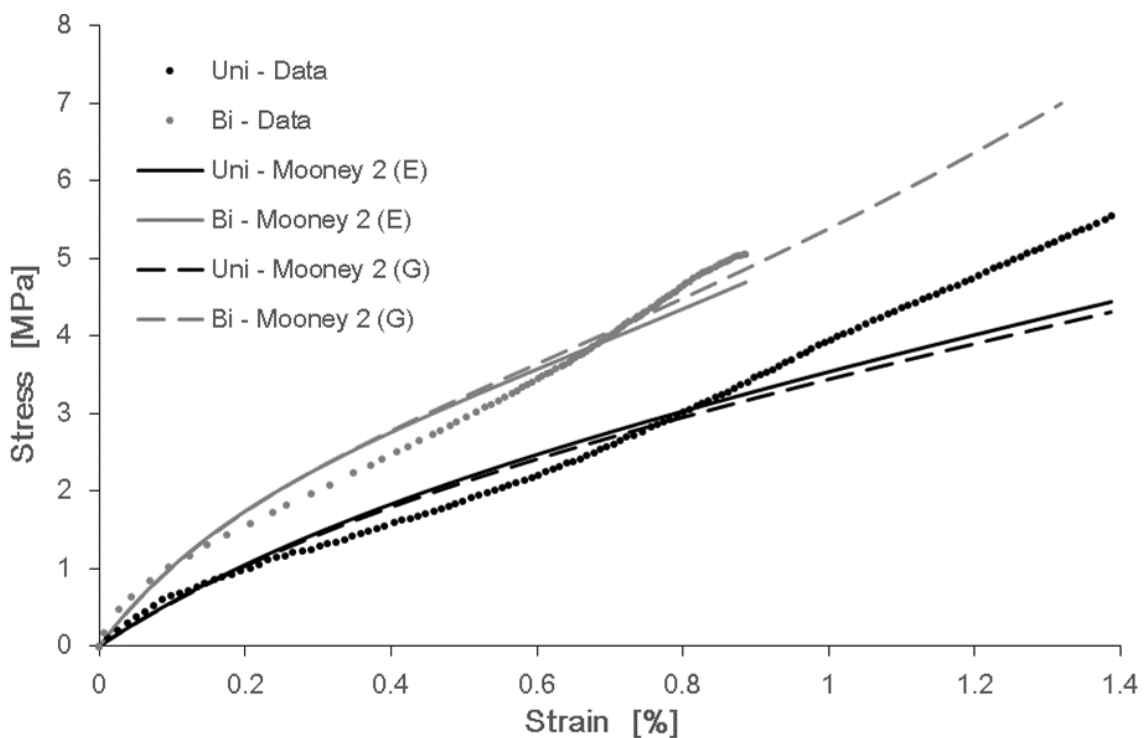**Fig. 5.32** Mooney-2 Model: Generated and real data comparison – M5

For the material M5, (Fig. 5.32) once again, biaxial and generated biaxial model curves are close to each other, but data set seems away from the models. In the case of uniaxial this is very much improved and all three are laying near to each other. Stresses are relatively high in this case.
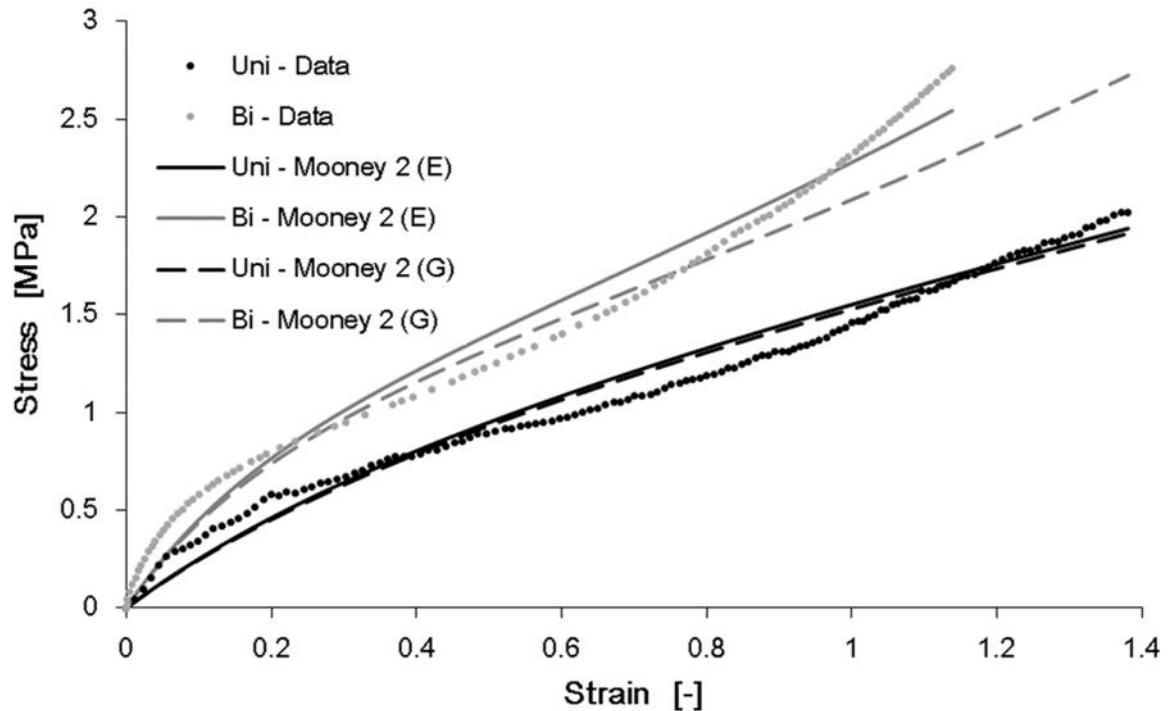


**Fig. 5.33** Mooney-2 Model: Generated and real data comparison – M6

In the case of M6, (Fig. 5.33) model curves are crammed between two data sets. This means, model is lower in the biaxial and higher in the uniaxial when it comes to represent respective data. However, for both instances, real and generated data fitted models give somewhat similar trajectories, though in biaxial case, at later part the generated curve is little off-shoot from the real one.

Altogether, data fitting for Mooney-2 model shows mixed results for six materials discussed. As these materials are different from one another in the way of hardness and carbon black content which consequently leads to property change, such variations could be expected.

# 6. DISCUSSION

## 6.1 Inadequacy of Data (Experiment 1)

The first experiment was done with the objective of finding the discrepancy in data fitting with single data set when compared with that of combined data fitting. Three hyperelastic models were selected for the comparison. Each model was examine related to three deformation forms, uniaxial, biaxial and pure shear.

Three deformation curves for Mooney-2 model (Fig. 5.1.a & b), show very clear improvement for the combined data fitting compared to single data set fitting. Mooney-3 parameter model also shows (Fig. 5.2.a & b) similar results. However, in this case, biaxial curve seems volatile in both the cases. Yeoh model (Fig. 5.3.a & b) seems the least responsive when it comes to the fitting method improvement.

Finally, as a concluding note for this experiment, following could be mentioned. Three models tested for single and combined data fitting showed mixed results. Mooney-2 seems the most improved due to the combined data fitting. Mooney-3 model could be considered partially improved with the multiple data set fitting, while Yeoh model seems not responsive to change in data fitting technique. However, discrepancies in all three models related to only uniaxial data fitted curves prove that method is not accurate and therefore less suitable for the mechanical characterization.

## 6.2 First Solution (Experiment 2)

Second experiment has two comparisons. First one is the data comparison. In this section, two biaxial data sets, real and generated are compared. For the generated data, there are three data sets, 0.6, 0.7 and 0.8 (Fig. 5.4). From visual inspection it could be selected the data set generated using 0.8 factor as the closest to the real data. A statistical examination subsequently carried out with three data sets also established the same conclusion.

In the second part of the experiment, data set generated by the method described is used to combine data fitting together with uniaxial data. Results obtained for this effort was compared with the only uniaxial data fitted curves. When we compare figure 5.5 with that of 5.1.a, one could observe a clear improvement related positions of all three curves in the case of combined data fitting. Biaxial curve seems the most improved. However, the generated biaxial data distribution needs further improvement as there is a clear deviation from real data which could be observed at the later stage of strains.

## 6.3  An Improvement to the Initial Solution (Experiment 3)

The third experiment was done as to improve the results of previous experiment. The method was changed to obtain a better trajectory for the generated data set.  From the figure 5.6, it could be observed that generated curve in this case is very much close to the real data. This is an indication to the success of this approach.

In the second part of the experiment, four models, Mooney 2, Mooney 3, Yeoh, and Ogden were tried with data fitting using real and generated data (Fig. 5.7 & 5.10) separately. Except for the Yeoh model, curves of all models show remarkable improvement related to the data fitting. Discrepancy showed by the Yeoh model might have been due to the fact that particular model is not suitable in representing this specific material characterization. Basically, it could be apportioned to a mismatch between the model and the material.

## 6.4  The Detailed Solution to the Problem (Final Experiments)

As given in results section, these experiments were done for six different materials. Each material has different ingredients and therefore physical behaviour is different from one another.  In order to get first hand opinion of the materials, physical examination and visual observation was done. Initial feel of materials suggest that M2 as the most soft. Materials M1 and M6 seems somewhat similar in toughness. M3 feels tougher than previous two materials. M5 comes next in toughness feel and M4 seems the toughest material.

If we consider regarding the carbon black content, according to data sheets, M1 has 50 Phr which is the lowest. M6 contains little more than M1while M3, M2 and M4 lies in the lower half of sixties in the ascending order.  M5 gives the highest carbon black content at 84 Phr. By referring once again, [43], it can be stated that this additive could affect the toughness of the overall material in compliment with oil content. According to the Dick [43], carbon black has three critical factors which influence the bulk material. That is particle size, shape and surface chemistry. However, in this particular case, lack of additional information regarding carbon black hinders a concrete prediction of effect of it on each material. Furthermore, there is no information about other additives. Hence, due to incomplete description of constituents of these material compounds, pre judgement of behaviour could not be possible. Additionally, this fact limits a suggestion of particular material model to be tested in the latter part of work too. Only possibility remain here is to test few models and select a better one in order to validate the results. However, it might not affect adversely as main objective of the work is rather less focused on a particular model, but on data.

Having discuss the initial state of these materials and thereby expected results according to the constituents of them, we are moving to examine the results of proceeding experiments. After series of uniaxial and eqi-biaxial experiments on each material, stress strain data were plotted and general appearance of these data distributions were examined and explained. In addition to that, it could be mentioned here as a general comment that while all four materials exhibit generalized data distribution pattern two materials, M4 and M5 markedly deviate from the group. This might have been due to their high toughness.

When it comes to discuss the final results, first of all, it is important to note that all the generated data sets are obtained through one unique exponential formula with one single exponent. Generated biaxial data were plotted together with real biaxial data, for each of these materials separately as given in results section (Fig. 5.13 – 5.18). Respective uniaxial data were also given as to show the relative position of biaxial data.

First figure from this set of graphs, which is given as Fig. 5.13, depicts the generated data for the material M1. Generated data very much resembling the real data in this case. Two data sets, real and generated, cross each other at around 110% strain level. Gap between two data sets is highest at the extreme end at strain level of nearly 140%. From the visual inspection, it can be noted that in this instance, generated data are successful in representing the experimental biaxial data all along the full range of tested strains.

Data distribution given in figure 5.14 is of material M2. In this case, uniaxial data shows some sag in the middle. As a result, generated data also possess that. Evidently, experimental biaxial data is without such sag. Therefore, there is a mismatch between two data sets, generated and experimental, after passing a certain strain value. Although generated data distribution trajectory seems out of place at the later stage, relative position of the generated data set in the stress-strain coordinate domain seems correct in this instance.

The third graph in this series is from the material M3 (Fig. 5.15). Once again, the sag in the uniaxial data which we were discussing could be observed here. Consequently, like in previous instance, this discrepancy migrate in to the generated data. The mismatch it has with the experimental data at the later stage of strain values could be apportioned to this. In this instance, highest stress level material reach is bigger than in M2. Relative position of the generated data seems correct this time as well.

Material M4 related data distributions given in Figure 5.16 depict a somewhat different picture compared to the material distributions so far discussed. In this case, data distributions, both uniaxial and biaxial, have visibly two segments.

They are, an initial rapid stress progression and, a gradual progression, which followed the former. However, rate of progression of stress, at initial stage is different from uniaxial to biaxial. Therefore, when it comes to develop a second data set, i.e. a hypothetical biaxial data set, based on uniaxial data, a mismatch between generated data set and real data set is obvious. This effect could have been eliminated if the approach was different. On the other hand, such effort could have bring unnecessary complication to the equation. When we consider the gradual progression, which follows the rapid one, visibly both uniaxial and biaxial data dispersions have, nearly similar stress development or progression rates. Despite such a similarity, generated data distribution could not be improved as that preliminary mismatch occurred during the initial stage, when reach the second stage carries a vertical shift.

Data distribution belongs to material M5 is given figure 5.17 shows very much promising result. Though uniaxial data in this case also show the same middle portion sag already discussed, similar sag prevail in the biaxial experimental data provided the perfect match required for the generated data to fit in.

Final material in the tested series is M6, and its related data distribution are given in figure 5.18. In this particular case, there are some oscillations in uniaxial data. These oscillations are visible throughout the entire length of the data distribution. It was not possible to locate the root cause for this abnormality and therefore, we had to live with it in the analysis and generate the secondary data with it. Despite these abnormality the data dispersion shows perfect match up to about 60% strain. Beyond that point, generated data, like in previous instances, seems deviating from the real data. Once again, location of the generated data in the stress-strain domain seems very much matching with the real data.

Having discussed the initial outcomes based on visual observations, at this stage it is appropriate to go in to detail analysis with results as to prove the viability of the method. Therefore, in order to statistically check how close the generated data dispersion to the real data is, we adopted the confident level testing method. Results of this effort were already given in the previous section and at this point, we would like to further discuss these results one by one. If the confidence interval is set to 95, the null hypothesis is to be accepted, the $p$ value should be above 0.05.

For the material M1, all the points show $p$ values higher than that. This indicates simply that, we cannot refuse the null hypothesis at each of these points and therefore two data groups are close to each other in 95 times out of 100 at each point. Materials M2 and M3 also gives similar results. However, as we expected, material M4 is out from the expected values at all tapping points. When

it comes to Material M5, first tapping point shows a minor value than 0.05. Initial discrepancy visible between generated and real data sets might have led to this result. However, if the confidence interval is changed, this might come within the acceptance range. Same outcome could be noticed from the M6 too.

Statistical proof of viability of method encouraged us to further examine the results in a way of data fitting. The results of this fitting exercise were given in previous section and in here, we would like to discuss about these results little further.

Combined data fitting results obtained with Mooney 2 model for material M1 (figure 5.28) show two close curves for both generated and experimental instances. In here, while there is no significant difference between two uniaxial curves, biaxial curves give some gap at the latter stage of strains. Both biaxial curves are somewhat deviating from the experimental data. In general, this data fitting results approve the answer we have so far obtained regarding the closeness of two biaxial data sets, generated and experimental.

Second material in the group, M2, poses a similar picture (figure 5.29). However, in this case, biaxial data set significantly differ from the model curves. Nevertheless, the main purpose of this exercise is to find out whether there is any significant difference between two combine data fitting cases, rather than evaluating fitting results with data. In that sense, results seems agreeable.

Material M3 data fitting graphs given in figure 5.30, though stress levels are higher, show similar picture like in previous two cases. The gap between two biaxial curves is widening over the strain. Once again, the biaxial data dispersion seems departing from the model curves for both experimental and generated cases.

Model curves for material M4 happened to be completely out of place from the data (figure 5.31). This behaviour can be expected as material seems in every way differ from the rest of the materials in this group. In this case, the gap between two combined biaxial data fitting curves seems rapidly widening.

Combined data fitting model curves given in figure 5.32 for material M5 show the closest trajectories to each other from all so far discussed. In this case, uniaxial data seems considerably deviating from model curves at the later part of strains. However, this behaviour could be observed equally for both uniaxial curves.

Final figure in this series, figure 5.33 depicts data fitting results from material M6. Once again, this shows similar trajectories we already discussed in M2 and M3. In this instance, data and the model curves are reasonably compatible as they should be. The deviation observed between data and biaxial curves at later stage

of strain might have been as mentioned by R. Schaefer [41] due to the selection of lower order of the Mooney model.

After discussion of data fitting results, it is suitable to discuss the additional effort we excreted in finding exact exponent for the exponential function we gave as a solution to the problem.

As already given in the results section, we did a least squire method analysis to minimize the gap between experimental data and the generated data. Each material was separately tested and finally, we went further by adding all material together to get a one unique solution for the material series. In each of these cases we obtained minimum values at different points of exponents' axis and they are given in table 5.4. Most of the time, exponent value is in the vicinity of 0.35. Material M5 and M4 are the only exception in this assumption. However, in this instance, value of material M4 could be excused as material itself is a misfit to this common group. The value related to M5 seems somewhat higher than normal and this might have been due to the excessive gap in those random tapping points the generated data could have created with experimental real data.

The overall curve in this analysis show a minimum value at 0.3525 and this could be very much justified. Therefore, with that result, we could suggest that most suitable exponential function as $e^{0.3525}$.

# 7. CONCLUSION

The research work included in this thesis touched the area of hyperelestic material characterization. As described in the text, materials of this nature are not the easiest to characterize. The only way forward through them is by fitting data to an appropriate model which could be selected from forty plus such models available to date. However, in order to get material constants, due to lack of enough data sets, usually one data set was selected for fitting. This practice proved to be erroneous. Therefore, effort was taken herein to solve this problem by generating an additional data set whenever one data set is available.

To begin with, error in the data fitting with one data set was established. In this effort, two data fittings, only uniaxial and combined uniaxial plus biaxial were done and results were compared. Biaxial data and curves were not in any way matching in the case of single data fitting, where as in combined fitting, curves were nicely seen near to respective data. With that results, it was proved the erroneous behaviour of the method of single data fitting.

Having done that, first proposal was given in the way of exponential function as to obtain a second data set from the available uniaxial data. The outcome of first effort showed promising results in the way of secondary data. Second data set obtained through the method was consequently used together with uniaxial data for combine data fitting. Clear improvement in fitting results could be observed both visually and statistically compared to only uniaxial data fitting.

Possibility of further improvement to the method of generating of secondary data was examined. In this method, uniaxial data was divided in two segments and each segment was separately addressed with different empirical formula to get the second data set. Final results of this experiment showed a further improvement to the overall fitting results. However, this method creates some complexities to the solution and therefore, was not further tested for application possibility.

Thereafter, final experiments were done using six different materials. Once again, exponential function was used with a different exponent. This time, overall results were encouraging and therefore continued with further testing. Out of six materials, five were reasonably successful. Only material M4 showed some resentment to the method. Later on, a statistical confidence interval test was done in order to check the closeness of two biaxial data dispersions. Students T table was used for this examination.

Consequently, a combined data fitting also was done with Mooney 2 model and results thus obtained once again were indicating to the useful nature of the method. However, Material M4 showed some incompatibilities in data fitting results as well.

Finally, exact exponent was searched for to use in exponential function in each material case. Certain type of lest squire method was used here. In this search, it was found out that most of the time exponent value oscillate as around 0.35. When method used with all material data together, value came to stand at 0.355 exact figure.

# CONTRIBUTION TO SCIENCE AND PRACTICE

This thesis aimed at providing a solution to a problematic situation that arises when there is not sufficient data sets available for data fitting in the mechanical characterization of hyperelestic materials. By providing secondary data set which resembles biaxial data, the problem could be overcome with reasonably accurate results. Such solution of the problem, contributed to the science in following manner.

- Method could improve the results by eliminating erroneous practice of single data set fitting.
- This is a cost-effective method of mechanical characterization of hyperelestic materials.
- The method reduces aggregate time consumed for characterization by way of additional experiments.
- Eliminate inaccuracies attached with biaxial testing as method nullifies the requirement for additional tests.
- The method open up a new area of research to find extra pure shear data set with similar type of method
- At the same time, method could be further developed to accommodate many more materials.

# REFERANCE

[1] SASSO, M. , PALMIERI, G., CHIAPPINI, G. AMODIO, D. Characterization of hyperelastic rubber like materials by biaxial and uniaxial stretching tests based on optical methods. J. Polymer Testing, 27 (2008), pp. 995–1004.

[2] GOUGH, J., MUHR, A.H., THOMAS, A.G. Material Characterisation for Finite Element Analysis of Rubber Components. J. Rubber Research, 1(4) (1998), pp. 222-239.

[3] ALI, A., HOSSEINI, M., SAHARI, B.B. A Review of Constitutive Models for Rubber-Like Materials. American J. of Engineering and Applied Sciences, 3 (1) (2010), pp. 232-239.

[4] ALI, A., HOSSEINI, M., SAHARI, B.B. A Review and comparison on some rubber elasticity models. J. of Scientific & Industrial Research, 69 (2010), pp. 495-500.

[5] YUAN, L., GU, Z., YIN, Z., XIAO, H. New compressible hyper-elastic models for rubberlike materials. J. Acta. Mech., 226 (2015), pp. 4059–4072.

[6] SCHAEFER, R. J. Mechanical properties of rubber.

[7] GENT, A.N. Engineering with Rubber.

[8] KUMAR, N., RAO, V. V. Hyperelastic Mooney-Rivlin Model: Determination and Physical Interpretation of Material Constants. MIT International J. of Mech. Engineering, 6(1) (2016), pp. 43-46.

[9] SHAHZAD, M., KAMRAN, A., SIDDIQUI, M.Z., FARHAN, M. Mechanical Characterization and FE Modelling of a Hyperelastic Material. J. Materials Research, 18(5) (2015), pp. 918-924.

[10] Visakh, P.M. and others. Advances in elastomers.

[11] SASSO, M., CHIAPPINI, G., PALMIERI, G., PAPALINI, S. Characterization of Time-Dependent Materials by Biaxial Stretching Tests. (2007)

[12] GUO, Z., SLUYS, L. J. Constitutive modelling of hyperelastic rubber-like materials. J. HERON, 53(3) (2008), pp. 109-132.

[13] VLASCEANU, D., GHEORGHIU, H., PASTRAMA, S. D. Experimental determination of the Mooney-Rivlin parameters for hyperelastic materials like rubber.

[14] JADHAV, A. N. BAHULIKAR, S.R., SIDDIQUI, M. Z., SAPATE, N.H. Comparative study of variation of Mooney-Rivlin hyperelastic material models under uniaxial tensile loading. Int. J. of Advance Research and Innovative Ideas in Education, 2(4) (2016), pp. 212-216.

[15] TRELOAR, A. R.G. Stress-strain data for vulcanised rubber under various types of deformation. Trans. Faraday Soc., 40, pp. 59-70.

[16] BOWER, A.F. Applied_Mechanics_of_Solids. CRC Press, Taylor & Francis Group, LLC. ISBN 978 1 4398 0247 2.

[17] RIVLIN, R. S. The Valanis-Landel Strain-Energy Function. J. of Elasticity, 73 (2003), pp. 291-297.

[18] STUMPF, F. T., MARCZAK, R. J. Optimization of constitutive parameters for hyperelastic models satisfying the Baker-Ericksen inequalities. Mecánica Computacional Vol XXIX (2010), pp. 2901-2916.

[19] AMIN, A. F. M. S., WIRAGUNA, S. I., BHUIYAN, A. R., OKUI., Y. Hyperelasticity model for finite element analysis of natural and high damping rubbers in compression and shear. J. of Engineering Mechanics, 132(1) (2006), pp. 54-64.

[20] LOPEZ-PAMIES, O. A new $I_1$-based hyperelastic model for rubber elastic materials. C. R. Mecanique 338 (2010) 3–11, www.sciencedirect.com

[21] BEDA, T. An approach for hyperelastic model-building and parameters estimation: a review of constitutive model. European Polymer Journal 50 (2014) 97–108.

[22] MANSOURI, M.R., DARIJANI, H. Constitutive modeling of isotropic hyperelastic materials in an exponential framework using a self-contained approach. International Journal of Solids and Structures 51 (2014) 4316–4326.

[23] ZHAO, F. Continuum Constitutive Modeling for Isotropic Hyperelastic Materials. J Advances in Pure Mathematics, 2016, 6, 571-582.

[24] KAKAVAS, P.A. A New Development of the Strain Energy Function forHyperelastic Materials Using a Logarithmic Strain Approach. Journal of Applied Polymer Science, Vol. 77, 660 – 672 (2000)

[25] HORGAN, C. O., Murphy, J. G. Limiting Chain Extensibility Constitutive Modelsof Valanis–Landel Type. J Elasticity (2007) 86:101–111, DOI 10.1007/s10659-006-9085-x

[26] SUSSMAN, T., BATHE, K. A model of incompressible isotropic hyperelastic material behaviour using spline interpolations of tension–compression test data. J. Commun. Numer. Meth. Engng (2009) ;25:53–63

[27] HOSS, L., MARCZAK, R. J. A New Constitutive Model for rubber-like Materials. J. Mecánica Computacional Vol XXIX, págs. 2759-2773

[28] OGDEN, R.W. Biaxial deformation of rubber-like solids: comparison of theory and experiment. J. Phys. D: Appl. Phys., Vol. 12 (1979).

[29] JAMES, A. G., GREEN, A., SIMPSON, G. M. Strain energy functions of rubber. I. Characterization of gum vulcanizates. J. Applied polymer science, 19 (1975), pp. 2033-2058.

[30] TEJASRI, P., BASAK, A. Comparative study of computational material models. Int. J. Applied engineering research, 13(10) (2018), pp. 8588-8595.

[31] DESTRADE, M., SACCOMANDI, G., SGURA, I. Methodical fitting for mathematical models of rubber-like materials. Int. J. Applied engineering research, http://dx.doi.org/10.1098/rspa.2016.0811.

[32] MARCKMANN, G., VERRON, E. Comparison of Hyperelastic Models for Rubber-Like Materials. J. Rubber Chemistry and Technology, American Chemical Society, 79 (5) (2006), pp. 835-858.

[33] KAYACI, S., SERBEST, A. K. Comparison of constitutive hyper-elastic material models in finite element theory. 6th Automotive technology congress, June 2012, Bursa, Turkey. http://otekon.org/dokuman/6thOtekonBook.pdf

[34] JOHANNKNECHT, R., JERRAMS, S. The need for equi-biaxial testing to determine elastomeric material properties. 1st European conference on constitutive models for rubber, August 1999, Vienna, Austria.

[35] MORROW, D. A., DONAHUE, T. H., ODEGARD, G. M., KAUFMAN, K. R. A method for assessing the fit of a constitutive material model to experimental stress–strain data. J. Comput. Methods Biomech. Biomed. Engin. 13 (2) (2010), pp. 247-256.

[36] HASSAN, M. A., ABOUEL_KASEM, A., EL-SHARIEF, M. A. Evaluation of the material constants of Nitrile Butadeine Rubber(NBR) with different Carbon Black(CB): FE-Simulation and experimental. J. of Engineering Sciences. 38 (1) (2010), pp. 119-134.

[37] OGDEN, R. W., SACCOMANDI, G., SGURA, I.. Fitting hyperelastic models to experimental data. J. Computational Mechanics (2004), DOI 10.1007/s00466-004-0593-y

[38] GAVIN, H. P. The Levenberg-Marquardt algorithm for nonlinear least squares curve-fitting problems. (2019) Gavin c ©. Corpus ID: 5708656

[39] MARCKMANN, G. & VERRON, E. Efficiency of hyperelastic models for rubber-like materials. J. Computational Mechanics (2004), DOI 10.1007/s00466-004-0593-y

[40] Science and Technology of Rubber, Third Edition

[41] Schaefer, R. J., Mechanical propeties of Rubber

[42] Erman, B. and others , Technology of Rubber , ISBN: 978-0-12-394584-6)
[43] DICK, J.S. Rubber Technology: Compounding and testing for performance. Hanser publishers, Munich, (2001). ISBN 3-446-19186-0.

[44] MARK, J. E., ERMAN, B., ROLAND, C. M. The Science and Technology of Rubber. Academic Press (2013 Elsevier Inc.), Oxford, OX5 1GB, UK.

[45] DE BORST, R., VAN DER BOGERT, P.A.J., ZEILMAKER, J. Modelling and analysis of rubber like materials, Science and Technology of Rubber, , Heron vol. 33 1988 no. 1

[46] KAMPER, M., BEKKER, A. Non-contact experimental methods to characterise the response of a hyper-elastic membrane. Int. J. of Mechanical and Materials Engineering. (2017), pp. 12-15.

[47] TOBAJAS, R., IBARZ, E., GRACIA, L. A comparative study of hyperelastic constitutive models to characterize the behaviour of a polymer used in automotive engines. MDPI, Basel, Switzerland.
http://creativecommons.org/licenses/by/4.0/

[48] MENDELSON, E. Schaum's outline of theory and problems of beginning calculus, 2nd ed. The McGraw-Hill Companies, Inc., ISBN 0-07-041733-4

[49] RACKL, M. (2015), Material testing and hyperelastic material model curve fitting for Ogden, Yeoh and Polynomial models , in 'ScilabTEC (7thInternational Scilab UsersConference)', Paris

[50] CHEVALIER, L., CALLOCH, S., HILD, F., MARCO, Y. Digital Image Correlation used to analyse the multiaxial behaviour of Rubber-like Materials. EU. J. of Mechanics - A/Solids. 20(2) (2001), pp. 169-187.

[51] JAVORIK, J., MANAS, D. The specimen optimization for the equibiaxial test of elastomers. ACMOS' 11 Proceedings of the 13th WSEAS international conference on Automatic control, modelling & simulation, May 2011, Canary Islands, Spain. pp. 121-124.

[52] BOJTOS, A., ABRAHAM, G., Optical measuring system for equibiaxial test of hyperelastic rubber-like materials, Ninth Youth symposium on experimental solid mechanics, Trieste, Italy (07/2010). ISBN 978-88-95940-30-4

[53] REUGE, N., SCHMIDT, F. M., MAOULT, Y.LE., RACHIK, M., ABBE, F. Elastomer biaxial characterization using bubble inflation technique. Numerical investigation of some constitutive models, J. Polymer engineering and science, 2001, Vol. 41(3), pp. 532-541.

[54] SEIBERT, H., SCHEFFER, T., DIEBELS, S., Biaxial testing of elestomers – experimental setup, measurement and experimental optimization of specimen's shape, J. Technische mechanik, 2014, Vol. 34 (2), pp.72-89

[55] MANSOURI, M.R., DARIJANI, H., BAGHANI, M. On the Correlation of FEM and Experimentsfor Hyperelastic Elastomers, J. Experimental Mechanics, 2016, DOI 10.1007/s11340-016-0236-0

[56] BRADLEY, G. L., CHANG, P. C., MCKENNA, G. B. Rubber modelling using uniaxial data, J. Applied Polymer Science, 2001, Vol. 81, pp. 837-848.

[57] YANG, L. M., SHIM, V. P. W., LIM, C. T. A visco-hyperelestic approach to modelling the constitutive behaviour of rubber, Int. J. Impact engineering, 2000, Vol. 24, pp.545-560.

[58] VLAD, C., PRISACARU, G., OLARU, D. FEM Simulation on Uniaxial Tension of Hyperelastic Elastomers, J. Applied Mechanics and Materials, 2014, Vol. 659, pp. 57-62.

[59] DESTRADE, M., SACCOMANDI, G., SGURA, I. Methodical fitting for mathematical models of rubber-like materials, Proc.R.Soc.A473: 20160811. http://dx.doi.org/10.1098/rspa.2016.0811

[60] CHAPRA, S. C. Applied Numerical Methods with MATLAB for engineers and scientists, McGraw-Hill Publishers, 2012, ISBN 978-0-07-340110-2.

[61] HUNT, B. R., LIPSMAN, R. L., ROSENBERG, J. M. A Guide to MATLAB: for Beginners and Experienced Users, Cambridge University Press, (2001), ISBN 10- 0-521-00859-x

[62] KNIGHT, A., Basics of MATLAB and Beyond, CRC Press LLC, ISBNO-8493-2039-9

[63] The Math Works, Inc., MATLAB User's Guide: Curve Fitting Toolbox: For Use with MATLAB

[64] MCFEDRIES, P., Excel 2013 Simplified, John Wiley & Sons, Inc., ISBN: 978-1-118-50542-7

[65] FREUND, S. M., JONES, M. B., STARKS, J. L. Microsoft Excel 2013: Complete, Cengage Learning, ISBN-10: 1-285-16844-5

[66] CRISFIELD, M.A. Non-linear Finite Element Analysis of Solids and Structures, (1997) John Wiley & Sons Ltd., ISBN 0 471 95649 X

[67] COOK, R.D. Finite Element Modelling for Stress Analysis, (1995) John Wiley & Sons Ltd., ISBN 0 471 10774 3

[68] CHEN, W., SALEEB, A. F. Constitutive Equations for Engineering Materials, Volume 1: Elasticity and Modelling, (1994) Elsevier Science B.V, ISBN: 0-444-88408-4

* Images obtained from free media in the internet.

# LIST OF TABLES

# LIST OF IMAGES

# LIST OF SYMBOLS AND ACRONYMS

| | | | |
|---|---|---|---|
| $a$ | - | **Factor** | - |
| $a_1, a_2, a_{3, \ldots} a_m$ | - | **Finite numbers** | - |
| $b, n$ | - | **Factors** | - |
| $C$ | - | **Right Cauchy-Green tensor** | - |
| $C_{i,j}, D, \lambda_L, \mu, \alpha$ | - | **Material constants** | - |
| $e$ | - | **Deformation measure** | - |
| $e'$ | - | **Error value** | - |
| $F$ | - | **deformation gradient** | - |
| $I$ | - | **Identity matrix** | - |
| $J$ | - | **Determinant of strain gradient** | - |
| $l$ | - | **Deformed speciman length** | **m** |
| $lo$ | - | **Undeformed specimen length** | **m** |
| $p$ | - | **applied pressure** | **MPa** |
| $R$ | - | **Rotation** | - |
| $r$ | - | **Radius of curvature** | **m** |
| $S_r$ | - | **Sum of squares of the residuals** | - |
| $S_{y/x}$ | - | **Standard error** | - |
| $to$ | - | **Initial thickness** | **m** |
| $U$ | - | **Pure deformation** | - |
| $W(e)$ | - | **Potential strain energy density function** | - |
| $X_{i\ (i=1,2,3)}$ | - | **Auxiliary  coordinate system** | - |
| $y_b$ | - | **Generated biaxial data** | - |
| $y_u$ | - | **Uniaxial stress** | **MPa** |

| $\gamma$ | - | **Green-Lagrange strain tensor** | - |
| $\xi_{i\ (i=1,2,3)}$ | - | **Coordinate system** | - |
| $\lambda_{i\ (i=1,2,3)}$ | - | **Principle stretch ratios** | - |
| $\lambda_{\theta\theta}$ | - | **Stretch ratio at the pole** | - |
| $\sigma_{ij}$ | - | **True (Cauchy) stresses** | **MPa** |
| $\sigma_{\theta\theta}$ | - | **Hoop stress** | **MPa** |

# LIST OF PUBLICATIONS BY AUTHOR

[1] **R. KEERTHIWANSA**, J. JAVORIK, J. KLEDROWETZ, P. NEKOKSA. Elastomer testing: The risk of using only uniaxial data for fitting the Mooney-Rivlin hyperelastic material model. J. Materials and technology, 52(1) (2017), pp. 003-008.

[2] **R. KEERTHIWANSA**, J. JAVORIK, J. KLEDROWETZ, P. NEKOKSA. Hyperelastic material characterization: A method of reducing the error of using only uniaxial data for fitting Mooney-Rivlin curve. J. Materials science forum, 919 (2018), pp. 292-298.

[3] **R. KEERTHIWANSA**, J. JAVORIK, J. KLEDROWETZ. Secondary biaxial data application in a process of a hyperelastic material characterization. J. Materials science forum, 952 (2019), pp. 275-281.

[4] **R. KEERTHIWANSA**, J. JAVORIK, J. KLEDROWETZ. Hyperelastic material characterization: A comparison of material constants. J. Materials and technology, 54(1) (2020), pp. 121-123.

[5] **R. KEERTHIWANSA**, J. JAVORIK, S. RUSNAKOVA, , P. GROSS, J. KLEDROWETZ. Hyperelastic material characterization: How the change in Mooney-Rivlin parameter values effect the model curve. J. Materials science forum, 994 (2020), pp. 265-271.

[6] J. JAVORIK, J. KLEDROWETZ, **R. KEERTHIWANSA**, P. NEKOKSA. The numerical analysis of axially loaded elastomeric bushing. J. Materials science forum, 919 (2018), pp. 315-324.

[7] J. KLEDROWETZ, J. JAVORIK, **R. KEERTHIWANSA**, P. NEKOKSA. Calculation of the tyre curing mould cavity shape using FEM. J. Manufacturing technology, 17(4) (2017), pp. 479-482

[8] J. KLEDROWETZ, J. JAVORIK, **R. KEERTHIWANSA**, P. NEKOKSA. FEM modelling techniques for three point bend test of rubber composites. J. Materials science forum, 919 (2018), pp. 257-265.

[9] J. KLEDROWETZ, J. JAVORIK, **R. KEERTHIWANSA**. Evaluation of a tyre tread pattern stiffness using FEA. J. Materials science forum, 952 (2019), pp. 243-249.

[10] J. KLEDROWETZ, J. JAVORIK, **R. KEERTHIWANSA,** P. Kratochvil, S. Rusnakova, P. Gross. FEM optimization of a steel belt of OTR tyres. J. Materials science forum, 994 (2020), pp. 272-279.

# CURRICULUM VITAE



*Personal data*

First Name / Name:     Rohitha Keerthowansa
Birth Date:            17.03.1966
Birth Place:           Colombo, Sri Lanka.
Nationality:           Sri-Lankan
Family States          Married
Address (Permanent):   67, Kingswood Park, Maya Mw.,   Kiribathgoda,
                       Sri Lanka.
Telephone:              00 420 605109785
E-Mail:                nihathamani@hotmail.com

*Studies*

1. **Tomas Bata University (2016-2020)**
    Zlin, Czech Republic.
    Ph.D. studies in Production Engineering

2. **Leibniz University of Hannover (2004-2008)**
    Hannover, Germany.
    Degree - Master of Science in Mechanical Engineering (M.Sc. (Eng.))
    Study field: Production Technology
    Specialization: Production Processes

3. **Technical University of Clausthal (2002-2003)**
    Clausthal–Zellerfeld, Germany.
    German Language Course

4. **University of Moratuwa  (2000-2001)**
    Faculty of Mechanical Engineering, Moratuwa, Sri Lanka.
    Degree - Postgraduate Diploma in Energy Technology

5. **University of Peradeniya**
    Faculty of Engineering, Peradeniya, Sri Lanka.
    Degree - Bachelor of Science in Mechanical Engineering (B.Sc.(Eng.))

*Work Experiances  in the Industry (1994 – 2013)*

-   Boehm+Leckner Multi Moulds (Pvt.) Ltd., Katunayake, Sri Lanka.
Workshop Engineer plus Controller (German Injection Mold Tool Making Company)
-   Central Engineering Consultancy Bureau, Digana, Sri Lanka.
Worked as a Mechanical Engineer Section design and construction of steel structures
-   Ceylon Biscuits (Pvt.) Ltd., Homagama, Sri Lanka.

Production shift Manager Had the responsibility for he Production Planning and control
- Tea Research Institute, Thalawakelle, Sri Lanka.

Worked as a technical assistant at department of statistics

*Work Experiances  as Lecturer (2011-2016)*
- Part time lecturing at University of Vocational Technology in Manufacturing Technology for B.Eng. students.
-  Lecturing at Seychelles Institute of Technology (SIT), Mahe, Republic of Seychelles, in Mechanical Engineering

*Skills and abilties*
- CAD/CAM programs (CATIA, Solid Works, NX 12)
- FEM/FEA programs (MSC Marc, MSC Patran)
- Programing (Matlab)
- Graphics (Photoshop, Coral Draw, Micro Graphics)

*Language skills*
- Sinhala – Mother tongue
- English – Fluent
- German - Fluent

Rohitha Keerthiwansa

96

# Design and Validation of the Methods for Comprehensive Characterization of the Hyperelastic Properties of Elastomers

# Návrh a validace metod pro komplexní charakterizaci hyperelastických vlastností elastomerů

Doctoral Thesis

Publication Year: 2020